



ETH

Eidgenössische Technische Hochschule Zürich
Swiss Federal Institute of Technology Zurich

How does forest structure affect landslide susceptibility?

Statistical prediction models for shallow landslides
integrating forest structure



Master thesis

**Christine Moos, Master in Environmental Science, ETH Zürich
März, 2014**

Supervisor: Dr. Peter Bebi, WSL-Institut für Schnee- und Lawinenforschung
(SLF), Davos

Co-Supervisor: Christian Rickli, Eidgenössisches Forschungsinstitut für Wald,
Schnee und Landschaft (WSL), Birmensdorf

Acknowledgments

This master thesis would not have been possible without the help of numerous people. First, I would like to thank my supervisor, Peter Bebi, who always helped in word and deed and made this thesis possible. I highly appreciated to have my office next to his and to find open doors when there was a problem. Thanks also go to my co-supervisor, Christian Rickli. He provided the landslide data and useful tips especially for the field work. Furthermore, I could always count on the support of Frank Graf, the leader of the SOSTANAH project. His expertise was indispensable for the statistical analysis. I am also grateful to Christian Rixen and the whole *mountain ecosystems* group of the SLF for methodological hints. Moreover, I thank Yves Bühler for his help with the GPS device. Special thanks go to my father, who assisted me with the field work under partially hard weather conditions. Last but not least, I would like to thank my family for the moral support and the whole team at the SLF for the great time in Davos.

Summary

Forests are assumed to have a generally positive effect on slope stability. However, field inventories of rainfall triggered shallow landslides in different regions in Switzerland show that landslide density in forest areas can be substantial. Thus, it can be assumed that not only the presence of forest plays an important role for slope stability, but also the forest structure. This master thesis aims to design statistical models to predict landslide susceptibility which include variables describing the forest structure along with terrain and hydrological parameters.

Two landslide inventories compiled by the Swiss Federal Institute for Forest, Snow and Landscape Research (WSL) in 1997 in Sachseln OW (136 landslide plots) and in 2005 in St. Antoenien GR (46 landslide plots) provide the basis of this study. For each point location of a landslide in the forest as well as for a comparable set of control points (same number and range of forest cover and steepness), variables characterising forest structure, topography, geomorphology and hydrology were measured in the field (St. Antoenien) and derived from LiDAR based elevation data (St. Antoenien and Sachseln) and from a stand classification (Sachseln). Subsequently, the data were analysed with univariate as well as with multivariate statistics. Three different multivariate models, namely logistic regression, classification trees and random forests, were used. I tested their performance with cross-validation on the entire data set using the area under the Receiver Operating Characteristic Curve (AUC) to quantify their prediction accuracy.

In addition to terrain features and hydrology, forest structure significantly influences slope stability. According to the field data of St. Antoenien, landslide susceptibility rises with decreasing tree coverage, increasing gap length and increasing distance between the (potential) release point and the nearest trees. The analysis of LiDAR data of St. Antoenien, however, only revealed significant effects for slope angle, curvature, the *weighted Topographic Wetness Index* (lower at landslide plots) and tree edge density (higher at landslide plots). In Sachseln, maximum and mean tree height as well as the standard deviation of tree height and tree edge density were significantly lower in landslide plots. Furthermore, there are more young and less deciduous stands in landslide plots compared to control plots. The performance of the three different classifiers was generally acceptable ($AUC \geq 0.7$), except for classification trees, which partially exhibited lower AUC values. Random forest was the best performing model, while logistic regression is expected to have best generalization capabilities. Multivariate models integrating forest structure performed better than models solely based on terrain and hydrological variables. Furthermore, models based on field variables yielded considerably higher AUC values than models based on LiDAR derived variables.

The study generally confirms the hypothesis that forest structural characteristics do have an influence on shallow landslide susceptibility. However, the varying results between the two study sites make evident that the influence of these variables depends strongly on regional and local conditions, such as vegetation zones, altitudinal range, size of the study area and the triggering rainfall event. Certain variables which highly affect slope stability according to the field investigation could not be ascertained with

the LiDAR data. This indicates that the resolution of digital elevation models used in this study (cell size = 2 m) is too low in order to detect local differences in forest structure which influence landslide susceptibility. In order to get more generalizable results, further analysis of larger data sets comprising different study areas are recommended.

Zusammenfassung

Im Allgemeinen wird angenommen, dass sich Vegetation und insbesondere Wald positiv auf die Hangstabilität auswirken. Feldinventuren von flachgründigen Rutschungen aus verschiedenen Regionen der Schweiz zeigen jedoch, dass der Rutschungsanteil in Wäldern beträchtlich sein kann. Dies lässt vermuten, dass nicht nur die Präsenz von Wald, sondern auch die Waldstruktur eine wichtige Rolle für die Hangstabilität spielt. Ziel der vorliegenden Masterarbeit ist es, statistische Modelle zur Vorhersage der Anfälligkeit für Hangrutschungen zu entwerfen, die neben geomorphologischen, topographischen und hydrologischen Parametern insbesondere auch verschiedene Waldstruktur-Variablen enthalten.

Die Grundlage der Studie bilden zwei Rutschungsinventuren, welche die Eidgenössische Forschungsanstalt für Wald, Schnee und Landschaft (WSL) 1997 in Sachseln OW (136 Rutschungspunkte) und 2005 in St. Antönien GR (46 Rutschungspunkte) durchgeführt hat. Für jede Rutschfläche sowie für eine gleiche Anzahl Kontrollflächen mit vergleichbarem Kronendeckungsgrad und Hangneigungswinkel wurden im Rahmen der vorliegenden Studie Variablen erhoben, die den Wald, das Terrain sowie die hydrologischen Verhältnisse beschreiben. Sie wurden im Feld gemessen (St. Antönien) und mittels LiDAR-basierten Höhenmodellen berechnet (St. Antönien und Sachseln), respektive von einer Bestandeskarte abgeleitet (Sachseln). Anschliessend wurden die Daten mit univariater und multivariater Statistik analysiert. Es kamen drei verschiedene multivariate Modelle – logistische Regression, Klassifikationsbäume und Random Forests – zur Anwendung. Die Güte der Modelle wurde jeweils mittels Kreuzvalidierung des gesamten Datensatzes erhoben. Dabei diente die Fläche unter der *Receiver Operating Characteristic Curve* (AUC) als Mass für die Klassifikationsgenauigkeit.

Nebst Gelände- und hydrologischen Faktoren hatte die Waldstruktur einen signifikanten Einfluss auf die Hangstabilität. Gemäss den Felddaten von St. Antönien steigt die Anfälligkeit gegenüber Hangrutschungen mit abnehmendem Kronendeckungsgrad, zunehmender Lückenlänge und einer zunehmenden Distanz zwischen dem (potentiellen) Auslösepunkt der Rutschung und den nächsten Bäumen. Die Analyse von Höhenmodellen von St. Antönien ergab hingegen nur signifikante Effekte für die Neigung, die Krümmung, den *weighted Topographic Wetness Index* (niedriger bei Rutschungen) und die Baumkantendichte (höher bei Rutschungen). In Sachseln waren die maximale und die minimale Baumhöhe, die Standardabweichung der Baumhöhe sowie die Baumkantendichte in Rutschflächen signifikant niedriger als in Kontrollflächen. Zudem werden Rutschflächen häufiger von Jungwuchs sowie von Nadel- und Mischwäldern dominiert. Kontrollflächen hingegen gehören generell zu älteren Beständen und haben einen höheren Laubbaumanteil. Die Güte der drei Klassifikationsmodellen war im Allgemeinen akzeptabel ($AUC \geq 0.7$). Eine Ausnahme bilden Klassifikationsbäume, welche teilweise tiefere Werte erreichen. Random Forest erwies sich als das Modell mit der höchsten Klassifikationsgenauigkeit, gefolgt von logistischer Regression. Multivariate Modelle, welche die Waldstruktur miteinbeziehen, erzielten eine höhere Leistung als Modelle, die nur auf Gelände- und hydrologischen

Variablen basieren. Ferner sind die AUC-Werte der Modelle basierend auf Feld-Variablen deutlich höher als jene der Modelle basierend auf LiDAR-Variablen.

Im Allgemeinen bestätigt die Studie die Hypothese, dass die Waldstruktur einen Einfluss auf die Anfälligkeit für flachgründigen Hangrutschungen hat. Die unterschiedlichen Resultate der beiden Untersuchungsgebiete zeigen jedoch, dass der Effekt der Waldstruktur stark von regionalen und lokalen Gegebenheiten, wie beispielsweise von den Vegetationszonen, den Höhenstufen, der Grösse des Untersuchungsgebietes und vom auslösenden Niederschlag, abhängt. Zudem konnten gewisse Variablen, die gemäss den Felddaten die Hangstabilität signifikant beeinflussen, mittels der LiDAR Daten nicht bestätigt werden. Dies deutet darauf hin, dass die Auflösung der hier verwendeten digitalen Höhenmodellen (*cell size* = 2 m) zu gering ist, um lokale Unterschiede in der Waldstruktur, welche die Anfälligkeit für Hangrutschungen beeinflussen, zu erkennen. Um die Resultate noch besser auf andere Gebiete übertragen zu können, empfehlen sich weitere Analysen mit grösseren Datensätzen in verschiedenen Untersuchungsgebieten.

Contents

Acknowledgments	i
Summary	ii
Zusammenfassung	iv
Contents	vi
Figures	viii
Tables	x
1. Introduction	1
2. Methods	3
2.1. Study areas	3
2.1.1. <i>St. Antoenien</i>	3
2.1.2. <i>Sachseln</i>	4
2.2. Data.....	6
2.2.1. <i>Landslide inventory</i>	6
2.2.2. <i>Geodata</i>	6
2.3. Determination of control points	7
2.4. Field investigation.....	8
2.5. Analysis of LiDAR data	11
2.5.1. <i>Tree height</i>	11
2.5.2. <i>Tree coverage</i>	11
2.5.3. <i>Gap length</i>	11
2.5.4. <i>Tree layers</i>	12
2.5.5. <i>Distance to the nearest tree</i>	12
2.5.6. <i>Topography</i>	12
2.5.7. <i>Weighted Topographic Wetness Index</i>	13
2.6. Verification of data actuality and accuracy	14
2.7. Statistical analysis	15
2.7.1. <i>Logistic regression</i>	15
2.7.2. <i>Classification and regression tree</i>	16
2.7.3. <i>Random forest</i>	16
2.7.4. <i>Explanatory variables</i>	17
2.7.5. <i>Model calibration and validation</i>	17
2.7.6. <i>Receiver Operating Characteristic</i>	18
3. Results	19
3.1. Univariate analysis.....	19
3.1.1. <i>St. Antoenien field data</i>	19

3.1.2.	<i>St. Antoenien LiDAR data</i>	24
3.1.3.	<i>Sachseln</i>	30
3.2.	Multivariate models.....	36
3.2.1.	<i>St. Antoenien field data</i>	36
3.2.2.	<i>St. Antoenien LiDAR data</i>	41
3.2.3.	<i>Sachseln</i>	44
4.	Discussion	49
4.1.	Explanatory variables	49
4.2.	Comparison LiDAR and field data.....	52
4.3.	Predictive power of statistical models	54
5.	Conclusions	56
6.	References	57
	Appendix A: Field protocol	64
	Appendix B: Correlation diagram	69
	Appendix C: Model Builder diagrams ArcGIS	76
	Appendix D: Explanatory variables	81
	Appendix E: Residual analysis logistic regression	92
	Appendix F: Declaration of originality	97

Figures

Fig. 1: Map of Switzerland with the two study areas Sachseln and St. Antoenien.....	3
Fig. 2: Study area in St. Antoenien with landslide and control points.....	4
Fig. 3: Study area in Sachseln with landslide and control points.....	5
Fig. 4: Landslide and control plot in St. Antoenien.....	8
Fig. 5: Distribution of slope angles measured at control and landslide points in St. Antoenien.	19
Fig. 6: Number of plots per geomorphology type in control and landslide plots.....	19
Fig. 7: Boxplot and barplot of tree coverage values estimated in control and landslide plots in St. Antoenien.....	20
Fig. 8: Distribution of lengths and widths of the largest gaps in control and landslide plots.....	20
Fig. 9: Distribution of the mean distance to the 5 nearest trees and the distance to the nearest tree measured in the field as well as on the orthophoto.....	21
Fig. 10: Distribution of the proxy-variable for root penetration of the nearest tree and the five nearest trees. The higher the value of the variable, the lower is the root penetration expected. Differences are for both variables significant.....	21
Fig. 11: Distribution of the estimated percentage of trees in the different diameter classes in control and landslide plots.....	22
Fig. 12: Distribution of LiDAR derived slope angles at the release point and averaged over an area of 30m x 30m.	24
Fig. 13: Distribution of curvature, profile curvature and plan curvature values in control and landslide plots.	25
Fig. 14: Distribution of tree edge density and the maximum tree height in control and landslide plots in St. Antoenien.....	25
Fig. 15: Distribution of distances from the (potential) release point to the nearest tree and lengths of the largest gap in control and landslide plots.	26
Fig. 16: Tree peaks extracted as local maxima from the CHM and forest gaps in two different sections of St. Antoenien.....	26
Fig. 17: Canopy Height Model for a section of the study area in St. Antoenien with landslide and control points.....	27
Fig. 18: Slope angle, wTWI and tree coverage in the study area of St. Antoenien.....	28
Fig. 19: Tree edge density, tree layers and maximum tree height in the study area of St. Antoenien.	29
Fig. 20: Distribution of slope angles at the release point and averaged over an area of 30m x 30m.....	30
Fig. 21: Distribution of the maximum and the mean tree height as well as the standard deviation of tree height and the tree edge density.	31

Fig. 22: Canopy Height Model for a section of the study area in Sachseln with landslide and control points.	32
Fig. 23: Number of control and landslide plots in the different successional stages....	32
Fig. 24: Number of control and landslide plots in coniferous, mixed and deciduous stands.....	33
Fig. 25: Mean slope angle and tree coverage in the study area of Sachseln.	34
Fig. 26: Successional stage and species mixture in the study area of Sachseln.....	35
Fig. 27: Classification tree to predict landslide occurrence in St. Antoenien based on hydrological and terrain variables assessed in the field (<i>CT topo</i>).....	37
Fig. 28: Classification tree to predict landslide occurrence in St. Antoenien based on hydrological, terrain and forest variables assessed in the field (<i>CT mix</i>).	38
Fig. 29: Explanatory variables of the random forest fitted with field data of St. Antoenien (<i>RF all</i> ; n = 93) and the corresponding variable importance.	39
Fig. 30: Receiver Operating Characteristics curves and corresponding AUC values of the logistic regression models, the classification trees and the random forest.....	40
Fig. 31: Classification tree to predict landslide occurrence in St. Antoenien based on LiDAR derived variables (<i>CT LiDAR</i>).	41
Fig. 32: Explanatory variables of the random forest fitted with LiDAR data of St. Antoenien (<i>RF LiDAR</i> ; n = 93) and the corresponding variable importance.....	42
Fig. 33: Receiver Operating Characteristics (ROC) curves and corresponding AUC values of the logistic regression model, the classification tree and the random forest based on LiDAR data of St. Antoenien.....	43
Fig. 34: Classification tree to predict landslide occurrence in Sachseln based on LiDAR derived variables (<i>CT Sachseln</i>).	45
Fig. 35: Classification tree to predict landslide occurrence in Sachseln based on variables derived from LiDAR data and the stand classification (<i>CT Sachseln+</i>).....	46
Fig. 36: Variable importance of the RF model fitted with LiDAR data only (<i>RF Sachseln</i>) and the RF model based on LiDAR data and the stand classification of Sachseln (<i>RF Sachseln+</i>).	47
Fig. 37: Receiver Operating Characteristics (ROC) curves and corresponding AUC values of the logistic regression models, the classification trees and the random forest models based on LiDAR data only and LiDAR data and stand classification.....	48

Tables

Tab. 1: Variables assessed in landslide and control plots in St. Antoenien.....	9
Tab. 2: Variables assessed in the field which significantly affect landslide occurrence in St. Antoenien and the corresponding p-values.....	23
Tab. 3: Variables derived from LiDAR data which significantly affect landslide occurrence in St. Antoenien and the corresponding p-values.....	27
Tab. 4: Variables derived from LiDAR data or the stand classification which significantly affect landslide occurrence in Sachseln and the corresponding p-values.	33
Tab. 5: Estimated regression coefficients, standard errors, Z-values and p-values of explanatory variables of the logistic regression model for St. Antoenien based on terrain and hydrological variables assessed in the field (<i>LOG topo</i>).....	36
Tab. 6: Estimated regression coefficients, standard errors, Z-values and p-values of explanatory variables of the logistic regression model for St. Antoenien based on terrain, hydrological and forest variables assessed in the field (<i>LOG mix</i>).....	37
Tab. 7: Estimated regression coefficients, standard errors, Z-values and p-values of explanatory variables of the logistic regression model for St. Antoenien based on variables derived from LiDAR data (<i>LOG LiDAR</i>).	41
Tab. 8: Estimated regression coefficients, standard errors, Z-values and p-values of explanatory variables of the logistic regression model based on variables derived from LiDAR data (<i>LOG Sachseln</i>).....	44
Tab. 9: Estimated regression coefficients, standard errors, Z-values and p-values of explanatory variables of the logistic regression model based on variables derived from LiDAR data and stand classification (<i>LOG Sachseln+</i>).	44

1. Introduction

Landslides pose a severe threat to infrastructure, agricultural land and even human life. Hence, accurate models are required to predict zones which are susceptible to landslide activity in a certain area and give a better understanding of landslide triggering factors (D'Amato Avanzi et al. 2004; Gorsevski et al. 2006; von Ruetten et al. 2011; Piacentini et al. 2012). Topographic, geomorphological and hydrological features are seen as primary factors controlling landslide susceptibility (e.g. Atkinson and Massari 1998; D'Amato Avanzi et al. 2004; Fernandes et al. 2004; Sidle 2006; Miller and Burnett 2007; Goetz et al. 2011). However, it is still controversially discussed how important the effect of vegetation and particularly forests is (Rickli and Graf 2009). Trees are expected to mechanically reinforce the soil (e.g. Abe and Ziemer 1991; Montgomery et al. 2000; Imaizumi et al. 2008; Bathurst et al. 2010; Kim et al. 2013) and positively influence its water household by interception, transpiration and improving soil permeability (e.g. Keim and Skaugset 2003; Gorsevski et al. 2006; Guns and Vanacker 2013). However, the surcharge from the weight of trees may decrease slope stability (Nilaweera and Nutalaya 1999). According to the Swiss federal recommendations for a sustainable protection forest, a small-scaled uneven-aged stand with high tree coverage and without large stand gaps best prevents landslides. Also important are tree species with a deep and intensive root penetration of the soil (Frehner et al. 2005). Despite the generally positive effect of trees on slope stability, six field inventories of rainfall triggered landslides in different regions in Switzerland show that landslide density in forest areas can be substantial. At one study site in St. Antoenien (canton of Graubunden), the amount of landslides in the forest even exceeded that in open land (Rickli and Graf 2009). For this reason, it can be concluded that not only the presence of forest plays an important role for slope stability, but also the forest structure (Schmidt et al. 2001; Rickli et al. 2002; Rickli and Graf 2009).

There are two main types of models which are used to detect landslide prone areas and the corresponding triggering factors: deterministic physically based and statistical models (e.g. Guzzetti et al. 1999; Vorpahl et al. 2012). Physically based models refer to physical processes and laws leading to slope failure (Montgomery and Dietrich 1994; Wu and Sidle 1995; Guzzetti et al. 1999). However, spatial information about the subsurface properties is often limited which is a clear disadvantage of physical approaches (Vorpahl et al. 2012). Statistical models are based on the assumption that future landslides will be triggered by the same factors as the observed ones. The landslide occurrence is the dependent variable which is related to a set of explanatory variables (Guzzetti et al. 1999). There is a wide range of different types of statistical models which are used for landslide susceptibility modelling, for example bivariate statistical approaches, discriminant function analysis, generalized linear models, classification trees, support vector machines and random forests (Guzzetti et al. 1999; cf. Brenning 2005; Vorpahl et al. 2012). The latter is a recent classification model combining a large number of tree predictors. It proved to be a robust classification method which keeps the bias low (Breiman 2001; Prasad et al. 2006). In this thesis, I applied generalized linear models, classification trees and random forests in combination with univariate statistics. The classifiers will be presented later in this work.

Explanatory variables are mostly extracted from aerial photos, elevation data, field measurements and thematic maps (Carrara et al. 2003; Carrara and Pike 2008). Elevation models constructed from LiDAR (Light Detection and Ranging) offer new opportunities to get comprehensive spatial information and reduce the cost of time-consuming field investigations (Lefsky et al. 2002; Liu et al. 2005; Dassot et al. 2011). They also facilitate the quantification of forest structures across large areas (Lefsky et al. 2002; Hyypä et al. 2008; Zellweger et al. 2013).

This master thesis is part of the project SOSTANAH of the National Research Programme NRP 68 “Soil as a Resource” (Graf et al. 2012). Its objective is to assess to what extent forest structure influences landslide occurrence. I therefore designed univariate and multivariate statistical models to predict landslide susceptibility which include variables describing forest structure along with geomorphological and topographic parameters. The term “landslide” is used for shallow landslides which are less than 2.0 m deep according to the Swiss recommendations (Lateltin 1997). Statistical models were calibrated with data from landslide inventories in St. Antoenien and Sachseln. Both are areas where a considerable amount of landslides was recorded in the forest (Rickli et al. 2002; Rickli and Graf 2009). The explanatory variables were measured in the field (St. Antoenien) and derived from elevation data constructed from LiDAR (St. Antoenien and Sachseln) and a stand classification (Sachseln). The following questions are to be addressed:

- Which factors are most determining for landslide activity based on statistical models for the two study areas St. Antoenien and Sachseln?
- Which forest structures have a positive influence on slope stability?
- Do the two study areas differ regarding landslide triggering factors?
- Are statistical models based on field data better performing than models based LiDAR derived variables?
- Do the statistical models differ regarding explanatory variables and model performance?

Based on these questions I hypothesise the following:

- In addition to terrain and hydrological factors, forest structure significantly influences slope stability.
- Landslide susceptibility declines with increasing tree coverage and decreasing gap size.
- Older and taller trees lead to a better root reinforcement and thus reduce landslide susceptibility.
- Forests with a vertically diverse structure and with a higher percentage of deciduous trees are less prone to landslides because they ensure better root penetration of all soil layers.
- Models predicting landslide susceptibility based on field variables are better performing than models based on LiDAR variables.
- The statistical method “random forests” achieve highest prediction accuracy compared to classification trees and logistic regression.

2. Methods

2.1. Study areas

The two study areas *St. Antoenien* and *Sachseln* (cf. Fig. 1) were chosen for this study because data from landslide inventories compiled by the Swiss Federal Institute for Forest, Snow and Landscape Research (WSL) in 1997 (*Sachseln*) and 2005 (*St. Antoenien*) were available for both sites. Additionally, more landslides occurred in the forest than in open land at *St. Antoenien*. A considerable amount of landslides was recorded also in forested areas of *Sachseln*. Hence, both areas are suitable to study the effect of forest structure on landslide occurrence. The two sites differ in their size and geology and the landslide inventories refer to two different rainfall events. Furthermore, the two sites have different forest composition: While a spruce dominated subalpine forest can be found in *St. Antoenien*, coniferous as well as deciduous stands at lower elevations occur in the study area of *Sachseln* (Rickli 2001; Rickli et al. 2008).

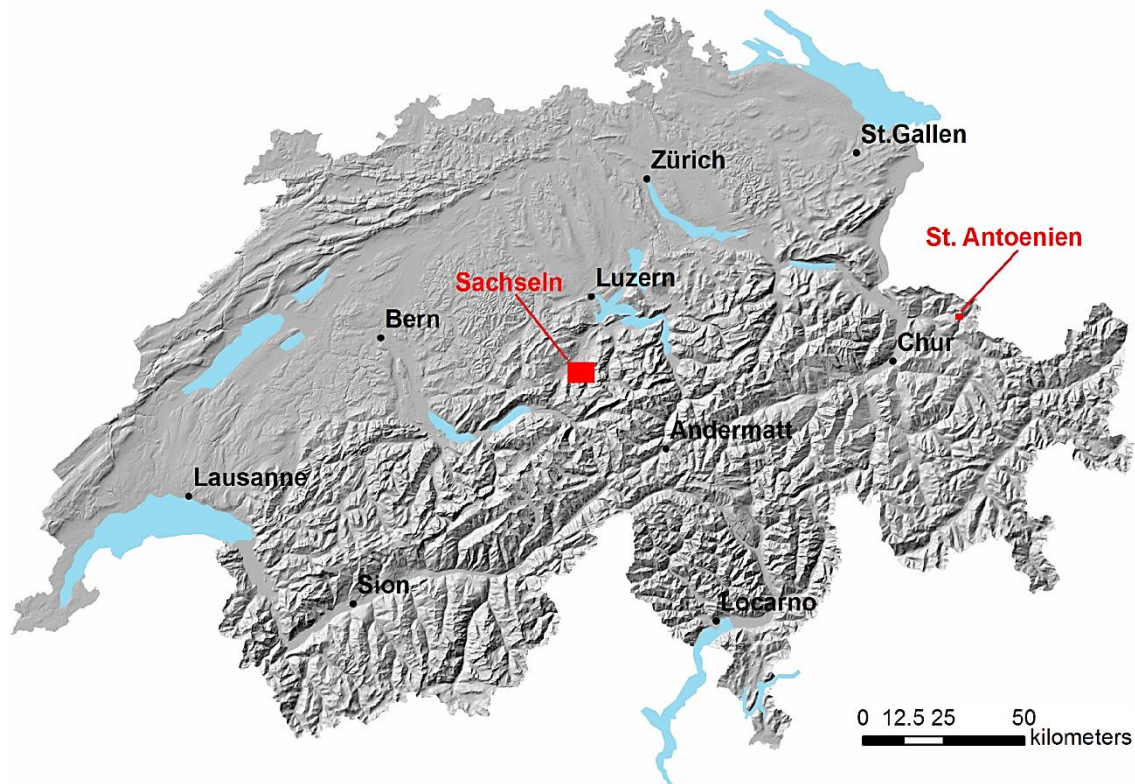


Fig. 1: Map of Switzerland with the two study areas *Sachseln* and *St. Antoenien*. The study areas (red rectangles) are drawn to scale.

2.1.1. *St. Antoenien*

The study area located in *St. Antoenien* (canton of Graubünden, Switzerland; cf. Fig. 2) has got a size of 0.77 km². It ranges from 1540 to 2000 m.a.s.l. and has got an average inclination of 31.2°. In about 3.0 % of the area, the geological unit *Praetigauer Flysch* can be found. In the other parts, till is dominant. After the heavy rainfall event of 2005, 36 shallow landslides were recorded in the forest (Rickli et al. 2008). This data set was complemented with eleven further landslides which were recorded during the

field investigation and which were not necessarily caused by the same rain event. Besides, 24 landslides were recorded in open land in 2005 (Rickli et al. 2008). The main triggering rainfall occurred from 21 to 23 August 2005. However, abundant precipitation had already fallen the days before. A precipitation level of 116.4 mm was measured in the village of St. Antoenien from 18 to 23 August 2005 (Rickli et al. 2008). The forest in the study area is dominated by spruce (*Picea abies*), accompanied by a few larches (*Larix decidua*) and rowans (*Sorbus aucuparia*). In the western part, stands mainly consist of strong timber. The eastern part is afforested (Rickli et al. 2008). A substantial area of the forest, especially in the western part, is pastured.

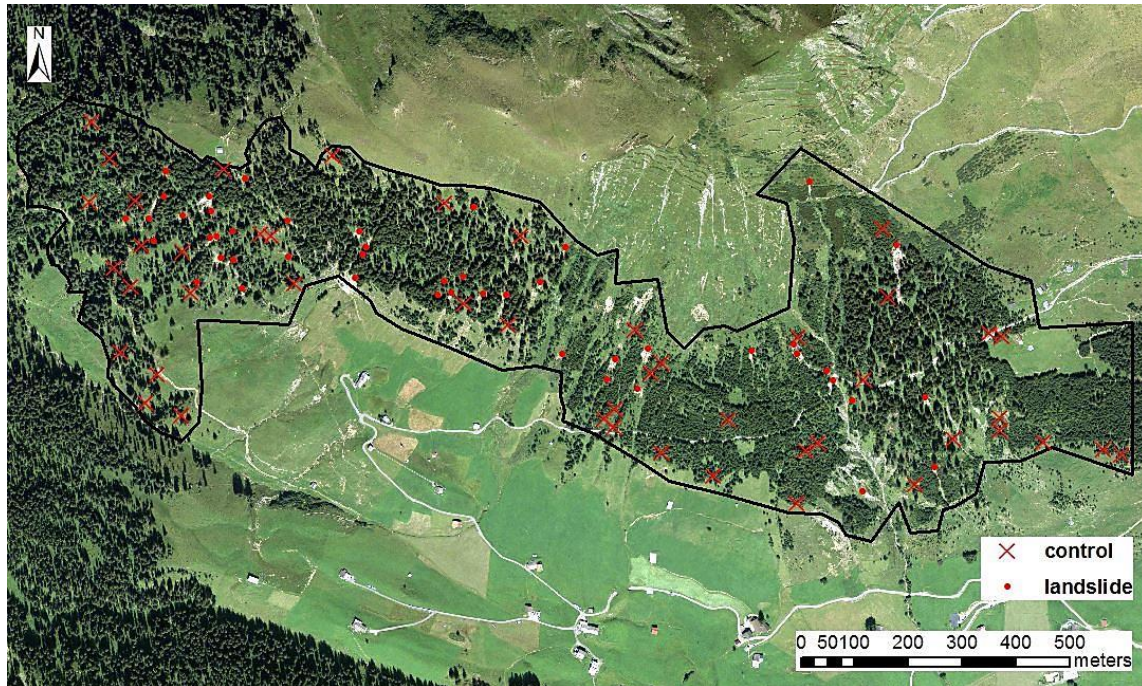


Fig. 2: Study area in St. Antoenien with landslide (dots) and control (crosses) points. Source: swissimage © 2014 swisstopo (5704000000)

2.1.2. Sachseln

The study area in Sachseln (canton of Obwalden, Switzerland; cf. Fig. 3) has got a size of 10.59 km² and ranges from 700 to 2000 m.a.s.l. with an average inclination of 36.07°. It comprises four hydrological catchment areas and is dominated by marly rocks (*Amdenermergel*, *Wildflysch*), sometimes in combination with limestone or sandstone. The landslide inventory of Sachseln was conducted after a heavy rainfall event in 1997. 136 landslides were recorded in forested area and 144 in open land (Rickli et al. 2002). The triggering precipitation fell within about two hours: On 15 August 1997, a severe thunderstorm accompanied by hail showers swept across the study area. The rainfall within these two hours was estimated at maximum 120 mm to 150 mm (Rickli 2001).

The forests at lower sites of the study area mainly consist of fir (*Abies alba*) and beech (*Fagus sylvatica*), whereby fir is highly underrepresented. At higher elevations, spruce dominates. The forest has been affected by several damaging effects, such as wind throw or infestations by bark beetles (Rickli 2001).

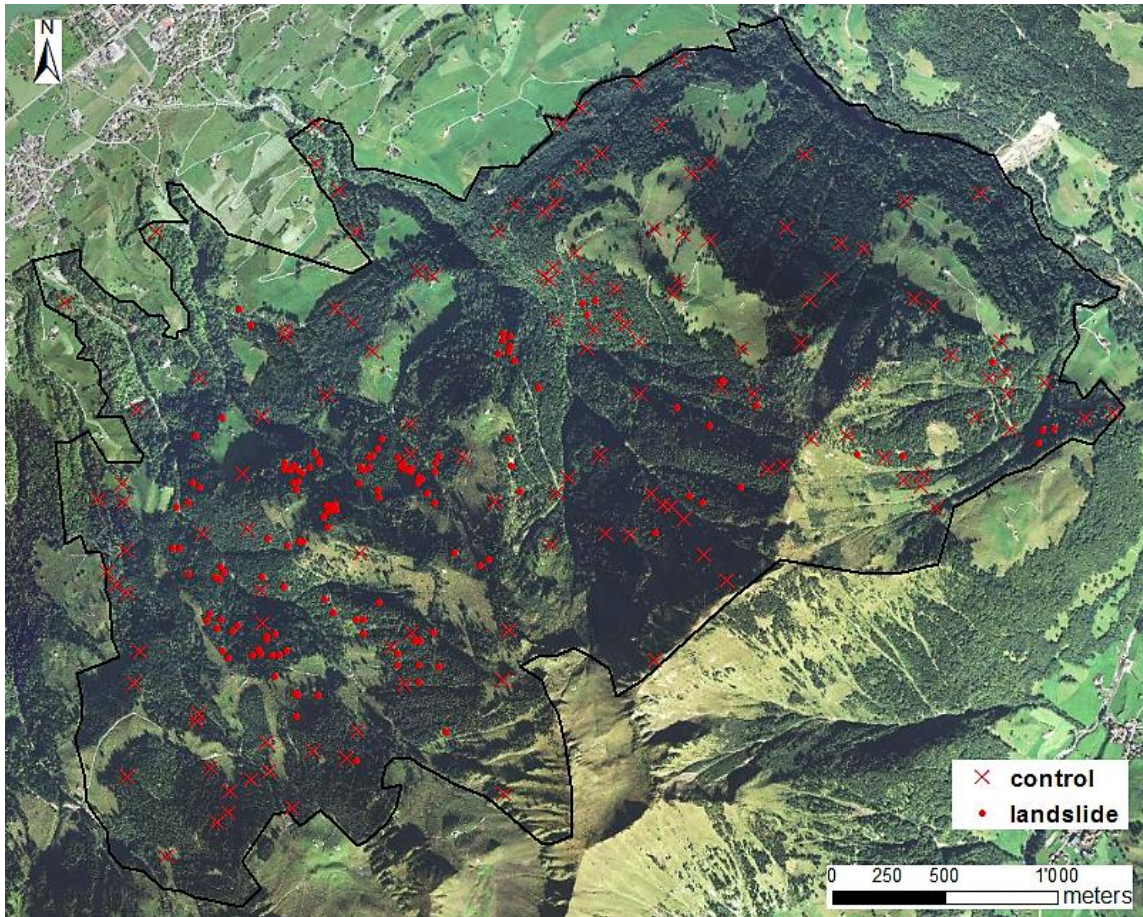


Fig. 3: Study area in Sachseln with landslide (dots) and control (crosses) points. Source: swissimage © 2014 swisstopo (5704000000)

2.2. Data

2.2.1. Landslide inventory

Two landslide inventories compiled by the Swiss Federal Institute for Forest, Snow and Landscape Research (WSL) in 1997 (Sachseln) and 2005 (St. Antoenien) provide the basis of this study (see further details in Rickli (2001) and Rickli et al. (2008)). The two inventories mainly consist of shallow landslides (maximum depth of 2 m) except for one landslide in St. Antoenien which was deeper and thus excluded here. I used all landslides where the vegetation was classified as forest. Apart from the position and the dimension of the landslides, the inventories also contain attributes describing soil, topography, hydrological conditions and vegetation. These will not be included in the statistical analysis presented in this study because they are only available for landslides and not for control points. The only exception constitutes a stand classification of the study area at Sachseln, which was extracted from existing forest classifications for the entire forest and used in the landslide survey. It contains information about the successional stage, the stocking level and the tree species mixture (Rickli 2001).

I complemented the inventory of St. Antoenien with eleven further landslides in the study area and re-measured the position of the landslides by GPS. For the analysis in Sachseln, landslide positions were taken over from the inventory. In total, the data set of St. Antoenien consists of 46 and that of Sachseln of 136 landslide points.

2.2.2. Geodata

Elevation data was used to extract terrain, hydrological and forest variables. Two digital elevation data sets constructed from LiDAR (Light Detection and Ranging) with a resolution of 2 m x 2 m were available (swisstopo 2014). The digital surface model (DSM) represents the elevation of the surface including vegetation and buildings. The digital terrain model (DTM), on the other hand, represents the elevation of the terrain without objects (Mathys 2005). The mean point density of the data is 1 point per 2 m² and the height accuracy 1.5 m in forested area (swisstopo 2014). The data was acquired in 2003 for St. Antoenien (before the landslide event). The area of Sachseln, however, was scanned nine years after the landslides, in 2006. Furthermore, orthophotos from 2003, 2005 and 2008 for St. Antoenien and from 1993, 1999 and 2013 for Sachseln served as verification data (swisstopo 2001).

2.3. Determination of control points

A set of control points where no landslides were recorded served as comparative data for the statistical analysis. As it can be expected that landslides do not occur at very flat or at especially densely forested slopes, the determination of control points was controlled by these two factors. First, I extracted the slope angle and tree coverage at the landslide points from 2005 in St. Antoenien from elevation data using a geographic information system (GIS; for further details see chapter 2.5). The slope angle varied between 20.01° and 49.79° (mean = 32.66°) and tree coverage between 0.00 % and 84.00 % (mean = 44.65 %). These values slightly differ from the values presented in the results of this thesis (cf. chapter 3.1) because the landslide data set was complemented and new coordinates were recorded. According to the ranges of the slope angle and the tree coverage of the landslides, I decided to cut the tree coverage at the 15 %- and the 85 %-quantile and hold it for the control plots in the corresponding range between 15 % and 70 %. The slope angle of the control points was hold between 20° and 50° which represents the whole range of the slope angle at landslide points. The area which meets these criteria was determined and 90 points were randomly set therein. Subsequently, I verified their suitability on an orthophoto and in the field. Points which were less distant than 30 m to a landslide or another control point were not considered. The same applied to control points which corresponded to landslides that are not included in the inventory of 2005. In this case, they were recorded as landslide points. Finally, I recorded 47 control points in St. Antoenien. The same method was applied to determine the control points in Sachseln. This resulted in 136 control points with a minimum distance of 30 m to each other and to the landslide points and a slope angle between 20° and 55° and tree coverage between 20 % and 70 %.

2.4. Field investigation

At each point location of a landslide in St. Antoenien as well as at the control points, I measured a set of variables which are expected to affect slope stability (cf. Tab. 1). I selected them according to the Swiss federal recommendations for a sustainable protection forest (Frehner et al., 2005) and other literature (cf. Tab. 1). The variables describing forest structure, geomorphology, hydrology and land use were assessed in an area of 30 m x 30 m around the (potential) release point. In landslide plots, the release point was defined as the middle of the landslide scar. The potential release point in control plots corresponds to the control points determined by GIS analysis (see chapter 2.3). Additionally, at each (potential) release point, the height above sea level, the exposition and the coordinates were recorded with a GPS device. Fig. 4 shows an example of a landslide (left) and control (right) plot.



Fig. 4: Landslide (left) and control (right) plot in St. Antoenien.

Tab. 1: Variables assessed in landslide and control plots (30 m x 30 m) in St. Antoenien.

Variable	Definition	Method	Expected effect on landslide activity
Slope angle	Slope angle at the (potential) release point, 15 m above and 15 m below	Measurement with an inclinometer with a precision of 2°	Gravitational driving forces increase with the slope angle (e.g. Vorpahl et al. 2012).
Geomorphology type	Geomorphology type after Rickli and Bucher (2003), describing the different landforms	Assessment of the dominant landform type according to the curvature in the line of slope and perpendicular to it	The geomorphology type influences acceleration / deceleration and convergence of water flow (Cha and Kim 2011).
Maximum tree height	Height of the highest tree in the plot	Measurement with a laser meter	The taller (and older) the trees the better the root penetration (Waisel et al. 2002).
Successional stage	Percentage of different dbh (diameter at breast height) classes and regeneration (Keller 2005)	Estimation in steps of 5 % for the dbh classes 13-30 cm, 30-50 cm, >50 cm and the regeneration (young growth (<40 cm height), thickening (40 cm height – 12 cm dbh))	Older (thicker) trees lead to a better reinforcement of the ground / multi-age forests ensure a better root penetration (Frehner et al. 2005).
Coverage in the stand layer	Share of different layers in tree coverage (Keller 2005).	Estimation in steps of 5 %, sub layer = 0.40 m – 1/3 x maximum height, middle layer = 1/3 – 2/3 x maximum height, upper layer = 2/3 x maximum tree height – maximum tree height	Multi-layered forests ensure a better root penetration (Frehner et al. 2005).
Tree coverage	Percentage of area covered by trees taller than 3 m (Keller 2005).	Estimation in steps of 5 %	A high canopy cover leads to higher interception and enhanced root penetration (Keim and Skaugset 2003; Frehner et al. 2005).
Deadwood	Distance between the (potential) release point and the nearest deadwood; state of the deadwood; percentage of lying and standing deadwood	Measurement of distance, estimation of the coverage of lying and standing dead wood in the categories: <1 %, 1-5 %, 5-20 %, >20 %	Landslide plots are expected to have a higher percentage of deadwoods, as the penetration of decaying roots decreases (e.g. Gray 1996; Preti 2013).
Ground vegetation coverage	Area covered by ground vegetation (h ≤ 1.3 m) (Keller 2005).	Estimation in the field in steps of 10 %	Ground vegetation enhances the reinforcement of the ground (Reubens et al. 2007).

Tree species	Dominant tree species, if else than <i>Picea abies</i>	Estimation in the field	The shallow roots of <i>P. abies</i> reinforce the ground worse than other trees (Frehner et al. 2005).
Stand gaps	Gap length and width of the largest gap in a plot	Estimation in meters. Gaps with a minimum width of half a tree length are considered.	In stand gaps, the stabilizing effect of roots is missing (e.g. Casadei et al. 2003).
Forest state	Forest state categories according to Rickli (2001)	<p>W1 ("relatively good forest state"): successional stage ≠ thickening, gaps ≤ 20 %</p> <p>W2 ("relatively bad forest state"): successional stage ≠ thickening, gaps ≥ 20 % and ≤ 70 %</p> <p>W3 ("very bad forest state" / damaged area): successional stage = thickening or gaps ≥ 70 %</p>	Landslides occur mainly in forest stands which are in a bad state according to Rickli (2001).
Distance to the 5 nearest trees	Distance between the (potential) release point and the 5 nearest trees and their dbh class	Measurement in the field	The smaller the distance to the next trees, the better the root penetration at the (potential) release point.
Root penetration	Product of dbh class (13-30 cm = 3, 30-50 cm = 2, >50 cm = 1) and distance between the tree and the (potential) release point.	Calculation with data assessed in the field (diameter class / distance to release point)	A high root penetration is expected, if the proxy-variable is small.
Old landslides	Signs of old soil movements (e.g. landform, tree growth)	Assessment in the field in the categories: <i>no, vague, high</i>	Landslides are expected to occur in areas which were already affected by slope instabilities (Rickli et al. 2008).
Hydrology	Signs of water logging / slope water discharge	Assessment in the field in the categories: <i>no, vague, high</i>	Landslides are more frequent at wet soils (e.g. Vorpahl et al. 2012).
Soil compaction	Signs of soil compaction (standing water, lanes)	Assessment in the field in the categories: <i>no, vague, high</i>	Compaction decreases the water permeability and enhances the risk of landslides (Rickli et al. 2008).
Grazing	Signs of grazing / agricultural land use (track ways of cows, cows, fences)	Assessment in the field in the categories: <i>no, weak, intensive</i>	Trampling by cattle enhances the risk of landslides (Rickli et al. 2008).

2.5. Analysis of LiDAR data

With the two digital elevation models generated by LiDAR (cf. chapter 2.2.2), I computed several parameters characterising forest structure, terrain and hydrological conditions. Most of them correspond to parameters assessed in the field. The raster data were processed in a geographic information system (GIS; software ESRI ArcGIS 10.2). The parameters were calculated either with a resolution of 2 m (e.g. slope angle) or 30 m (analogous to the size of the study plots) and then extracted for landslide and control points.

2.5.1. *Tree height*

In a first step, the so called canopy height model (CHM) was calculated. This was done by subtracting the digital terrain model (DTM) from the digital surface model (DSM). The CHM represents the height of above ground features like vegetation or buildings. As there are no non-vegetative structures in the study area in St. Antoenien, it was not necessary to differentiate between houses and trees. In Sachseln, however, buildings had to be removed from the CHM (dataset Vector25, swisstopo 2013). Furthermore, I set negative height values zero, assuming them to be measurement errors. Subsequently, I computed the maximum and the mean tree height, which are an indicator of forest age (Hediger 2012), in a moving window with a size of 30 m x 30 m. In order to avoid noise from topography, only vegetation with a minimum height of 1 m was considered. Moreover, the standard deviation of the vegetation height (from 1 m on) was calculated. The latter is assumed to give an idea about the diversity of the vertical structure (Hediger 2012).

2.5.2. *Tree coverage*

The raster cells of the CHM were split into stocked cells with a vegetation height of minimum 3 m and unstocked cells. The same threshold is applied in the Swiss Forest Inventory (Ginzler et al. 2005). Finally, the proportion of stocked cells was computed in a moving window with a size of 30 m x 30 m.

2.5.3. *Gap length*

In order to identify forest gaps, I implemented the method of Koukoulas and Blackburn (2004) with slight adaptations. First, the unstocked cells were determined applying a threshold of 3 m to the CHM. Following this, the gap raster was resampled to a cell size of 1 m and shrunken by one, three and five cells in order to isolate individual gaps from the interconnected raster cells. The resulting rasters were converted to polygons. All polygons with a low area-perimeter ratio were removed. The thresholds for the area-perimeter ratio were chosen following Koukoulas and Blackburn (2004) and by manually selecting polygons. I set them to 1.0 for polygons shrunken by one cell, 0.5 for polygons shrunken by three cells and 0.67 for polygons shrunken by five cells. Subsequently, all polygons shrunken by one or three cells which completely contained a polygon shrunken by five cells were excluded. As the remaining polygons were initially shrunken and did not represent the whole extension of the gaps, a buffer

according to the number of shrunken cells was added. Finally, the polygons were merged and gaps bigger than 20'000 m², which can be considered as open land, were removed (Temperli 2006).

In a next step, I reconverted the resulting polygons to a raster with their identification numbers as raster values and summed them up with the DTM. Following this, the maximum and the minimum value of each gap was identified and finally subtracted from each other. The resulting raster corresponds to the elevation difference between the highest and the lowest point in a gap. These height differences were divided by the sinus of the mean slope angles of the gaps in order to get the gap lengths. The detailed model implemented in ESRI ArcGIS 10.2 can be found in Appendix C3.

2.5.4. *Tree layers*

Before the different tree layers could be determined, the single tree crowns or tree groups, respectively, had to be delineated (cf. Appendix C2). This was done by inverse watershed segmentation, a commonly applied method to determine individual trees, which segments the inverted CHM into “catchment basins” associated with tree crowns (e.g. Andersen 2009; Edson and Wing 2011). First, I isolated the vegetation with a minimum height of 1 m from the CHM in order to exclude noise from the topography. The resulting forest raster was inverted and smoothed. Subsequently, the local minima (tree peaks / peaks of tree groups) and their respective watersheds were determined (tools *Flow Accumulation* and *Watershed* in ESRI ArcGIS 10.2). The watersheds correspond to the crowns of the trees and were finally assigned to a tree layer according to their height. I differentiated between the sub layer (1 m – 1/3 x maximum tree height), the middle layer (1/3 x maximum tree height – 2/3 x maximum tree height) and the upper layer (2/3 x maximum tree height – maximum tree height) (Keller 2005).

2.5.5. *Distance to the nearest tree*

From each landslide and control point, the distance to the nearest tree peak was calculated. The ArcGIS tool *Path Distance* was used, which accommodates for the real surface distance (ESRI 2013). How the individual trees were delineated is described in chapter 2.5.4 (see also Appendix C2).

2.5.6. *Topography*

I computed the slope angle for each cell based on the algorithm by Burrough and McDonnell (1998), which considers the largest height difference between the cell and its eight neighbours. Subsequently, I averaged the slope angle for an area of 30 m x 30 m. Furthermore, the curvature of the DTM was calculated. The curvature is the second derivative of the surface and is fitted through the cell and its eight surrounding neighbours (Zevenbergen and Throne 1987). It controls the direction, acceleration and deceleration of the water flow (Cha and Kim 2011; von Ruetten et al. 2011). Two curvature types are distinguished: The profile curvature is in the direction of the maximum slope angle and the plan curvature is perpendicular to the direction of the maximum slope angle. A positive profile curvature indicates an upwardly convex, a

negative profile curvature an upwardly concave surface. A positive plan curvature indicates an upwardly concave, a negative plan curvature an upwardly convex surface (Peckham 2011).

2.5.7. *Weighted Topographic Wetness Index*

The *Topographic Wetness Index* (TWI) is a measure derived from topography to estimate the moisture of a site. It is calculated from the local upslope contributing area of a cell (a) and its inclination (β) according to the following equation:

$$TWI = \frac{\ln(a)}{\tan(\beta)}$$

A high TWI corresponds to a high potential moisture based on topography (Sørensen et al. 2006). In this study, the so-called *weighted Topographic Wetness Index* (wTWI) according to Ma et al. (2010), was applied. In this extended version of the TWI, the exposition and the topographic position are included as weighting factors. More importance is given to northern (shadowy) expositions as well as valleys compared to southern (sunny) expositions and ridges. The wTWI was calculated with a resolution of 2 m x 2 m and then averaged for an area of 30 m x 30 m (cf. Appendix C5).

2.6. Verification of data actuality and accuracy

One major problem I faced in this study was the actuality and accuracy of the data. The field investigations at St. Antoenien were made eight years after landslide occurrence and it cannot be ruled out that the landslides substantially changed the forest structure, for example by removing trees. Especially tree coverage, the distance to the nearest tree and the gap size could have been influenced by landslides. In order to be sure that the post hoc assessment is still representative for the situation before the event, orthophotos before (2003) and after (2005) the landslides were compared. I assessed whether there was a considerable change in tree coverage. Furthermore, the distance from the release point to the nearest tree was measured on the orthophoto of 2003 and then compared to the distances measured in the field.

The question of actuality also rises for the LiDAR derived variables. As the elevation data of St. Antoenien were raised in 2003, it can be assumed that it well represents the situation before the landslides. For Sachseln, however, elevation data were only available for 2006, meaning nine years after the landslide event. Thus, the forest canopies before and after the landslides were also compared at each landslide point. Orthophotos were available for the years 1993 and 1999.

Besides changes in the forest structure caused by slope movements, vegetation naturally evolved between the events and the present survey. However, these changes can be regarded as marginal because the study area at St. Antoenien belongs to the subalpine and that at Sachseln to the montane and subalpine vegetation zones, where vegetation develops rather slowly (Frehner et al. 2005). Moreover, vegetation changed at landslide as well as at control plots why the differences between both should not be influenced significantly.

2.7. Statistical analysis

In a first step, the data were analysed univariately. For each of the variables measured in the field or derived from LiDAR, it was assessed whether there is a significant difference between landslide and control plots with the *Wilcoxon rank-sum test* (continuous variables) or the *Chi-squared test* (categorical variables) and *logistic regression*. The Wilcoxon rank-sum test is a non-parametric test used to test the hypothesis that two samples come from distributions with the same mean. It is a robust alternative to the t-test in the case that the assumption of normally distributed data is not met (Dalgaard 2008). The Chi-squared test (X^2 test) is also a distribution-free test which can be applied to nominal as well as categorical data. Logistic regression (LOG; see also chapter 2.7.1) is a widely used method to describe the relationship between a discrete (here a binary) outcome variable and one or more independent (or explanatory) variables (Hosmer and Lemeshow 2000). Although the error terms from the logistic model are not assumed to be normally distributed, it is not non-parameteric (or distribution-free), as a binomial distribution is specified for the response variable (Moore and McCabe 2005).

Besides the univariate tests, multivariate statistics were applied in order to analyse several explanatory variables simultaneously. Three different models, namely logistic regression, classification tree and random forest, were used and are described hereafter. All statistical analyses were performed within the open-source data analysis environment R (R Development Core Team 2012).

2.7.1. Logistic regression

As outlined above, logistic regression (LOG) is a suitable method to model binary outcome variables and is one of the most frequently used techniques in landslide susceptibility modelling (e.g. Atkinson and Massari 1998; Dai and Lee 2002; Ayalew and Yamagishi 2005; Brenning 2005; von Ruetten et al. 2011; Vorpahl et al. 2012). Opposite to simple linear regression, probabilities are modelled on a transformed scale so that only values between zero and one are predicted. The model can be set up as:

$$\text{logit } p_i = \beta_0 + \beta_1 x_1 + \beta_2 x_2 + \dots + \beta_k x_k$$

where $\text{logit } p_i$ is the logistic link function $\log[p_i/(1-p_i)]$ and p_i the probability associated with a given observation i . β_0 is the intercept of the model, the k β_i are the regression coefficients and the k x_i the independent variables. An important difference to linear regression is the conditional distribution of the outcome variable, as there is no error term. The β coefficients were estimated based on maximum likelihood (Hosmer and Lemeshow 2000; Dalgaard 2008).

The final logistic regression models were determined using stepwise backward variable selection with the aim to minimize the *Akaike Information Criterion* (AIC). The quality of the models was examined with customary residual diagnostic plots (Stahel 2013; cf. Appendix E). The plots did not indicate any need for transformation of the data.

2.7.2. Classification and regression tree

Classification and regression trees (CT) are a non-parametric regression approach which recursively partitions the space spanned by all explanatory variables. At each node, the data is split into two groups based on a single predictor (Vorpahl et al. 2012). The splitting variable is selected aiming at impurity reduction. This means that daughter nodes have to be as homogeneous (“pure”) as possible. CT have been applied in landslide susceptibility modelling by a few authors (e.g. Nefeslioglu et al. 2010; Yeon et al. 2010; Felicísimo et al. 2012). They have the advantage that predictor variables and interactions among them are easily interpretable (De'Ath and Fabricius 2000).

We performed conditional inference trees, using the *ctree* function of the *party* package in the statistical software R (Hothorn et al. 2013). In order to avoid overfitting, the value of the test statistic that must be exceeded in order to implement a split (the so-called *mincriterion*) was held at 0.95. This means that the p-value must be smaller than 0.05 to split a certain node (Hothorn et al. 2013).

2.7.3. Random forest

A random forest (RF) is a combination of tree-structured classifiers where each tree depends on the values of a random vector of predictor variables sampled independently (Breiman 2001). The random selection of splitting variables allows “weak” predictor variables to enter the collection of trees. After a large number of trees have been generated, the predictions of individual trees need to be combined. Each tree returns a predicted class for a certain subject and the class most trees “vote” for is returned as the prediction of the classifier (Breiman 2001; Strobl et al. 2009). In order to learn which explanatory variables are most predictive in the RF, their importance can be calculated. This is done by randomly permuting the values of a predictor variable, so that its original association with the response is broken. The difference in prediction accuracy before and after the permutation of the variable denotes its importance (so-called permutation accuracy importance; Strobl et al. 2009). We implemented the conditional permutation scheme after Strobl et al. (2008), which leads to more reliable results if predictor variables are correlated. Their importance is computed by permuting within a grid which is defined by the covariates associated to the variable of interest (see Strobl et al. 2008 for further details). A distinct advantage of random forests is that they do not overfit the data because a large number of trees are grown (Prasad et al. 2006; Strobl et al. 2009). In landslide susceptibility modelling, however, they have rarely been used (Vorpahl et al. 2012; Catani et al. 2013).

Random forest models were implemented utilizing conditional inference trees as base learners in the *cforest* function of the *party* package in the statistical software R (Hothorn et al. 2013). The number of input variables randomly sampled as candidates at each node (*mtry*) was integrated as a tuning parameter and the model with the best performance was finally chosen.

2.7.4. *Explanatory variables*

Variables compiled during the field investigation in St. Antoenien as well as variables derived from LiDAR data were used as explanatory variables. For St. Antoenien, models were first fitted based on topographic, geomorphological and hydrological field variables. In a next step, the set of explanatory variables was complemented with forest variables and finally, models were fitted based on LiDAR derived variables. For Sachseln, models were fitted on the one hand with LiDAR derived variables and on the other hand with LiDAR derived variables in combination with variables from the stand classification. In order to avoid over-fitting, only variables which had a significant effect on slope stability in the univariate analysis were used for logistic regression and classification trees. In case that two of the corresponding variables were substantially correlated (cf. correlation diagrams in Appendix B), only the variable with the lower p-value in the univariate analysis or the variable which led to a better model performance was considered. I regarded variables as substantially correlated if the correlation coefficient (*Spearman* correlation) was greater or equal 0.4, which is a moderate correlation according to Dancey and Reidy (2011). Random forests, however, were fitted with all variables regardless of their significance in the univariate analysis because they are more resistant against overfitting (Breiman 2001; Strobl et al. 2009).

2.7.5. *Model calibration and validation*

The multivariate models were calibrated for the landslide data of St. Antoenien and Sachseln using different sets of explanatory variables (cf. chapter 2.7.4). Due to the relatively small data basis of St. Antoenien, it was decided to use all data for calibration (in St. Antoenien as well as in Sachseln). The performance of the model was tested on the training data set (all data). As ROC curves (cf. chapter 2.7.6) generated for the calibration data tend to be too optimistic (e.g. Steyerberg et al. 2001; Leathwick et al. 2006), three times repeated 10-fold cross-validation was accomplished and the average performance across the hold-out predictions was calculated. In cross-validation, a small proportion of the data set (in our case one-tenth) is removed when building the model and subsequently used as testing set (Hastie et al. 2008; Starweather 2011).

2.7.6. Receiver Operating Characteristic

Receiver Operating Characteristic (ROC) curves were used to compare the predictive performance of the different models. ROC curves indicate the ability of a model to discriminate between positives (here landslides) and negatives (here control points) (Zweig and Campbell 1993; Leathwick et al. 2006). The so-called *True Positive rate* (correctly classified positives / total positives) is plotted against the *False Positive rate* (incorrectly classified negatives / total negatives) (Fawcett 2003). The area under the ROC curve (AUC; Hosmer and Lemeshow 2000) serves as measure of the model performance. A value of 0.5 indicates that the discrimination is completely random, while a value of one indicates that negatives and positives are perfectly discriminated (Leathwick et al. 2006). According to Hosmer and Lemeshow (2000), an AUC value of 0.7 is an acceptable and 0.8 an excellent discrimination.

3. Results

3.1. Univariate analysis

3.1.1. St. Antoenien field data

The slope angle measured in the field is significantly higher in landslide than in control plots ($p^1 = 0.001$; cf. Fig. 5) although the slope angle of control plots was controlled (cf. chapter 2.3). Most of the landslides have a slope angle between 40° and 60° , whereas the slope angle in control plots mainly ranges between 20° and 40° . No significant differences were found for slope angles 15 m above and below the release point. However, landslide and control plots significantly differ in their geomorphology ($p = 0.003$; cf. Fig. 6). The geomorphology types 2, 3, 7 and 8 (after Rickli and Bucher 2003) are more frequent in landslide than in control plots. Significant differences were also found for hydrological features. Landslide plots show more frequent signs of slope water discharge ($p = 0.016$) and are more prone to high or vague water logging ($p = 0.010$). Graphs of these variables as well as of other variables which are not illustrated here can be found in Appendix D.

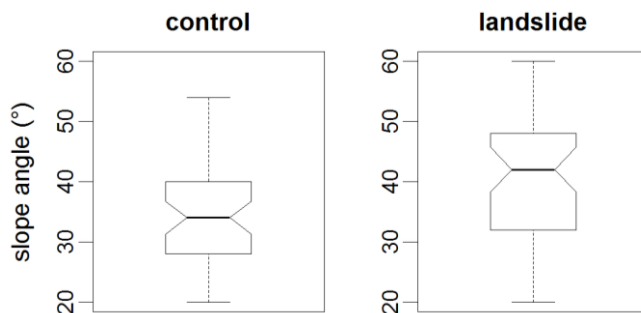


Fig. 5: Distribution of slope angles measured at control (left) and landslide (right) points in St. Antoenien. The slope angle is significantly higher in landslide plots.

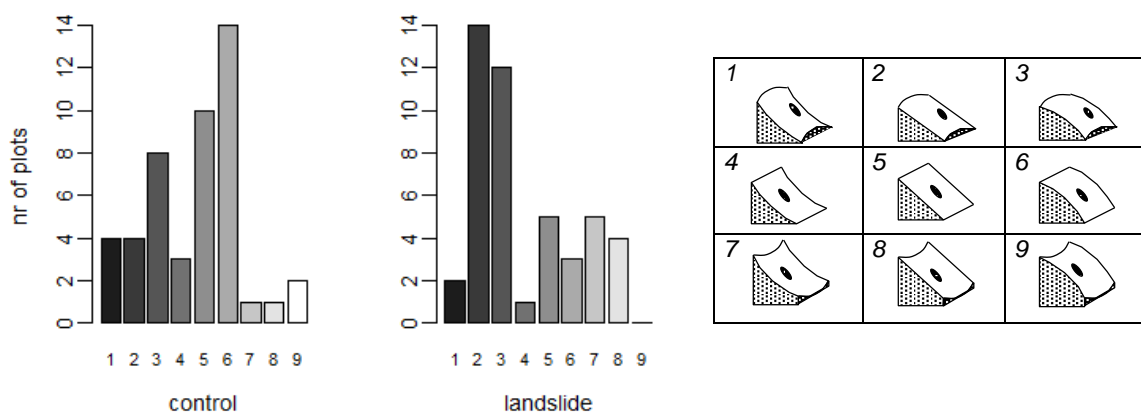


Fig. 6: Number of plots per geomorphology type after Rickli and Bucher (2003) (explanation on the right) in control and landslide plots (significant difference).

¹ P-values reported in brackets correspond to the Wilcoxon rank sum test for continuous or the Chi-squared test for categorical data. P-values higher than 0.05 are considered as significant.

Analogous to the slope angle, the tree coverage estimated in the field is significantly lower in landslide than in control plots despite controlling this factor ($p = 0.001$; cf. Fig. 7). The mean tree coverage in control plots is 48.09 % and in landslide plots 36.20 %. The comparison of the orthophotos from 2003 and 2005 revealed for 27.3 % of the landslide plots a decrease in tree coverage. A significant difference could also be observed for gap length ($p < 0.001$; cf. Fig. 8). The largest gap is on average longer in landslide than in control plots. This does not account for gap width where control and landslide plots do not differ significantly. Because gap length is correlated with tree coverage (*Spearman* correlation coefficient = 0.42), only gap length was used as explanatory variable for the logistic regression model and the classification tree.

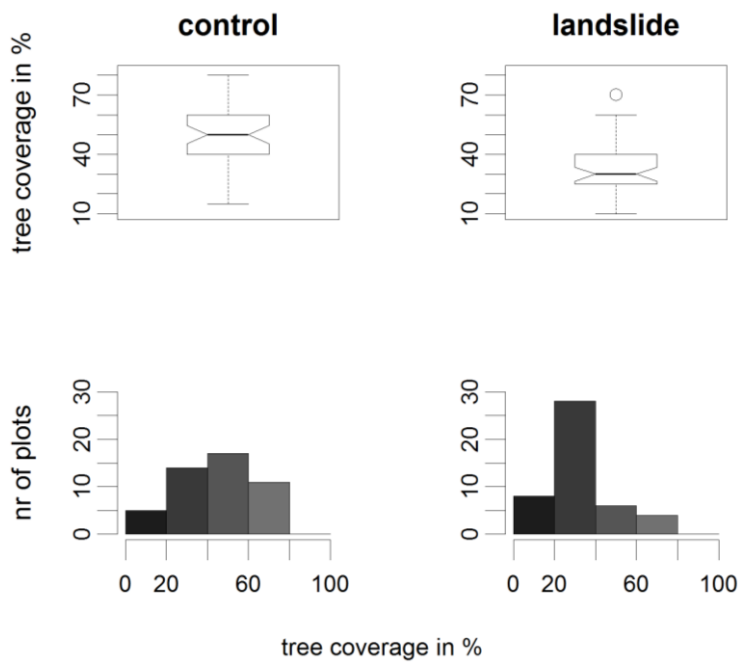


Fig. 7: Boxplot (above) and barplot (below) of tree coverage values estimated in control (left) and landslide (right) plots in St. Antoenien (significant difference).

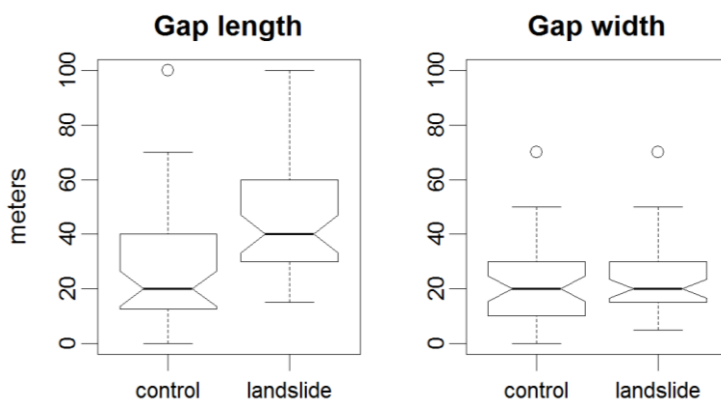


Fig. 8: Distribution of lengths (left; significant) and widths (right; not significant) of the largest gaps in control and landslide plots.

The mean distance from the (potential) release point to the five nearest trees as well as the distance to the nearest tree is in landslide plots significantly higher than in control plots ($p = 0.001$; $p = 0.002$; cf. Fig. 9). The same result was obtained for the distance measured on the orthophoto of 2003 ($p = 6.04 \cdot 10^{-4}$; cf. Fig. 9). Moreover, the distances to the nearest tree on the orthophoto do not significantly differ from the distances measured in the field. The proxy-variable for root penetration of the nearest tree and the five nearest trees is significantly higher in landslide than in control plots ($p = 7.72 \cdot 10^{-4}$; $p = 8.91 \cdot 10^{-5}$; cf. Fig. 10). This means that root penetration is expected to be higher in control plots. As the variable for root penetration is deduced from the distance to the nearest tree, only root penetration was considered in the multivariate analysis.

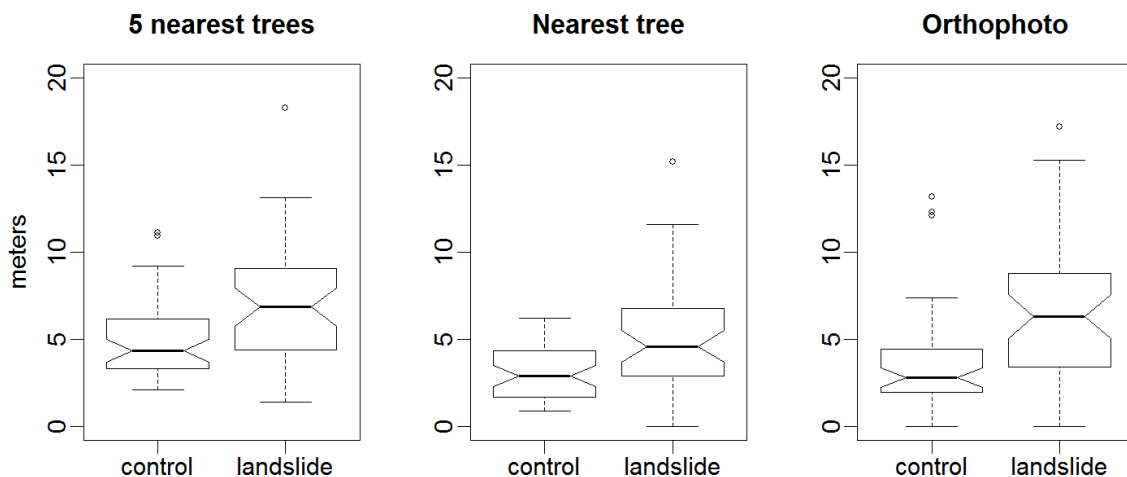


Fig. 9: Distribution of the mean distance to the 5 nearest trees (left) and the distance to the nearest tree measured in the field (middle) as well as on the orthophoto. All variables show significant differences.

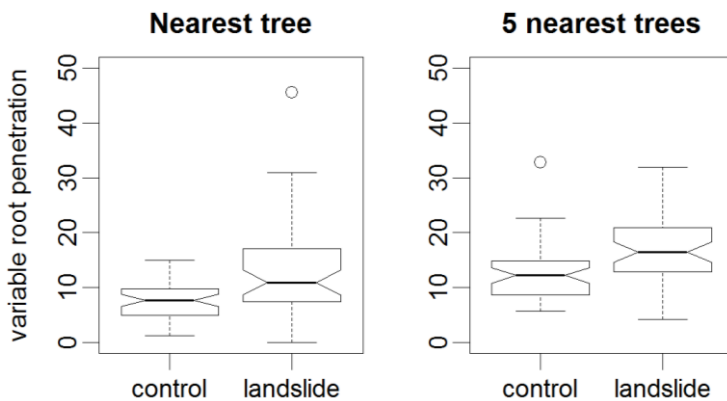


Fig. 10: Distribution of the proxy-variable for root penetration of the nearest tree (left) and the five nearest trees (right). The higher the value of the variable, the lower is the root penetration expected. Differences are for both variables significant.

On the other hand, no significant difference could be detected for the maximum tree height and the successional stage (cf. Fig. 11). The percentage of trees with a dbh between 30 and 50 cm is considerably higher in landslide plots, but not significantly according to the Wilcoxon rank sum test ($p = 0.052$). However, a significant p-value resulted from logistic regression ($p = 0.035$). For the dbh classes 13 to 30 cm and > 50

cm, only slight differences were found. The percentage of regeneration did not differ distinctly between landslide and control plots, too.

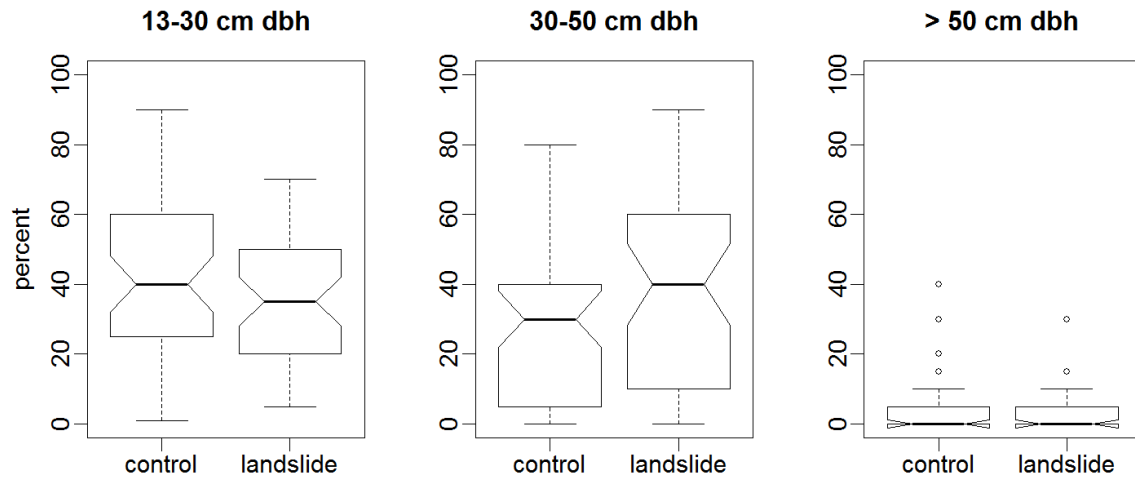


Fig. 11: Distribution of the estimated percentage of trees in the different diameter classes (13-30 cm dbh (left), 30-50 cm dbh (middle), > 50 cm dbh (right)) in control and landslide plots (no significant difference).

Forest stands also showed no significant difference concerning their vertical structure. Landslide as well as control plots are mainly single-layered (coverage of the sub and middle layer < 20 %). Tree coverage of the sub and the middle layer only slightly differs between landslide and control plots, whereas the coverage of the upper layer is significantly higher in control plots ($p = 0.002$). It should be mentioned, however, that this value is highly correlated with tree coverage (*Spearman* correlation coefficient = 0.84), as the coverage of the lower layers is nearly zero. Therefore, the variable was not considered in logistic regression and the classification tree. The forest state in landslide as well as in control plots was predominantly classified as “relatively” or “very bad” (categories W2 and W3 after Rickli (2001)). Consequently, no significant difference was found although there are slightly more control plots with a “relatively good” forest state. Furthermore, landslide and control plots do not significantly differ regarding ground vegetation coverage, amount and type of deadwood, soil compaction, signs of old landslides and grazing. Tab. 2 summarises the p-values of all significant variables assessed in the field.

Tab. 2: Variables assessed in the field which significantly affect landslide occurrence in St. Antoenien and the corresponding p-values of the Wilcoxon rank sum test (continuous variables), the Chi-squared test (categorical variables) and logistic regression (LOG). The effect of the continuous variables on landslide susceptibility is indicated with + (increase in the variable leads to an increase in landslide susceptibility) and – (increase in the variable leads to a decrease in landslide susceptibility).

	Wilcoxon-Test	X²-Test	LOG
Slope angle (+)	0.001		0.002
Geomorphology type		0.003	0.001
Tree coverage (-)	0.001		0.002
Gap length (+)	$5.195 \cdot 10^{-6}$		0.0002
Mean distance 5 nearest trees (+)	0.001		0.002
Distance nearest tree (+)	0.002		0.002
Distance nearest tree orthophoto 2003 (+)	$6.035 \cdot 10^{-4}$		0.002
Proxy-variable root penetration nearest tree (+)	$7.721 \cdot 10^{-4}$		0.002
Proxy-variable root penetration 5 nearest tree (+)	$8.906 \cdot 10^{-5}$		0.001
Water logging		0.010	0.009
Slope water discharge		0.016	0.009
Coverage upper layer (-)	0.002		0.003

3.1.2. St. Antoenien LiDAR data

In general, slope angles derived from elevation data are lower than slope angles measured in the field. Analogous to the results from the field data, the slope angle at the (potential) release point calculated with the DTM is significantly higher in landslide than in control plots ($p = 0.019$; cf. Fig. 12 and Fig. 18). The same accounts for the mean slope angle in the study plots (30 m x 30 m), where the difference is even more pronounced ($p = 7.519 \cdot 10^{-4}$, cf. Fig. 12). The two variables are highly correlated (*Spearman* correlation coefficient = 0.71) and therefore, I only included the mean slope angle in logistic regression and the classification tree.

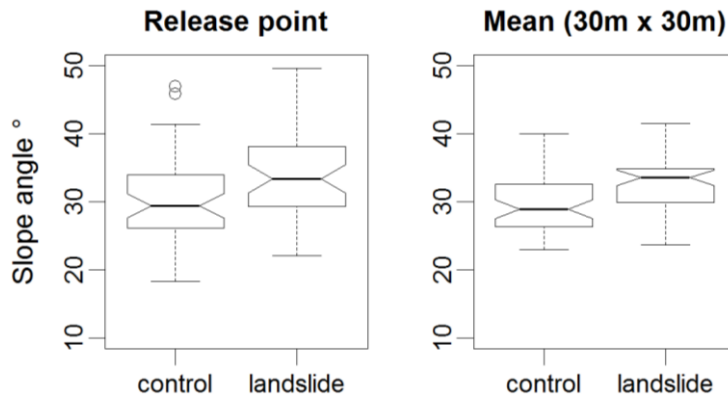


Fig. 12: Distribution of LiDAR derived slope angles at the release point (left) and averaged over an area of 30m x 30m (right) in control and landslide plots in St. Antoenien. The differences between control and landslide plots are significant.

Significant differences were also found for the curvature as well as the profile and plan curvature averaged for an area of 30 m x 30 m ($p = 0.003$; 0.009; 0.008; cf. Fig. 13). The curvature and the plan curvature are on average lower in landslide plots, meaning that the slope is more concave. The profile curvature is higher in landslides plots, what also indicates a more concave shape. As profile and plan curvature are highly correlated with curvature (*Spearman* correlation coefficient = 0.91; 0.92; cf. Appendix B2), only the latter was included in the logistic regression model and the classification tree. Furthermore, the *weighted Topographic Wetness Index* (wTWI) averaged for an area of 30 m x 30 m (cf. Fig. 18) is significantly lower in landslide than in control plots. Hence, water accumulation based on topographic position is expected to be higher in control plots. However, no significant difference between landslide and control plots was found for the wTWI at the release point.

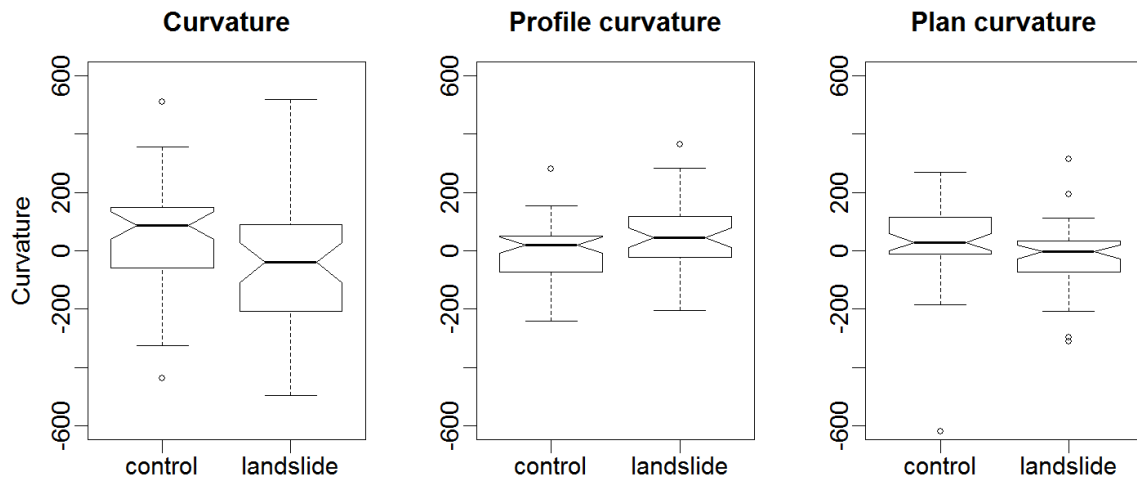


Fig. 13: Distribution of curvature (left), profile curvature (middle) and plan curvature (right) values in control and landslide plots. Differences between control and landslide plots are for all three variables significant.

Tree edge density on a tree height of 10 m is significantly higher in landslide plots compared to control plots ($p = 0.037$; cf. Fig. 14 and Fig. 19). The maximum and the mean tree height as well as the standard deviation of tree height, however, do not differ significantly. Similar to the field data, landslide and control plots show no substantial difference regarding coverage of the different layers. The stands are mainly single-layered (coverage of the lower and middle layer $< 20\%$; cf. Fig. 19). Moreover, no significant difference was found for tree coverage (cf. Fig. 18), which was controlled for the determination of the control points.

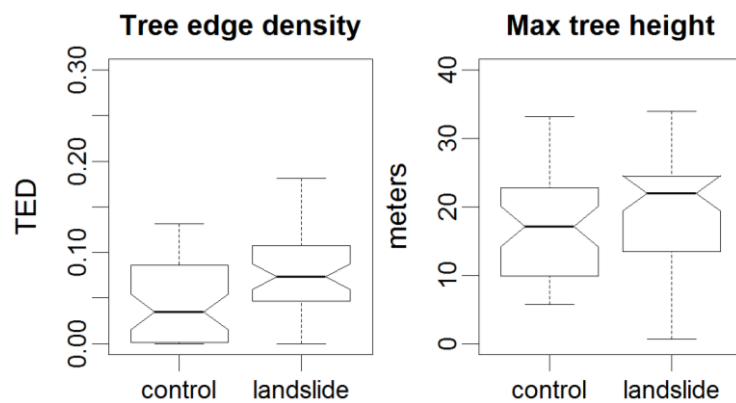


Fig. 14: Distribution of tree edge density (TED; left) and the maximum tree height (right) in control and landslide plots in St. Antoenien. TED is significantly higher in landslide plots, whereas there is no significant difference regarding the maximum tree height.

The distance to the nearest tree (or tree group) is in landslide plots slightly higher than in control plots (cf. Fig. 15). In contrast to the field data, the difference is not significant. The same accounts for the maximum gap length, which is even slightly higher in control plots (cf. Fig. 15). However, comparing the gaps extracted from the CHM to the orthophoto makes apparent that they do not represent the forest gaps accurately (cf. Fig. 16). The tree peaks, too, were not completely recorded.

P-values of the significant variables are listed in Tab. 3. A section of the CHM in the study area can be seen in Fig. 17 and a selection of variables derived from LiDAR data is illustrated in Fig. 18 and Fig. 19.

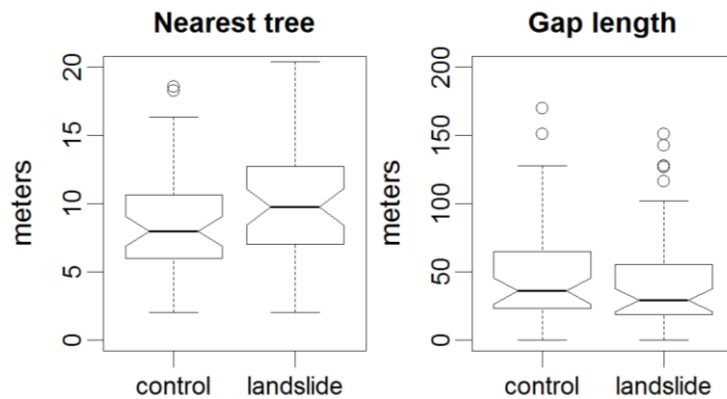


Fig. 15: Distribution of distances from the (potential) release point to the nearest tree (left) and lengths of the largest gap (right) in control and landslide plots. Differences are not significant.

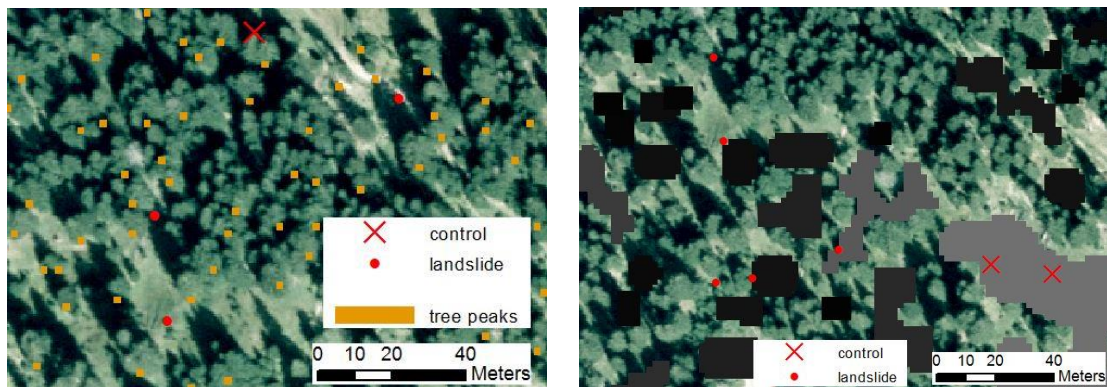


Fig. 16: Tree peaks extracted as local maxima from the CHM (left) and forest gaps (right) in two different sections of St. Antoenien. Source: DTM-AV DOM-AV and swissimage © 2014 swisstopo (5704000000).

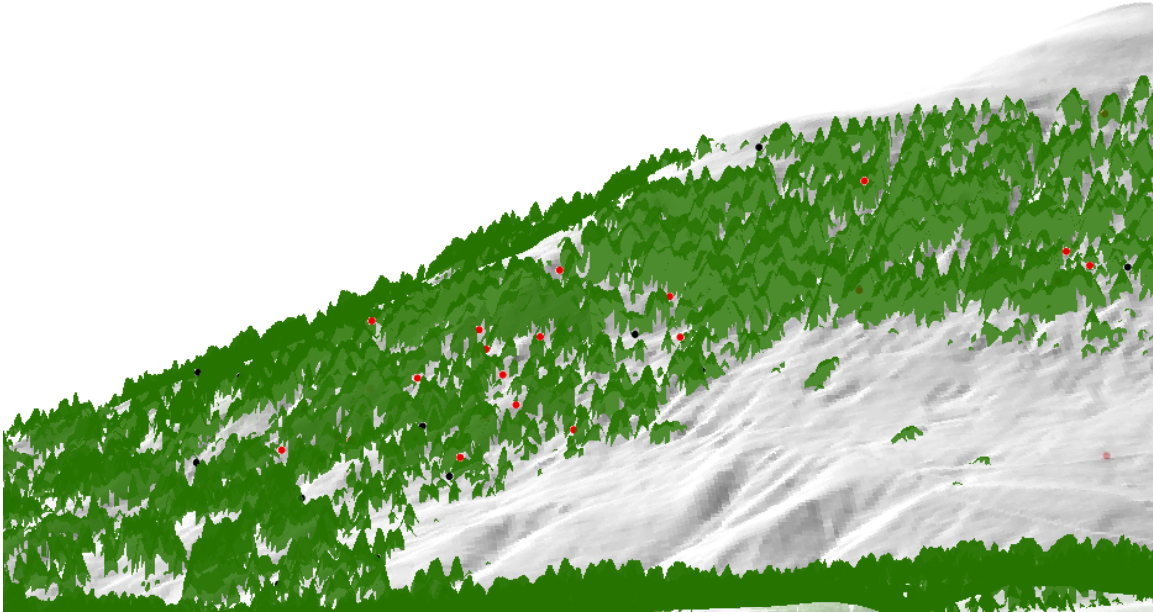


Fig. 17: Canopy Height Model (CHM) displayed in 3D for a section of the study area in St. Antoenien with landslide (red) and control (black) points. Source: DTM-AV DOM-AV © 2014 swisstopo (5704 000 000).

Tab. 3: Variables derived from LiDAR data which significantly affect landslide occurrence in St. Antoenien and the corresponding p-values of the Wilcoxon rank sum test (continuous variables), the Chi-squared test (categorical variables) and logistic regression. The effect of the continuous variables on landslide susceptibility is indicated with + (increase in the variable leads to an increase in landslide susceptibility) and – (increase in the variable leads to a decrease in landslide susceptibility).

	Wilcoxon-Test	LOG
Slope angle release point (+)	0.019	0.026
Mean slope angle 30m x 30m (+)	$7.519 \cdot 10^{-4}$	0.002
Curvature 30m x 30m (-)	0.003	0.011
Profile curvature 30m x 30m (+)	0.009	0.009
Plan curvature 30m x 30m (-)	0.008	0.030
Tree edge density (+)	0.037	0.013
Mean wTWI 30m x 30m (-)	0.005	0.003

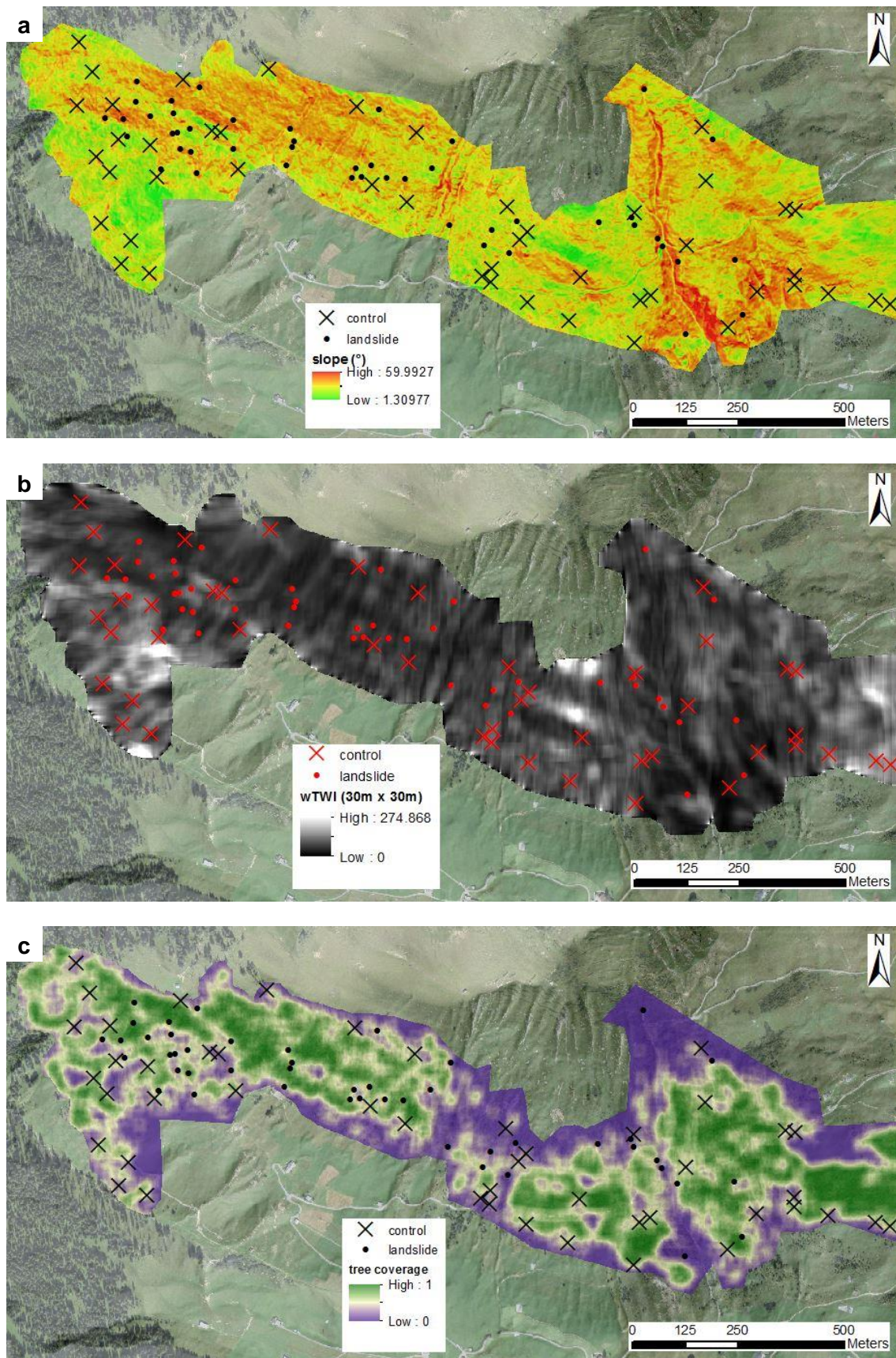


Fig. 18: Slope angle (a), wTWI (b) and tree coverage (c) (calculated with the DTM and the CHM, respectively) in the study area of St. Antoenien. Source: DTM-AV DOM-AV and swissimage © 2014 swisstopo (5704000000).

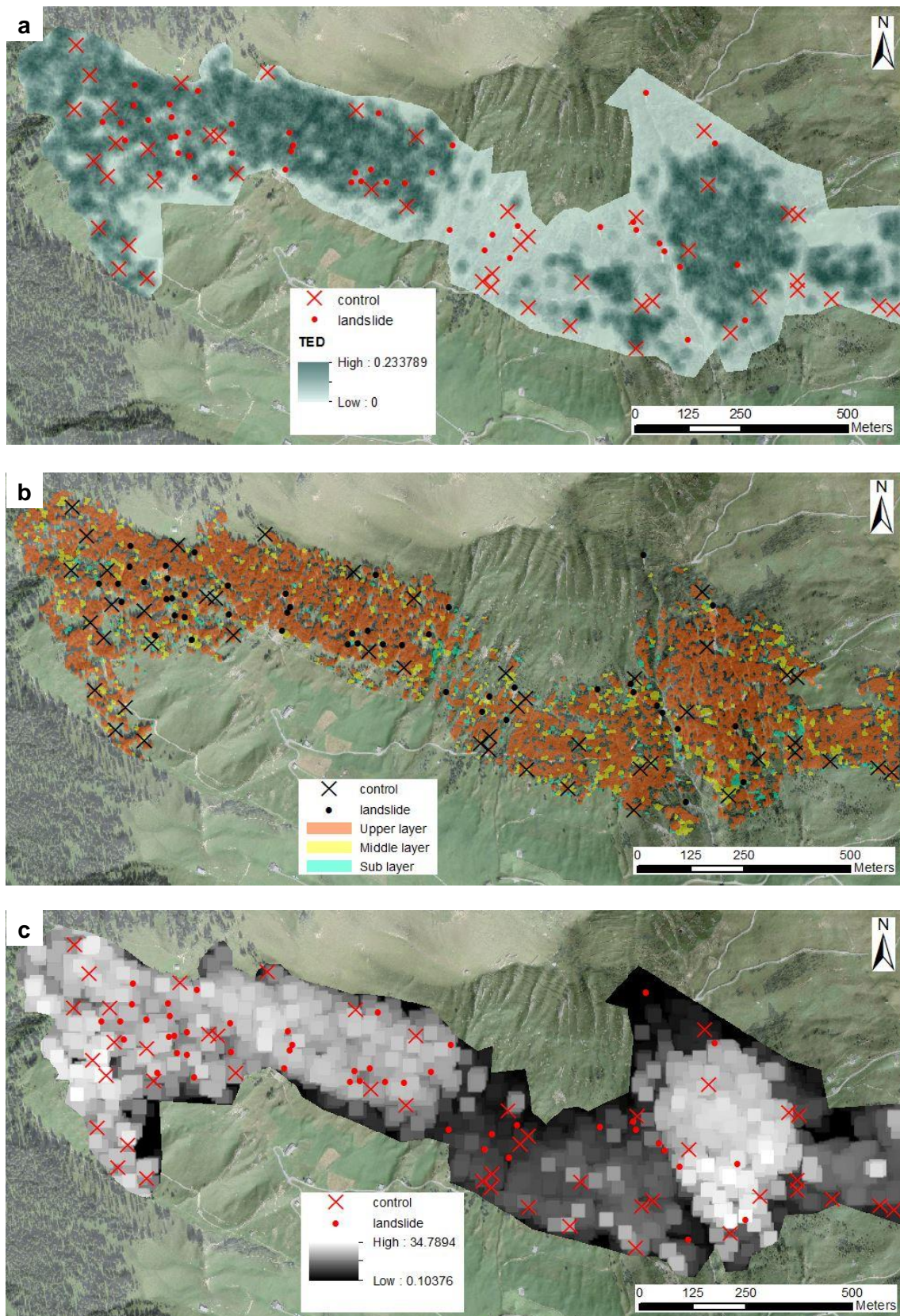


Fig. 19: Tree edge density (a), tree layers (b) and maximum tree height (c) (calculated with the CHM) in the study area of St. Antoenien. Source: DTM-AV DOM-AV and swissimage © 2014 swisstopo (5704000000).

3.1.3. Sachseln

Slope angles at the (potential) release point are higher in Sachseln compared to St. Antoenien (LiDAR data; cf. chapter 3.1.2). The mean slope angle at landslide points is 38.1° (St. Antoenien: 33.5°) and 37.0° at control points (St. Antoenien: 30.4°). The slope angle at the release point does not significantly differ between landslide and control points in Sachseln. The slope angle averaged over an area of 30 m x 30 m, however, is significantly higher in landslide plots (cf. Fig. 20). Furthermore, no significant differences were found regarding the curvature and the wTWI at the release point. The wTWI averaged over the study plots is slightly higher in control plots. The difference is not significant according to the Wilcoxon rank sum test ($p = 0.107$), however according to logistic regression ($p = 0.008$).

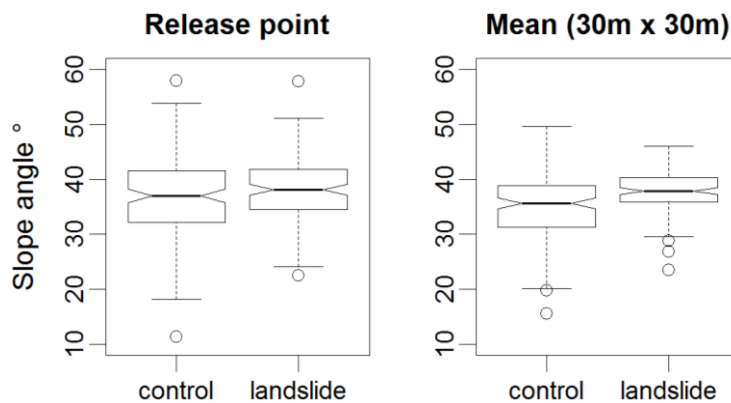


Fig. 20: Distribution of slope angles at the release point (left) and averaged over an area of 30m x 30m (right) in control and landslide plots in Sachseln. The mean slope angle significantly differs between control and landslide plots; the slope angle at the release point does not.

The tree height significantly differs between control and landslide plots (cf. Fig. 21). The maximum and the mean tree height as well as the standard deviation of the tree height are significantly lower in landslide plots ($p = 1.307 \cdot 10^{-5}$; 0.001; $4.333 \cdot 10^{-6}$). Additionally, the tree edge density at a height of 10 m is significantly lower in landslide plots. As the tree height variables and tree edge density are highly correlated, only the standard deviation of tree height (lowest p-value) was integrated in the logistic regression model and the classification tree.

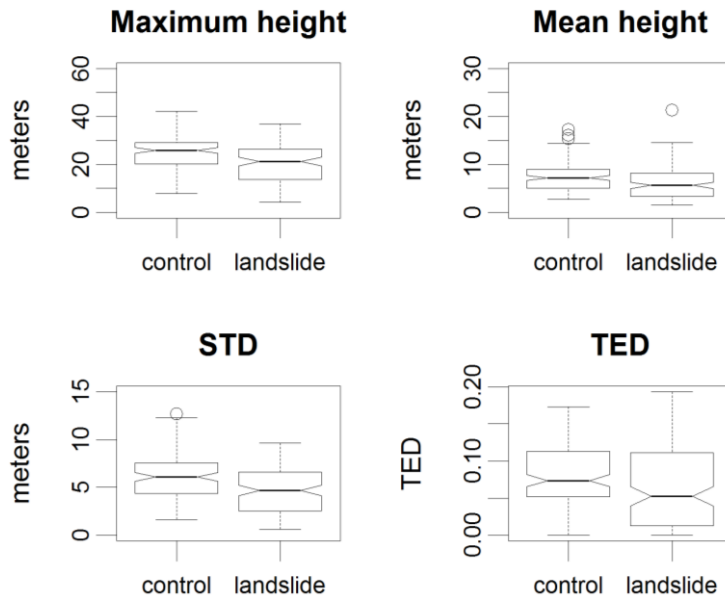


Fig. 21: Distribution of the maximum (above left) and the mean (above right) tree height as well as the standard deviation of tree height (STD; below left) and the tree edge density (TED; below right). Differences between control and landslide plots are for all variables significant.

Similar to St. Antoenien, no significant difference was found regarding the vertical forest structure. Forests are predominantly single-layered (coverage of the sub and middle layer < 20 %), whereby the percentage of multi-layered stands is in Sachseln generally higher than in St. Antoenien (32.0 % in Sachseln; 8.6 % in St. Antoenien). Landslide and control plots do not significantly differ in tree coverage, too. The comparison of the orthophotos from 1993 and 1999 revealed minor to moderate changes in tree coverage for 26.5 % of the landslide plots. Furthermore, the distance from the (potential) release point to the nearest tree is slightly higher in control plots, but not significantly. The same accounts for the length of the biggest gap. However, for Sachseln, too, the comparison to the orthophoto showed that forest gaps and tree peaks were not delineated accurately from the CHM. A section of the CHM for Sachseln is shown in Fig. 22.

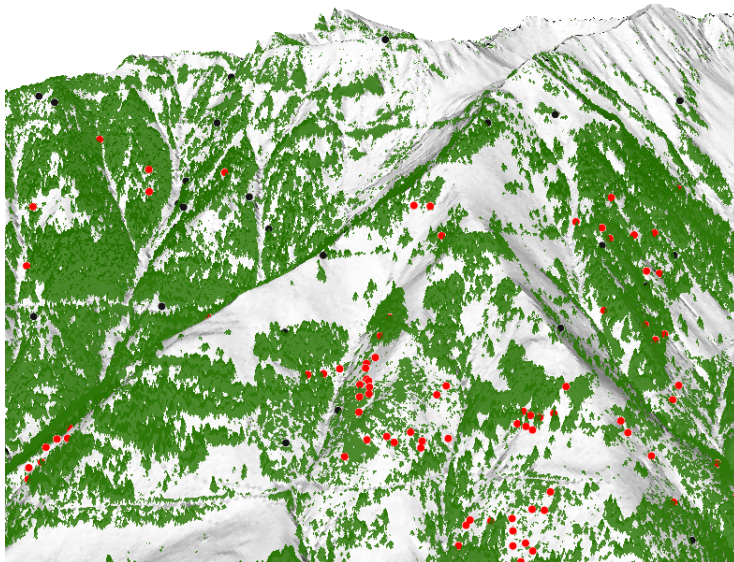


Fig. 22: Canopy Height Model (CHM; green) displayed in 3D for a section of the study area in Sachseln with landslide (red) and control (black) points. Source: DTM-AV DOM-AV and swissimage © 2014 swisstopo (5704000000).

There are significantly more landslide plots which were classified as young growth in the stand classification (Rickli 2001), whereas control plots mainly belong to stands with a dbh between 35 and 50 cm or to multi-layered stands (cf. Fig. 23). In addition, landslide and control plots significantly differ in their species mixture (cf. Fig. 24). Significantly more control plots are in deciduous stands. No significant difference, however, was found for the stocking level.

P-values of variables significantly affecting landslide occurrence in Sachseln are outlined in Tab. 4 and a selection of variables is shown in Fig. 25 and Fig. 26.

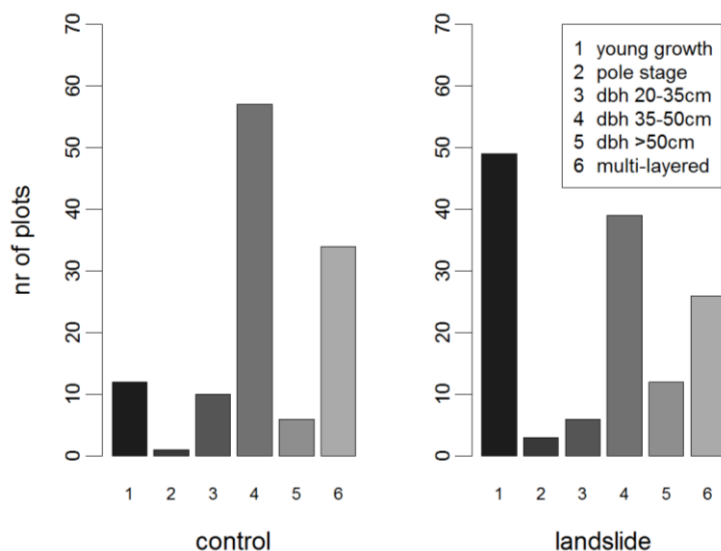


Fig. 23: Number of control (left) and landslide (right) plots in the different successional stages (legend on the right).

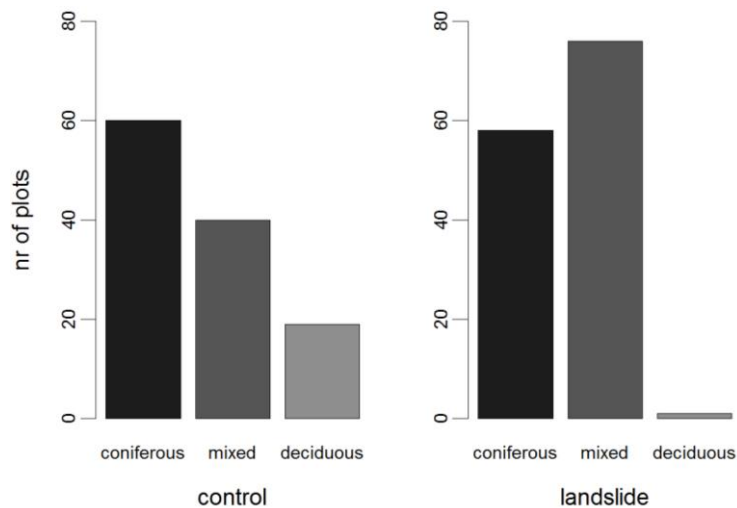


Fig. 24: Number of control (left) and landslide (right) plots in coniferous, mixed and deciduous stands.

Tab. 4: Variables derived from LiDAR data or the stand classification which significantly affect landslide occurrence in Sachseln and the corresponding p-values of the Wilcoxon rank sum test (continuous variables), the Chi-squared test (categorical variables) and logistic regression. The effect of the continuous variables on landslide susceptibility is indicated with + (increase in the variable leads to an increase in landslide susceptibility) and – (increase in the variable leads to a decrease in landslide susceptibility).

	Wilcoxon-Test	X ² -Test	LOG
Mean slope angle 30m x 30m (+)	4.207*10 ⁻⁶		1.290*10 ⁻⁵
Mean tree height (-)	0.001		0.007
Maximum tree height (-)	1.307*10 ⁻⁵		7.060*10 ⁻⁶
Standard deviation tree height (-)	4.333*10 ⁻⁶		3.340*10 ⁻⁶
Tree edge density (-)	0.002		0.014
Successional stage		1.406*10 ⁻⁵	6.654*10 ⁻⁶
Species mixture		1.757*10 ⁻⁶	2.810*10 ⁻⁷

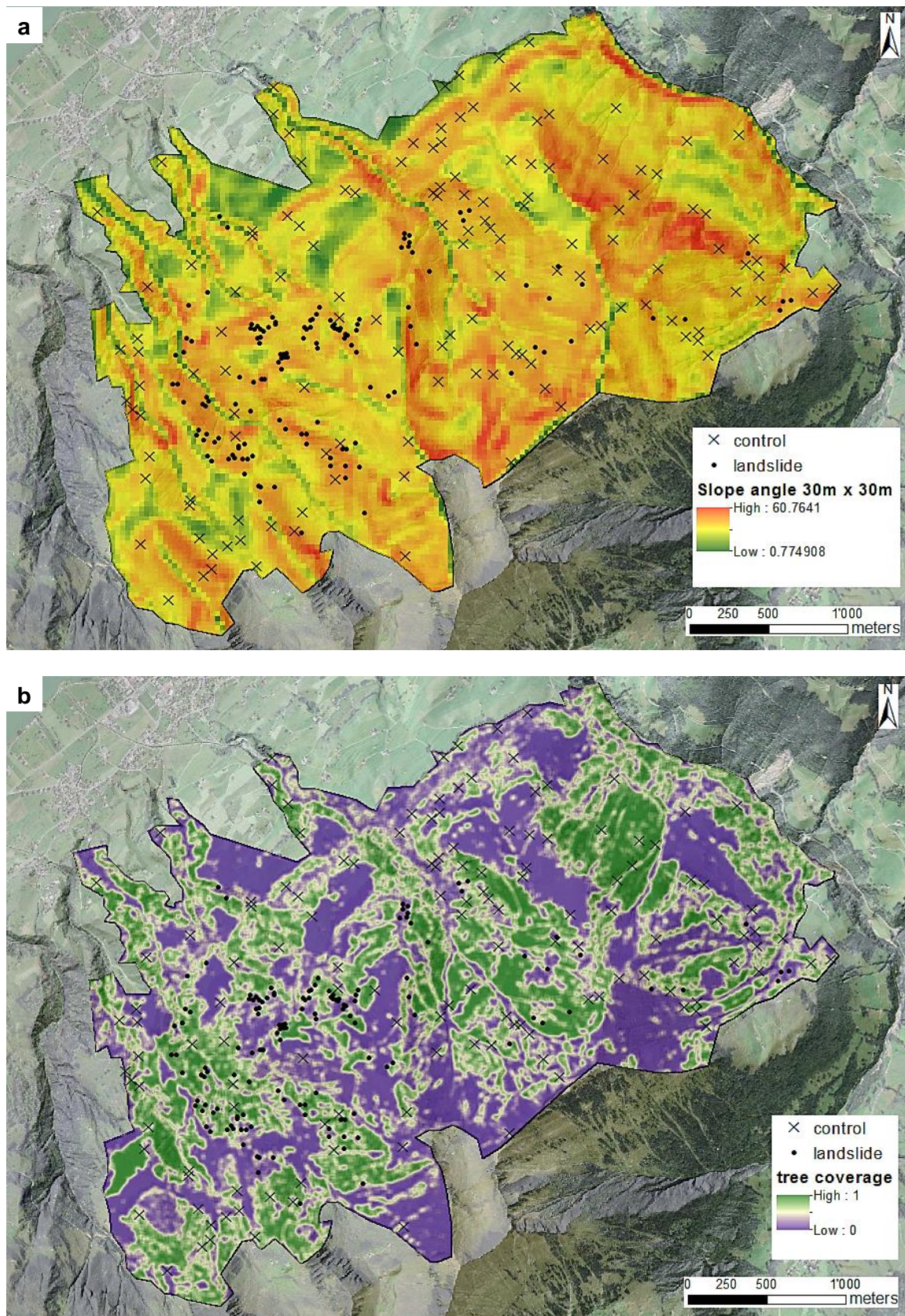


Fig. 25: Mean slope angle (a) and tree coverage (b) (calculated with the DTM and the CHM, respectively) in the study area of Sachseln. Source: DTM-AV DOM-AV and swissimage © 2014 swisstopo (5704000000).

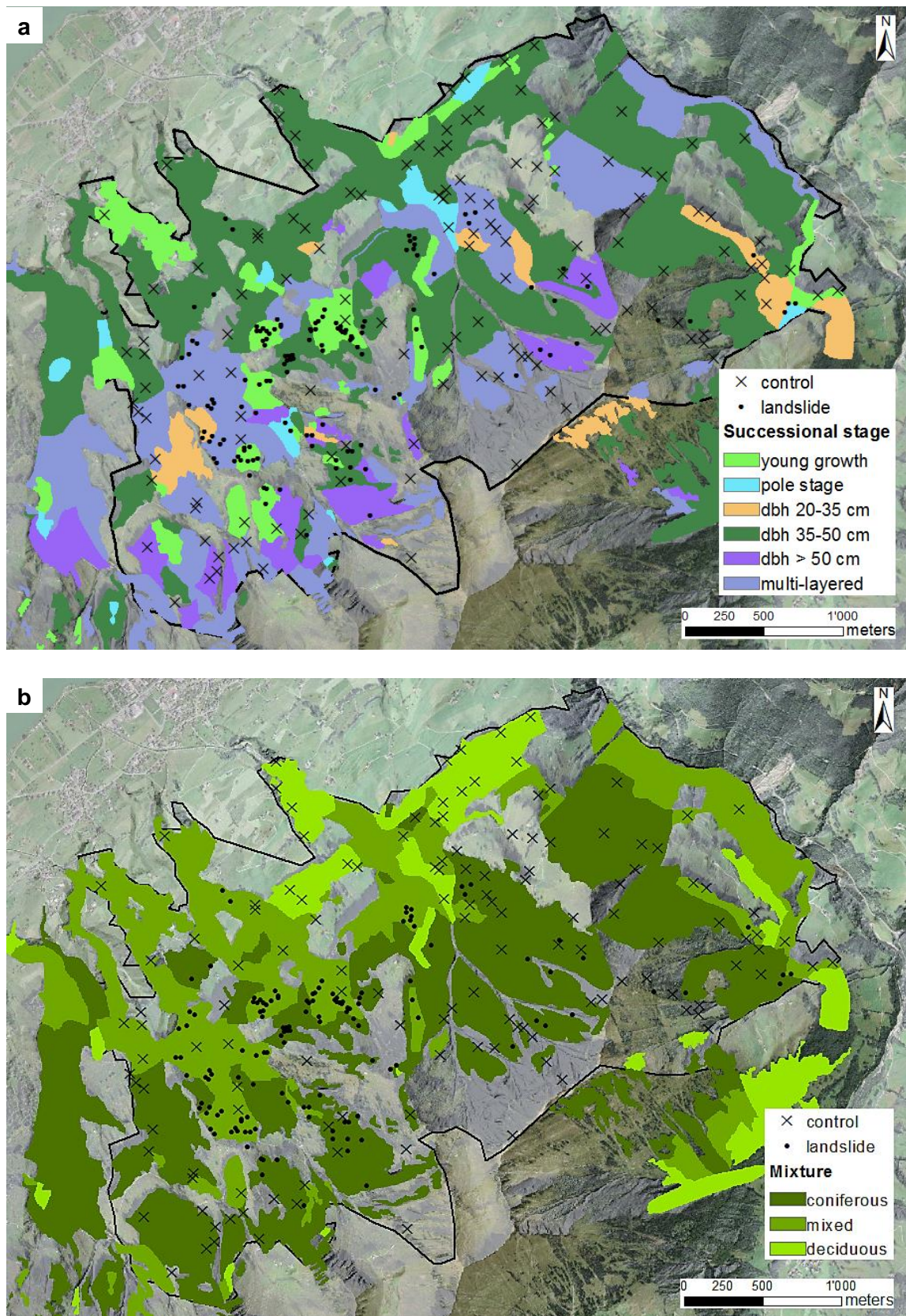


Fig. 26: Successional stage and species mixture (derived from a stand classification) in the study area of Sachseln. Source: Rickli (2001) and swissimage © 2014 swisstopo (5704000000).

3.2. Multivariate models

3.2.1. St. Antoenien field data

According to the final regression model calibrated with terrain and hydrological variables assessed in the field (*LOG topo*), geomorphology type, slope angle at the release point and water logging are the most important factors affecting landslide susceptibility in St. Antoenien. The estimated regression coefficients, their standard errors, the Z-values and the corresponding p-values are listed in Tab. 5. The positive regression coefficient of the slope angle means that landslide susceptibility increases with an increasing slope angle. The geomorphology types 6 and 9 have got negative, types 2 and 8 positive regression coefficients. This indicates a lower susceptibility at vertically convex slopes (6, 9) and a higher susceptibility at horizontally convex (2) and concave (8) slopes. The negative coefficients of *no* and *vague* water logging indicate a decline of landslide susceptibility if the soil is not or only little wet. The p-values of the geomorphology type 9 and of *vague* water logging are not significant. As eliminating these variables increased the Akaike-Information-Criterion (AIC) distinctly, they were kept in the model. Fig. 30 shows the ROC curve of *LOG topo*. The area under the curve is 0.87 and 0.75 with cross-validation, respectively. The AIC of the model is 100.63.

Tab. 5: Estimated regression coefficients, standard errors, Z-values (ratio of estimate and standard error) and p-values of explanatory variables of the logistic regression model for St. Antoenien based on terrain and hydrological variables assessed in the field (*LOG topo*). The model was fitted with the whole data set ($n = 93$).

	Estimate	Std. Error	Z-value	p (> z)
(Intercept)	-2.562	1.147	-2.234	0.025
Geo 2	1.475	0.730	-2.198	0.028
Geo 6	-1.883	0.857	-2.198	0.028
Geo 8	2.625	1.438	1.825	0.068
Geo 9	-16.754	1517.856	-0.011	0.991
Slope angle	0.099	0.032	3.117	0.002
Water logging (no)	-2.754	0.792	-3.476	5.090*10 ⁻⁴
Water logging (vague)	-1.086	0.689	-1.563	0.118

When including forest variables along with hydrological and terrain features, the stepwise procedure for variable selection stopped with a model consisting of five explanatory variables (*LOG mix*; cf. Tab. 6). In addition to slope angle, water logging and geomorphology type, gap length and the proxy-variable for root penetration of the nearest tree were included. Furthermore, geomorphology type 3 and 4 along with 2 and 8 were kept in the model, but not 6 and 9. They all have a positive regression coefficient, indicating enhanced landslide susceptibility at horizontally convex (2), horizontally and vertically convex (3), vertically concave (4) and horizontally concave (8) slopes. The regression coefficients of gap length and the proxy-variable for root penetration are also positive. This means that landslide susceptibility rises with longer gaps and a weaker root penetration of the soil. The AIC of *LOG mix* is 88.58, thus distinctly lower than the AIC of *LOG topo* (100.63; cf. Fig. 30). Moreover, *LOG mix* has got a larger AUC value (0.91; 0.80 with cross-validation; cf. Fig. 30).

Tab. 6: Estimated regression coefficients, standard errors, Z-values (ratio of estimate and standard error) and p-values of explanatory variables of the logistic regression model for St. Antoenien based on terrain, hydrological and forest variables assessed in the field (*LOG mix*). The model was fitted with the whole data set ($n = 93$).

	Estimate	Std. Error	Z-value	p (> z)
(Intercept)	-7.187	1.855	-3.875	$1.070 \cdot 10^{-4}$
Geo 2	2.135	0.959	2.226	0.026
Geo 3	1.576	0.848	1.858	0.063
Geo 4	2.357	1.528	1.542	0.123
Geo 8	2.317	1.704	1.359	0.174
Slope angle	0.111	0.039	2.845	0.004
Gap length	0.048	0.016	2.984	0.003
Water logging (no)	-2.798	0.982	-2.850	0.004
Water logging (vague)	-1.179	0.761	-1.550	0.121
Root penetration nearest tree	0.134	0.049	2.747	0.006

The slope angle at the release point and water logging were used to split the data of St. Antoenien into controls and landslides in the classification tree fitted with topographic, geomorphological and hydrological variables (*CT topo*; Fig. 27). In the first node, a threshold of 36° is applied to the slope angle. Thus, a data point is with a probability of about 0.7 a control point if its slope angle is less or equal 36° . Otherwise, the data point is classified as control point, in case there is no water logging (water logging *no* = 1). The area under the ROC curve of *CT topo* (0.74) is considerably lower than that of *LOG topo* (0.87; cf. Fig. 30). The AUC with cross-validation (0.56) is even under 0.7, which is the minimum value for an acceptable model according to Hosmer and Lemeshow (2000).

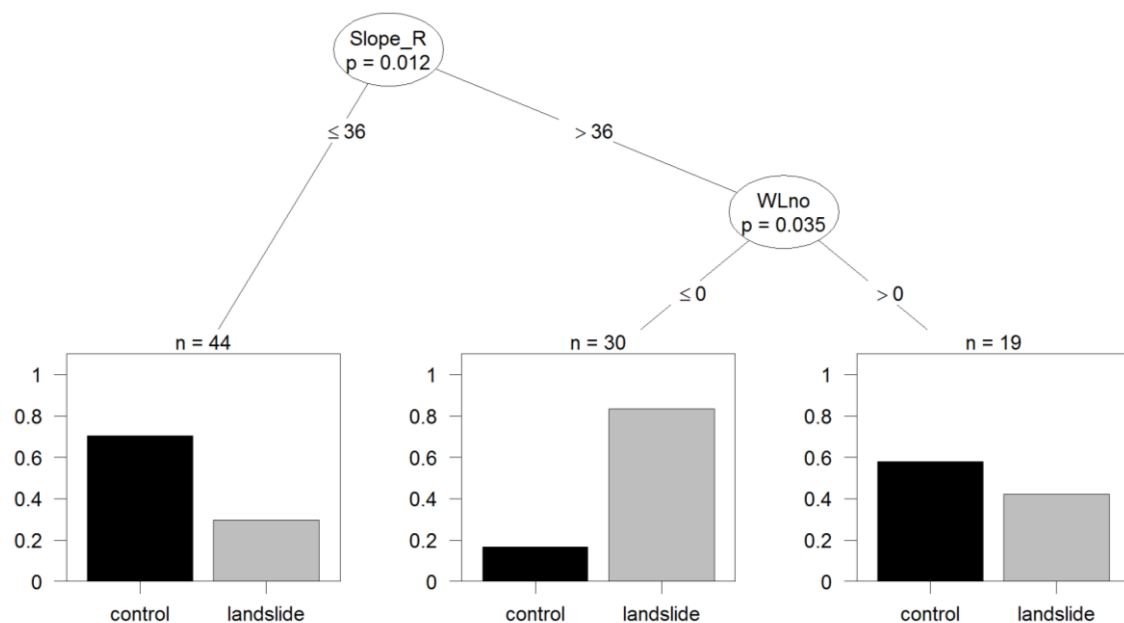


Fig. 27: Classification tree to predict landslide occurrence in St. Antoenien based on hydrological and terrain variables assessed in the field (*CT topo*). The model was fitted with the whole data set of St. Antoenien ($n = 93$). The n-values exhibit the number of cases which are explained by the corresponding variable. *Slope_R*: Slope at the release point; *WLno*: water logging *no*

In the classification tree including forest variables (*CT mix*), the length of the biggest gap and the slope angle at the release point are used to split the data (cf. Fig. 28). At the first node, the data set is partitioned based on gap length (threshold = 20 m). In case the biggest gap is longer than 20 m, the second node splits the remaining data points according to their slope angle. Similar to logistic regression, the AUC of *CT mix* (0.84; 0.77 with cross-validation) is larger than the AUC of *CT topo*, but lower than the AUC of *LOG mix* (0.91; 0.80 with cross-validation; cf. Fig. 30).

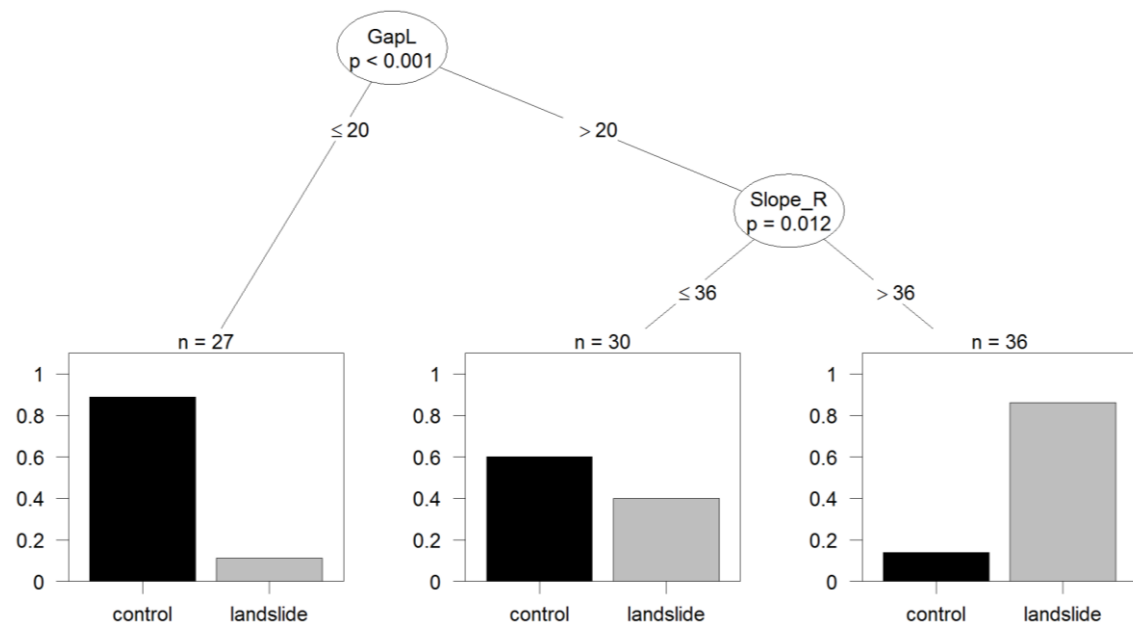


Fig. 28: Classification tree to predict landslide occurrence in St. Antoenien based on hydrological, terrain and forest variables assessed in the field (*CT mix*). The model was fitted with the whole data set of St. Antoenien ($n = 93$). The n -values exhibit the number of cases which are explained by the corresponding variable. *Slope_R*: Slope at the release point; *GapL*: Length of largest gap

Gap length, root penetration of the five nearest trees and slope angle are also in the random forest (*RF all*) the most predictive variables. The importance of the explanatory variables can be seen in Fig. 29 (only the first 14 variables are shown). In the final model, 22 variables were randomly sampled as splitting candidates at each node (*mtry*). It is conspicuous, that gap width as well as regeneration coverage of 10 % to 25 % (*Regeneration 3* in Fig. 29) have got a relatively high importance, although they were not significant in the univariate analysis. The AUC of *RF all* amounts to 0.98 and 0.84 with cross-validation, respectively. Fig. 30 gives an overview of the AUC values of the different classification models based on the field data of St. Antoenien.

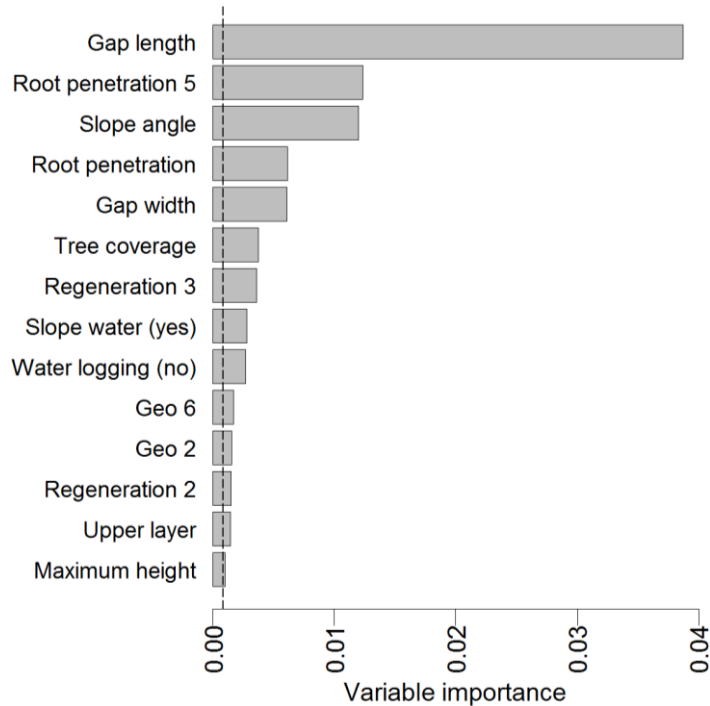


Fig. 29: Explanatory variables of the random forest fitted with field data of St. Antoenien (*RF all*; $n = 93$) and the corresponding variable importance. Only the 19 most important variables are shown. The dotted line corresponds to the amplitude of the largest negative value. The importance of variables below this value can be regarded as random (Strobl et al. 2009). *Regeneration 3*: regeneration coverage of 10-25 %; *Regeneration 2*: regeneration coverage of 1-9 %.

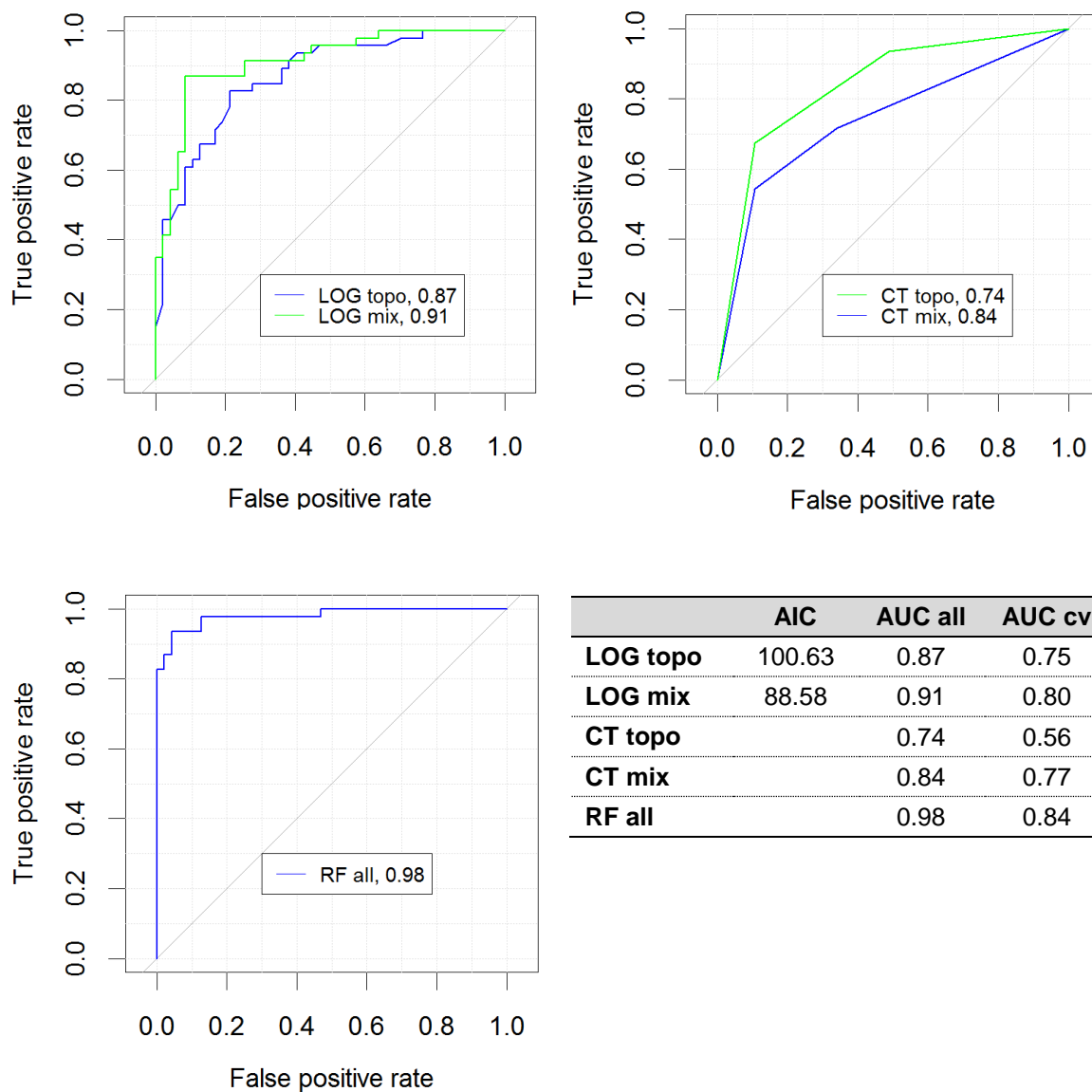


Fig. 30: Receiver Operating Characteristics (ROC) curves and corresponding AUC values (validation with the whole data set) of the logistic regression models (top left), the classification trees (top right) and the random forest (bottom left). All classification models are based on the field data of St. Antoenien ($n = 93$). The table (bottom right) exhibits a summary of the AIC of logistic regression and AUC values of the validation with the whole data set (AUC_{all}) as well as with three times repeated 10-fold cross-validation (AUC_{cv}).

3.2.2. St. Antoenien LiDAR data

Curvature, wTWI and tree edge density were kept in the logistic regression model fitted with the LiDAR derived variables (*LOG LiDAR*; cf. Tab. 7). The estimated regression coefficient of the curvature is negative. Consequently, higher landslide susceptibility is expected at concave slopes (negative curvature). The wTWI also has a negative regression coefficient, indicating enhanced landslide susceptibility with a decreasing wTWI and thus a less wet soil based on topography and exposition. As the regression coefficient of tree edge density is positive, more landslides are expected if tree edge density is high. The AIC of *LOG LiDAR* is 111.43 and the AUC value 0.79 and 0.75 with cross-validation (cf. Fig. 33). Compared to the logistic regression models fitted with the field data, the performance of *LOG LiDAR* is worse. However, the difference between the AUC values with and without cross-validation is smaller (cf. Fig. 33).

Tab. 7: Estimated regression coefficients, standard errors, Z-values (ratio of estimate and standard error) and p-values of explanatory variables of the logistic regression model for St. Antoenien based on variables derived from LiDAR data (*LOG LiDAR*). The model was fitted with the whole data set ($n = 93$).

	Estimate	Std. Error	Z-value	p (> z)
(Intercept)	3.386	1.306	2.593	0.01
Curvature 30m	-0.004	0.001	-3.078	0.002
wTWI 30m	-0.527	0.164	-3.203	0.001
Tree edge density	7.141	4.899	1.457	0.145

In the classification tree for the LiDAR data of St. Antoenien (*CT LiDAR*, cf. Fig. 31), only the mean slope angle for an area of 30 m x 30 m was used as a splitting variable. The applied threshold was 29.59°, meaning that a data point is classified as landslide point if its mean slope angle is larger than this value. The AUC value of *CT LiDAR* is 0.68 and 0.58 with cross-validation, respectively, and thus distinctly lower than the AUC value of the LOG model.

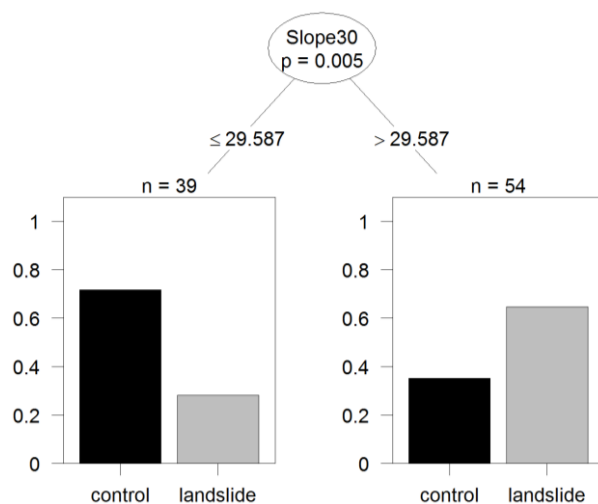


Fig. 31: Classification tree to predict landslide occurrence in St. Antoenien based on LiDAR derived variables (*CT LiDAR*). The model was fitted with the whole data set ($n = 93$). The n-values exhibit the number of cases which are explained by the corresponding variable. *Slope30*: Slope angle averaged for an area of 30 m x 30 m.

The variable with the highest importance in the random forest model (*RF LiDAR*, cf. Fig. 32) is mean wTWI (30 m x 30 m), followed by mean profile curvature, tree edge density, mean slope and mean curvature. In the final model, 16 variables were randomly sampled as splitting candidates (*mtry*). The performance of *RF LiDAR* tested on the training data set (all data) is with an AUC value of 0.96 substantially higher than the performance of *LOG LiDAR* and *CT LiDAR*. On the other hand, the AUC value with cross-validation (0.77) only slightly exceeds that of *LOG LiDAR*. Fig. 33 gives an overview of the AUC values of the different models.

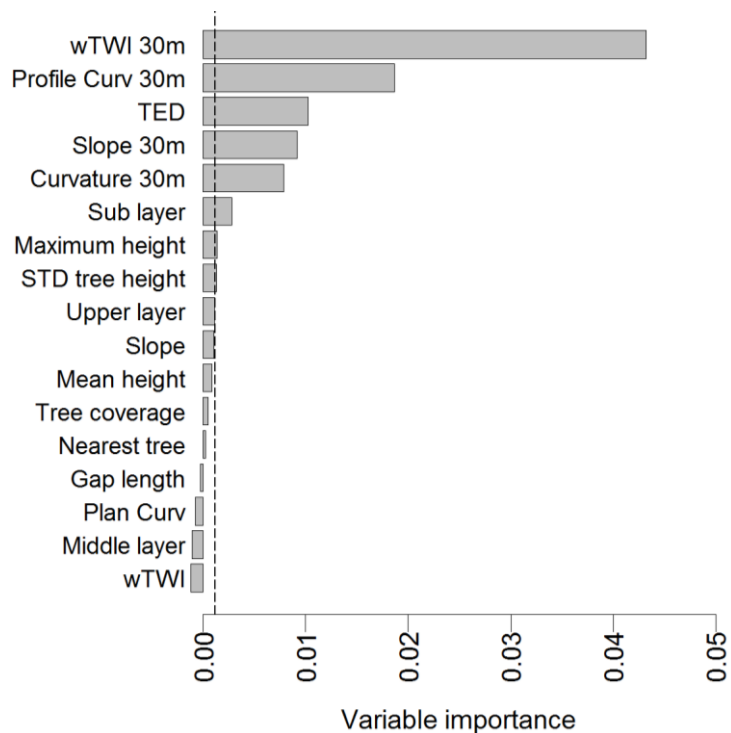


Fig. 32: Explanatory variables of the random forest fitted with LiDAR data of St. Antoenien (*RF LiDAR*; $n = 93$) and the corresponding variable importance. The dotted line corresponds to the amplitude of the largest negative value. The importance of variables below this value can be regarded as random (Strobl et al. 2009). *TED*: tree edge density; *STD tree height*: standard deviation of tree height.

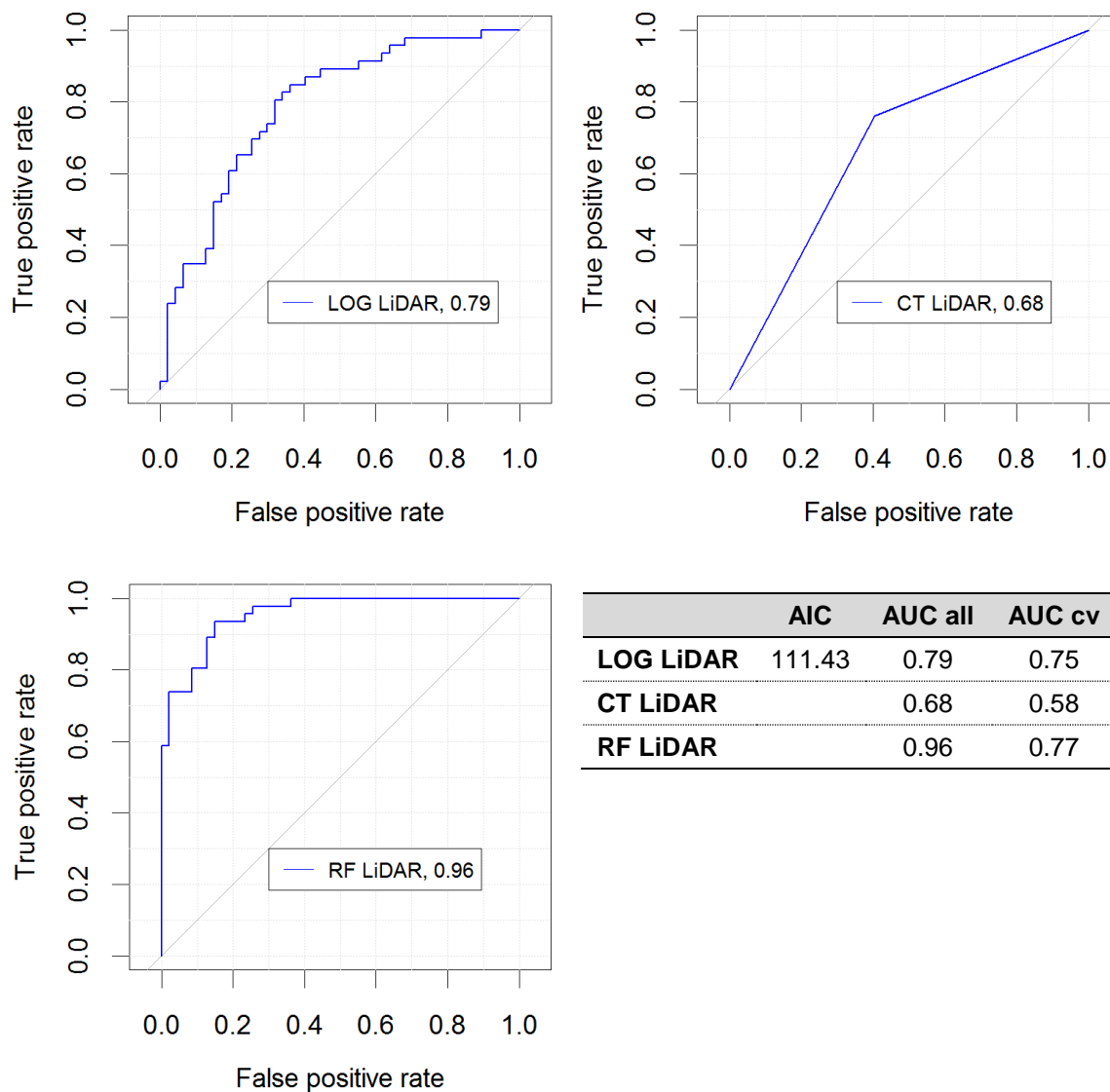


Fig. 33: Receiver Operating Characteristics (ROC) curves and corresponding AUC values (validation with the whole data set) of the logistic regression model (top left), the classification tree (top right) and the random forest (bottom left) based on LiDAR data of St. Antoenien ($n = 93$). The table (bottom right) exhibits a summary of the AIC of logistic regression and AUC values of the validation with the whole data set (*AUC all*) as well as with three times repeated 10-fold cross-validation (*AUC cv*).

3.2.3. *Sachseln*

For the LiDAR derived data of *Sachseln*, the final logistic regression model (*LOG Sachseln*) consists of the variables mean slope angle and standard deviation of tree height (cf. Tab. 8). The mean slope angle has got a positive, the standard deviation of tree height a negative regression coefficient. This indicates rising landslide susceptibility with an increasing slope angle and a decreasing standard deviation of the tree height. Both explanatory variables have got a highly significant p-value (mean slope: $1.380 \cdot 10^{-5}$, standard deviation: $4.070 \cdot 10^{-6}$). The AUC value of *LOG Sachseln* with cross-validation (0.71) is only slightly lower than that without (0.72). Furthermore, the model has got an AIC of 336.92 (cf. Fig. 30).

Tab. 8: Estimated regression coefficients, standard errors, Z-values (ratio of estimate and standard error) and p-values of explanatory variables of the logistic regression model based on variables derived from LiDAR data (*LOG Sachseln*). The model was fitted with the whole data set ($n = 272$). *STD tree height*: Standard deviation of tree height.

	Estimate	Std. Error	Z-value	p (> z)
(Intercept)	-3.019	1.065	-2.834	0.005
Mean slope 30m	0.124	0.028	4.347	$1.38 \cdot 10^{-5}$
STD tree height	-0.281	0.061	-4.608	$4.070 \cdot 10^{-6}$

When including the significant variables derived from the stand classification in the logistic regression, the final model (*LOG Sachseln+*; cf. Tab. 9) contains species mixture (*deciduous*) and successional stage (*dbh 20-35 cm*, *dbh 35-50 cm* and *multi-layered*) in addition to the slope angle and the standard deviation of tree height as explanatory variables. The regression coefficient for deciduous forest (*mixture deciduous*) is negative, meaning that landslide susceptibility is higher in coniferous or mixed forest. The coefficients for *dbh 20-35 cm*, *dbh 35-50 cm* and *multi-layered* are negative, too. Hence, forests dominated by trees in these successional stages are less prone to landslides than forests which mainly consist of young or very old ($dbh > 50$ cm) stands. *LOG Sachseln+* has got an AUC of 0.79 and 0.76 with cross-validation, respectively. Both values are higher than the AUC values of *LOG Sachseln*. In addition, the AIC of *LOG Sachseln+* is considerably lower (cf. Fig. 37).

Tab. 9: Estimated regression coefficients, standard errors, Z-values (ratio of estimate and standard error) and p-values of explanatory variables of the logistic regression model based on variables derived from LiDAR data and stand classification (*LOG Sachseln+*). The model was fitted with the whole data set ($n = 272$). *STD tree height*: Standard deviation of tree height.

	Estimate	Std. Error	Z-value	p (> z)
(Intercept)	-0.830	1.239	-0.670	0.503
Mean slope 30m	0.094	0.032	2.966	0.003
STD tree height	-0.304	1.078	-3.000	$3.610 \cdot 10^{-5}$
Mixture <i>deciduous</i>	-3.235	1.108	-3.000	0.0027
dbh 20-35 cm	-1.412	0.636	-2.221	0.026
dbh 35-50 cm	-0.823	0.389	-2.134	0.033
Multi-layered	-0.988	0.410	-2.408	0.016

The standard deviation of tree height and the mean slope angle were also used as splitting variables in the classification tree based on the LiDAR derived variables of Sachseln (*CT Sachseln*; cf. Fig. 34). For the standard deviation, a threshold of 2.928 was applied. In a second step, the data points are split according to their mean slope angle with a threshold of 32.567° (standard deviation ≤ 2.928) or 35.155° (standard deviation > 2.928). The AUC of *CT Sachseln* for the whole data set (0.76; cf. Fig. 37) is slightly higher than the AUC of *LOG Sachseln* (0.72). Applying cross-validation, however, substantially reduces the AUC (0.46).

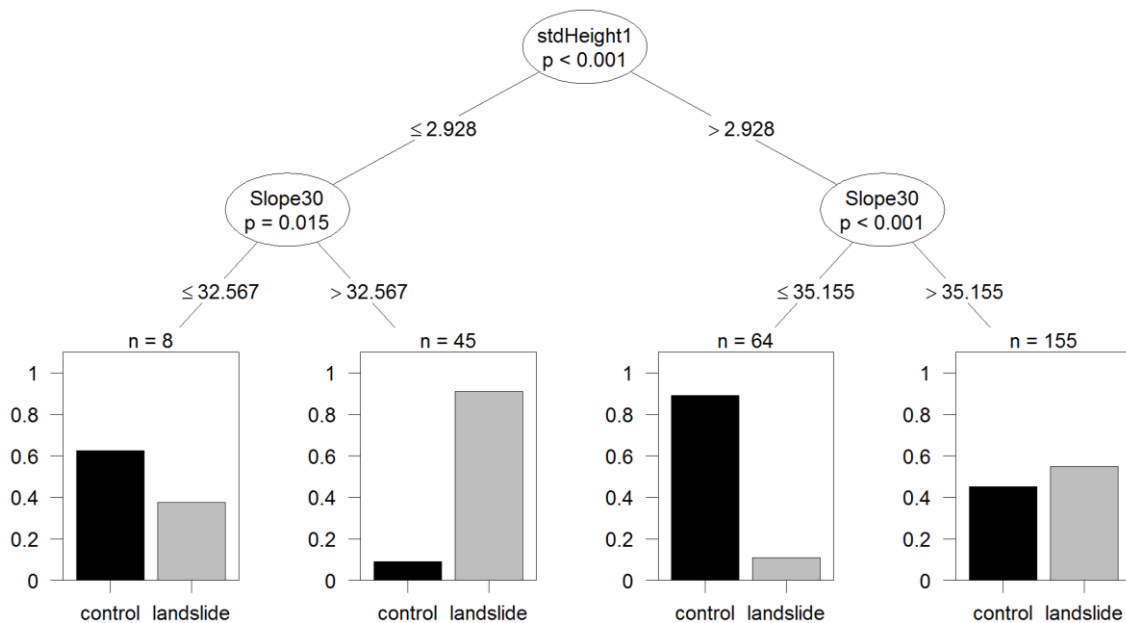


Fig. 34: Classification tree to predict landslide occurrence in Sachseln based on LiDAR derived variables (*CT Sachseln*). The model was fitted with the whole data set ($n = 272$). The n -values exhibit the number of cases which are explained by the corresponding variable. *stdHeight1*: standard deviation of tree height; *Slope30*: slope angle averaged for an area of 30m x 30m.

In addition to the standard deviation of tree height and the mean slope angle, the species mixture ($Mix3 = deciduous$) serves as splitting variable in the classification tree including the variables derived from the stand classification ($CT\ Sachseln+$; Fig. 35). The first node splits the data according to the standard deviation of tree height. If it is equal or less than 2.989, the data point is classified as landslide. The data with a larger standard deviation is split in data points with deciduous and non-deciduous (coniferous or mixed) forest. Deciduous data points are classified as control points, coniferous and mixed points are further split based on their mean slope angle (threshold = 32.132°). The AUC of $CT\ Sachseln+$ is 0.77 and thus only marginally larger than the AUC of $CT\ Sachseln$ (0.76; cf. Fig. 37). The AUC with cross-validation (0.40) is also below 0.5 and even smaller than that of $CT\ Sachseln$ (0.46).

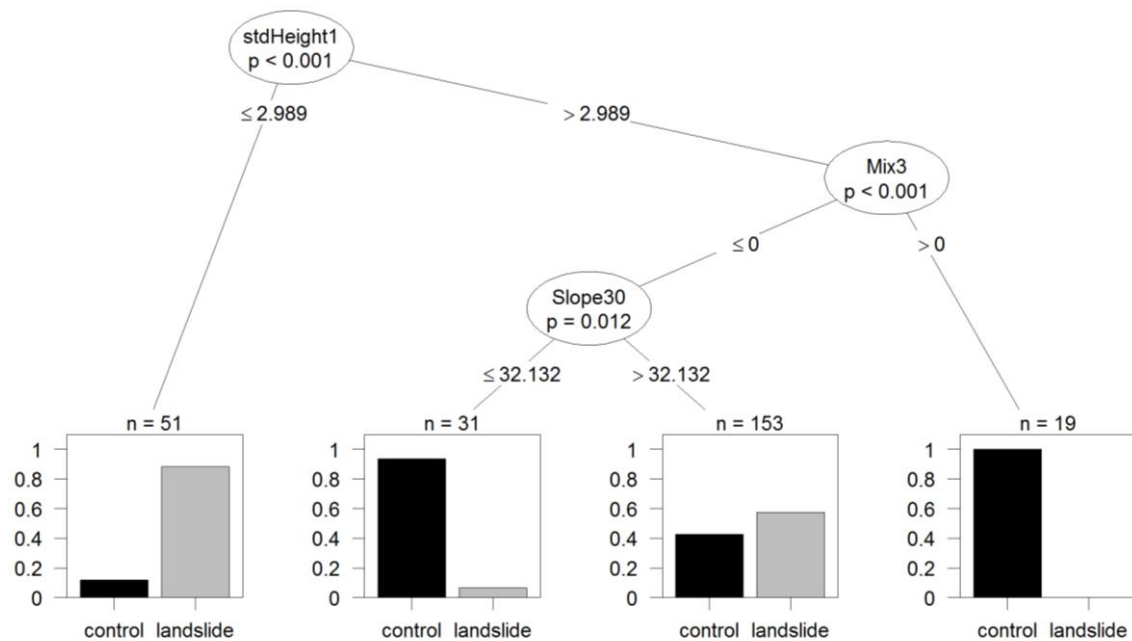


Fig. 35: Classification tree to predict landslide occurrence in Sachseln based on variables derived from LiDAR data and the stand classification ($CT\ Sachseln+$). The model was fitted with the whole data set ($n = 272$). The n -values exhibit the number of cases which are explained by the corresponding variable. *stdHeight1*: standard deviation of tree height; *Mix3*: species mixture *deciduous*; *Slope30*: slope angle averaged for an area of 30m x 30m.

In the final random forest model based on LiDAR data of Sachseln (*RF Sachseln*), three variables were randomly sampled as splitting candidates at tree nodes (*mtry*). As it can be seen in Fig. 36 (left), the mean slope angle is by far the most important variable. Tree height (standard deviation, maximum, minimum) as well as tree edge density also show a high importance. Additionally, tree coverage, coverage of the upper layer, profile curvature and wTWI are also relatively important, although they were not significant in the univariate analysis. *RF Sachseln* has got an AUC of 0.91 and 0.79 with cross-validation (cf. Fig. 37). When integrating the variables derived from the stand classification (*RF Sachseln+*; Fig. 36 right), the mean slope angle still has the highest variable importance. The tree height and tree edge density are again very important variables. Furthermore, the species mixture (*deciduous*, *mixed* in Fig. 36) and the successional stage (*dbh 35-50 cm* in Fig. 36) are under the most important variables. The AUC value of *RF Sachseln+* is 0.94 and thus slightly higher than that of *RF Sachseln* (cf. Fig. 37). In cross-validation, the AUC value is reduced to 0.81.

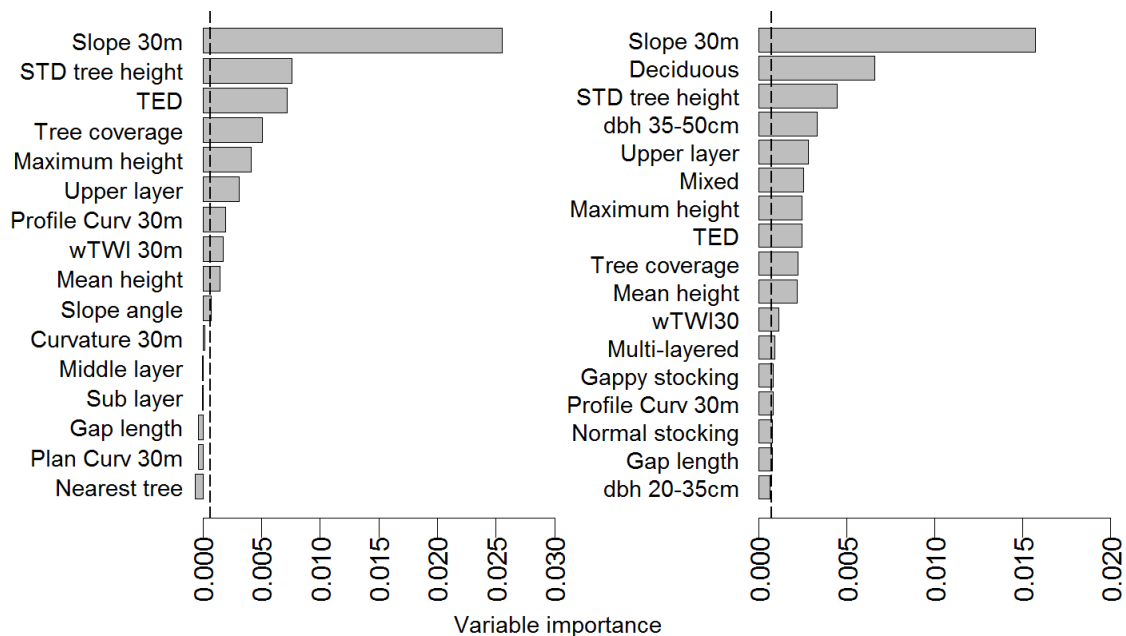


Fig. 36: Variable importance of the RF model fitted with LiDAR data only (*RF Sachseln*; left) and the RF model based on LiDAR data and the stand classification of Sachseln (*RF Sachseln+*; right). The dotted line corresponds to the amplitude of the largest negative value. The importance of variables below this value can be regarded as random (Strobl et al. 2009). *STD tree height*: standard deviation of tree height; *TED*: tree edge density.

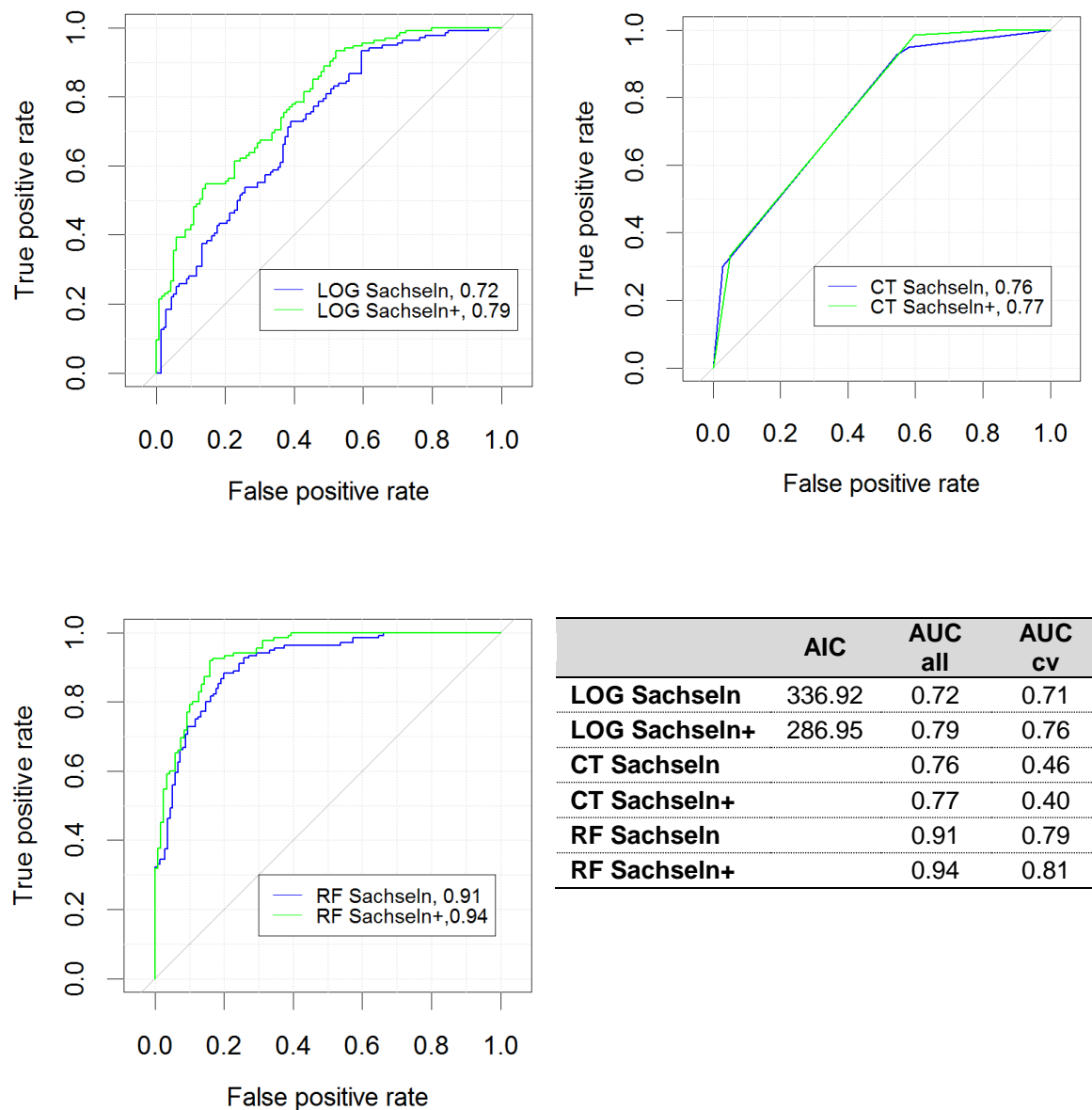


Fig. 37: Receiver Operating Characteristics (ROC) curves and corresponding AUC values (validation with the whole data set) of the logistic regression models (top left), the classification trees (top right) and the random forest models (bottom left) based on LiDAR data only (*Sachseln*, blue) and LiDAR data and stand classification (*Sachseln+*, green). The table (bottom right) exhibits a summary of the AIC of logistic regression and the AUC values of the validation with the whole data set (*AUC all*) as well as with three times repeated 10-fold cross-validation (*AUC cv*).

4. Discussion

4.1. Explanatory variables

In the present study, I designed univariate and multivariate statistical models for a set of landslide and control points in the two study areas St. Antoenien and Sachseln in order to assess whether forest structure affects slope stability. Three different multivariate classifiers were used and models were designed for predictor variables assessed in the field and derived from LiDAR data. As it can be expected that landslides do not occur in very flat or in densely forested areas, only control points with a slope angle and tree coverage similar to that of landslide points were selected. It became evident that in addition to topographic and hydrological factors, forest structure can considerably influence landslide susceptibility. Significant effects were found for gap length, the proxy-variable for root penetration of the nearest trees, tree height, tree edge density, successional stage and tree species. These variables are all associated with root penetration and confirm previous findings which showed that root reinforcement enhances soil cohesion and thus slope stability (e.g. Wu and Sidle 1995; Gorsevski et al. 2006; Preti 2013).

The importance of explanatory variables for landslide susceptibility differed between the two study areas. According to the statistical models based on data of the field investigation of St. Antoenien, gap length and the proxy-variable for root penetration highly influence slope stability, but tree height, successional stage and tree species, which were significant in Sachseln, do not. This may be explained by the fact that the study area in St. Antoenien is dominated by a relatively uniform subalpine spruce forest with only little vertical variation. Because of the spatially highly aggregated forest structure ("Rottenstruktur", typical for subalpine spruce forests), gaps are a defining feature of the forest. Consequently, gap length can be expected to strongly influence landslide occurrence in subalpine forests comparable to St. Antoenien because the root reinforcement in the direction of slope decreases with gap length. This also supports the findings of Casadei et al. (2003). They hypothesise that during storm events, landslides occur in gappy forests where increased pore pressures develop in patches of lower root strength and thicker soil. Sachseln, on the other hand, has a larger altitudinal range and is dominated by deciduous or mixed forest stands in the lower parts. These forests are relatively fast-growing and vary in their vertical structure, but they are less characterized by a grouped structure (Frehner et al. 2005). The analysis of LiDAR data of Sachseln showed that trees are on average taller and have a bigger diameter at breast height (dbh) in control than in landslide plots indicating enhanced reinforcement of the soil with increasing tree age. This is congruent with the findings of Rickli (2001), who classified the landslides predominantly as damaged area and young growth. The forest stands were affected by windthrow and beetle infestations in the 1970s and then again in 1990 (storm "Vivian"). We can therefore assume that landslides occurred in a critical post-disturbance phase in which roots of dead trees did not reinforce the soil anymore and roots of the upcoming young growth were too small to stabilize the soil. According to Ammann et al. (2009), the strength of the decaying roots of spruces which had died about eight years previously declines by approximately 40 % of the original strength. Several other authors also report a

decreased slope stability after tree removal (e.g. Gray 1973; Sidle 1992; Vergani et al. 2012). Moreover, control plots can be distinguished by a higher standard deviation of tree height and a higher tree edge density, which suggest a more diverse vertical structure and thus a better root penetration of the different soil layers (Frehner et al. 2005; Hediger 2012). The statistical models designed for Sachseln also support my hypothesis that deciduous forests are less prone to landslides than coniferous forests because root systems of the latter are mainly developed in the uppermost soil horizon (Waisel et al. 2002). Against expectations, there were more landslide plots classified as mixed forests than control plots. Mixed forests, mainly consisting of beeches and firs, are assumed to stabilize the soil better than spruce forests because of their deep root systems (Frehner et al. 2005). The unexpected result might be explained by the fact that many landslide plots with mixed forest belong to young stands and damaged areas where the root penetration is mainly limited by tree age and not by tree species.

The two study sites do not only differ in vegetation and altitudinal range, but also in geology and rainfall events. In St. Antoenien, landslides were triggered by a rainfall of 116.5 mm during three days (Rickli et al. 2008), whereas about the same amount of rain fell within two hours in Sachseln (Rickli 2001). The amount and duration of rainfall can strongly influence the effect of vegetation (Keim and Skaugset 2003). Hydrological effects of the forest on slope stability can presumably be neglected in Sachseln as the interception capacity was probably exceeded rather quickly (Ward and Trimble 2004). In St. Antoenien, on the other hand, interception might have played a role in preventing slope failure. It should also be mentioned that the different sizes of study areas (Sachseln 10.59 km²; St. Antoenien 0.77 km²) and the associated sample sizes may have influenced the outcome of the study. Miller and Burnett (2007), for example, found highest landslide densities in older forests, when sampled over tens of square kilometres, and in recently harvested and younger forests, when sampled over hundreds of square kilometres.

Despite the differences between the study areas, the results of this study can be regarded as fairly consistent with the Swiss federal recommendations for a sustainable protection forest (NaiS; Frehner et al. 2005). As a minimum requirement, they recommend a maximum gap size of 600 m², tree coverage of minimum 40 % and tree species mixture typical for the location. The analysis of the field data of St. Antoenien supports the importance of gap size, but shows that especially gap length strongly influences slope stability. The mean tree coverage derived from LiDAR data was for control and landslide plots in St. Antoenien as well as in Sachseln slightly above 40 %, meaning that the minimum requirement was on average met in landslide plots. This indicates that the threshold is slightly too optimistic (for extreme rainfall events) and eventually supports the hypothesis that tree coverage is not the only forest variable affecting landslide susceptibility. NaiS also recommends small-scale uneven-aged stands in order to guarantee a widespread and deep root penetration. This complies with the results of Sachseln, where landslide plots had a significantly lower tree edge density and standard deviation of tree height, but contradicts the results of St. Antoenien, where tree edge density was significantly higher in landslide plots.

The statistical analyses of this study also confirmed that terrain and hydrological factors can be recognized as primary factors controlling landslide susceptibility (e.g. Atkinson

and Massari 1998; D'Amato Avanzi et al. 2004; Fernandes et al. 2004; Sidle 2006; Miller and Burnett 2007; Goetz et al. 2011). Especially the slope angle was in almost all multivariate models a highly significant predictive variable, although slope angles of control points were held in the same range as those of the landslide points. In St. Antoenien, geomorphology also plays an important role. Landslide plots were predominantly classified as curved-shaped (field data) and concave, respectively (LiDAR data). In Sachseln, on the other hand, curvature did not have a significant influence on slope stability. This is only partially consistent with the results of former landslide assessments in the study areas, where landslides in Sachseln as well as in St. Antoenien were mainly classified as flat (Rickli et al. 2008). These statistics, however, also contain landslides in open land. Furthermore, landslides in St. Antoenien exhibit significantly more signs of water logging and slope water discharge compared to control plots. Surprisingly, the *weighted Topographic Wetness Index* (wTWI) derived from LiDAR data contrasts with this finding from the field data. In Sachseln, no significant difference regarding wTWI was found. A reason for this might be that, due to the extreme storm event, landslide triggering did not depend on whether the release zone was already wet.

Although the importance of topographic and hydrological factors for predicting landslide susceptibility is undisputed, the present study demonstrates that forest structure distinctly contributes to slope stability. Multivariate models solely based on terrain and hydrological variables performed considerably worse than models integrating forest structure.

4.2. Comparison LiDAR and field data

In addition to regional variations, results were not congruent between LiDAR and field data. First, tree coverage estimated in the field was significantly higher in control than in landslide plots, whereas tree coverage calculated with the canopy height model (CHM) did not significantly differ. This might be a consequence of the time lag between the landslide event and the field investigation. We cannot completely trace changes in forest cover caused by landslides and a distinct reduction of tree coverage in landslide plots cannot be ruled out. LiDAR data, on the other hand, were collected before the event (2003) and the calculation of tree coverage based on the CHM can be regarded as reliable (e.g. Ulrich 2008; Hediger 2012). However, we ascertained only for 27.8 % of the landslide plots in St. Antoenien minor to moderate changes in forest cover when comparing orthophotos before (2003) and after (2005) the event. Therefore, it is more plausible that the tree coverage estimation in the field was biased. The largest gap in landslide plots was in most cases right below the release point (centre of the plot). This did not necessarily apply to control plots and thus could have influenced the estimation. Also, the study plots in the field do not completely correspond to the moving window (30 m x 30 m) of the GIS analysis. The former were aligned in the direction of slope and the latter horizontally. For this reason, study plots in the field are expected to have a higher proportion of gaps than the calculation units in the GIS analysis because gaps are usually oriented in the direction of slope, too. Furthermore, certain trees which were shorter than 3 m in 2003 and thus not classified as forest may have outgrown this threshold in between and caused general changes in tree coverage.

Second, I found significant effects on slope stability for gap length and the distance to the nearest tree assessed in the field, but could not assert them with the LiDAR derived variables. This might also be due to the time lag between landslide event and field investigation. On the other hand, distances to the nearest tree measured on the orthophoto of 2003 were also significantly larger for landslides. Moreover, the comparison with the orthophoto made evident that gaps and single tree peaks were not extracted satisfactorily. According to Morsdorf (2011), a DSM with a point density of $0.25/m^2$ is not suitable for single tree delineation. Nevertheless, the nearest tree peaks are slightly more distant in landslide than in control plots suggesting a tendency to decreasing slope stability with rising tree distance. Implementing more complex watershed segmentation algorithms might lead to better results (e.g. Popescu and Wynne 2004; Wang 2004; Jing et al. 2012; Chen and Zhu 2013). The resolution of the LiDAR data does not appear to be the main problem for gap detection, because non-forested cells were extracted accurately from the CHM. Instead, the isolation of single forest gaps turned out to be challenging due to the almost continuous connectivity of the non-forested area, which is especially pronounced in mountainous forests. For this reason, the high accuracy of the gap definition method introduced by Koukoulas and Blackburn (2004) could not be proved. This is plausible since they developed the method for a semi-natural broadleaved deciduous forest. In addition, gap length had to be calculated indirectly what also may have affected the correctness of the results.

As already mentioned, the results from the field investigation and the LiDAR data also differ regarding water logging. Landslide plots in St. Antoenien were assessed to be significantly more affected by water logging, whereas the wTWI was significantly higher

in control plots. A reason for this may be that the wTWI is only based on topography and exposition and thus does not absolutely reflect the actual moisture conditions, which are also influenced by vegetation and soil properties (e.g. Pachepsky et al. 2004). The discrepancy might even point out the importance of the hydrological effect of vegetation and slope water discharge in the study area of St. Antoenien. Furthermore, the wTWI is possibly slightly biased as the single flow direction used in the calculation is not very exact (Ma et al. 2010).

Compared to the multivariate models based on LiDAR data, the models fitted with field variables performed considerably better. For Sachseln, too, the model performance could be enhanced by integrating variables derived from a stand classification. This implies that the resolution of the digital elevation model used in this study (cell size = 2 m) is too low to accurately detect local differences in forest structure influencing landslide susceptibility. In order to obtain more accurate results, elevation models with higher resolution are recommended (e.g. Morsdorf et al. 2004; Popescu and Wynne 2004; Wang 2004). However, acquisition of such data is associated with higher costs because they are not available for most regions. Given their availability, the usage of high precision elevation models from LiDAR would facilitate a more comprehensive assessment of landslide susceptibility in forested area and costs caused by time-consuming field investigations in mostly remote areas could be reduced. On the other hand, field investigations have the advantage that not only the measured variables but also the position of the release and the control points can be verified. In doing so, it can be prevented that control points also lie in landslide zones and thus distort.

Not only the spatial but also the temporal resolution of the LiDAR data is relevant to the accuracy of the results. The digital elevation models from 2003 available for St. Antoenien are expected to accurately represent the forest state before the landslides. The elevation models of Sachseln, however, date from 2006. For this reason, a bias because of the time lag cannot be excluded. Nevertheless, a relatively high validity of the here presented results can be assumed as the comparison of orthophotos did not reveal fundamental changes of forest cover in most of the plots. In order to guarantee undoubted accuracy, LiDAR data from shortly before and after the landslide event are required. Then, it would also be possible to derive changes in the forest structure caused by landslides from LiDAR data.

4.3. Predictive power of statistical models

For St. Antoenien as well as for Sachseln, random forest models (RF) are the best performing models based on the area under the ROC curve. The AUC values from the validation with the whole data set are in all cases higher than 0.9, which is an excellent discrimination according to Hosmer and Lemeshow (2000). Applying ten-fold cross-validation results in AUC values between 0.75 (*RF LiDAR*) and 0.84 (*RF all*). This confirms previous studies which evaluated random forest as a very successful classification model (e.g. Prasad et al. 2006; Barbeito et al. 2012; Vorpahl et al. 2012; Catani et al. 2013) and proves its suitability for landslide prediction modelling. The performance of logistic regression (LOG) was also satisfactory for all cases as the AUC value with and without cross-validation always exceeded 0.7. Classification trees (CT) achieved the worst performance. AUC values with cross-validation of CT based on topographic field variables (*CT topo*) or LiDAR data of St. Antoenien and Sachseln (*CT LiDAR*, *CT Sachseln*, *CT Sachseln+*) are below 0.6 and thus, the prediction accuracy is nearly random. This conforms to Vorpahl et al. (2012), who compared different classifiers for landslide prediction and found random forest and logistic regression among the best performing models, whereas classification trees exhibited worst performance.

The AUC values of all models distinctly decreased when implementing cross-validation. This proves that validation with the training data set positively biases the prediction accuracy (Brenning 2005; von Ruetten et al. 2011). Cross-validation, on the other hand, is regarded to provide a realistic picture of the model performance for an independent data set (von Ruetten et al. 2011). Aiming at even more realistic validation results, Brenning (2005) and Petschko et al. (2014) suggest spatial cross-validation which is based on spatial sub-sampling. The decline in the AUC value is especially pronounced for random forest and classification tree models. This indicates that they tend to overfit the data (Vorpahl et al. 2012), although random forests are regarded to be resistant against over-fitting (Breiman 2001; Strobl et al. 2009). Logistic regression appears to be the most robust model for the application to other regions. Brenning (2005) and Schicker and Moon (2012) also found best generalization capabilities for logistic regression compared to other classification models. In order to further assess whether the models are transferable to other regions, it would be recommended to validate them with a test data set. I decided to omit this because of the relatively small sample size. Partitioning of the data set would have engendered instable models and decreased their transferability (Petschko et al. 2014). Moreover, models designed for St. Antoenien were not applied to Sachseln and vice versa, because the statistical analysis showed that the two study sites strongly differ in landslide triggering factors and outcomes can hardly be generalized.

As the distances between the data points used in this study are rather small (smallest distance ≈ 10 m), they are expected to be autocorrelated and therefore, models might have yielded biased significance statements (Legendre 1993; Fortin and Dale 2005). Different methods have been proposed to cope with spatial autocorrelation by modifying logistic regression (e.g. Brenning 2005) or classification tree models (e.g. Bel et al. 2009; Zhao and Li 2011; Stojanova et al. 2013). Another method dealing with spatial nonstationarity is *Geographically Weighted Regression*, which estimates the

actual regression parameters for each location in space (see Brunsdon et al. 1996 for further details). However, a model which accurately represents spatial dependence is not required to achieve good predictive properties according to Brenning (2005). Furthermore, most authors modelling landslide susceptibility do not account for spatial autocorrelation (e.g. Atkinson and Massari 1998; von Ruetten et al. 2011; Vorpahl et al. 2012; Catani et al. 2013; Conforti et al. 2014). For this reasons, I did not consider it in this study.

Despite the drawbacks outlined above, the investigation methods proved to be suitable and revealed relevant information about the influence of the forest structure on landslide occurrence. It became evident, however, that further analysis with variables derived from field investigations and small footprint LiDAR data of larger data sets are required in order to get more generalisable results. Future work may also integrate physically based models which consider vegetation into statistical models in order to better comprehend root reinforcement processes.

5. Conclusions

The univariate and multivariate statistical analyses of this study show that forest structure substantially influences slope stability in forested areas. In addition to terrain features and tree coverage, gap length, the proxy-variable for root penetration of the nearest trees, tree height, tree edge density, successional stage and tree species significantly affected landslide susceptibility. The varying results between the two study sites indicate that the influence of these forest structural variables depends strongly on regional and local conditions, such as vegetation zones, altitudinal range, size of the study area and the triggering rainfall event. While plots with long gaps and low root penetration are more prone to landslides in St. Antoenien, the landslide susceptibility in Sachseln is mainly influenced by the vertical structure and forest composition as landslides predominantly occurred in young and coniferous or mixed stands.

The performance of the three different classifiers was generally acceptable (AUC \geq 0.7), except for classification trees, which partially exhibited lower AUC values. Random forest was the best performing model, followed by logistic regression. It can be assumed that terrain feature and forest structure do not solely determine slope failure, since the multivariate models did not exhibit excellent performance in most cases. Variables of soil properties and geology, which were not considered here, have thus probably also an important influence on landslide occurrence.

Differences were also found between variables assessed in the field and those derived from LiDAR data. Certain factors (e.g. gap length or distance to the nearest tree), which highly affect slope stability according to the field investigation, could not be ascertained with the LiDAR data. Furthermore, multivariate models based on LiDAR derived variables performed considerably worse than the models based on field data. Therefore, I conclude that digital elevation models with a resolution of 2 m are too imprecise in order to detect local differences in forest structure which influence slope stability.

Despite obvious limitations of the assessment methods and the sample size, the findings of this study expand the knowledge about the effects of forest structure on slope stability and might help to develop more small-scale, physically based models which integrate root reinforcement. Future research should also include field and LiDAR based analyses of larger data sets, comprising different study areas, in order to get more general results which are useful for practitioners in natural hazard management and protection forests.

6. References

- ABE, K. AND R. R. ZIEMER (1991). Effects of tree roots on a shear zone: modeling reinforced shear stress. *Canadian Journal of Forest Research* **21**: 1012-1019.
- AMMANN, M., A. BÖLL, C. RICKLI, T. SPECK AND O. HOLDENRIEDER (2009). Significance of tree root decomposition for shallow landslides. *Forest, Snow and Landscape Research* **82**(1): 79-94.
- ANDERSEN, H.-E. (2009). Using airborne light detection and ranging (LIDAR) to characterize forest stand condition on the Kenai Peninsula of Alaska. *Western journal of applied forestry* **24**(2): 95-102.
- ATKINSON, P. M. AND R. MASSARI (1998). Generalised linear modelling of susceptibility to landsliding in the central Apennines, Italy. *Computers & Geosciences* **24**(4): 373-385.
- AYALEW, L. AND H. YAMAGISHI (2005). The application of GIS-based logistic regression for landslide susceptibility mapping in the Kakuda-Yahiko Mountains, Central Japan. *Geomorphology* **65**(1-2): 15-31.
- BARBEITO, I., M. A. DAWES, C. RIXEN, J. SENN AND P. BEBI (2012). Factors driving mortality and growth at treeline: a 30-year experiment of 92 000 conifers. *Ecology* **93**(2): 389-401.
- BATHURST, J. C., C. I. BOVOLO AND F. CISNEROS (2010). Modelling the effect of forest cover on shallow landslides at the river basin scale. *Ecological Engineering* **36**(3): 317-327.
- BEL, L., D. ALLARD, J. M. LAURENT, R. CHEDDADI AND A. BAR-HEN (2009). CART algorithm for spatial data: Application to environmental and ecological data. *Computational Statistics & Data Analysis* **53**(8): 3082-3093.
- BREIMAN, L. (2001). Random Forests. *Machine Learning* **45**: 5.
- BRENNING, A. (2005). Spatial prediction models for landslide hazard: review, comparison, evaluation. *Natural Hazards and Earth System Sciences* **5**(6): 853-862.
- BRUNSDON, C., A. S. FOTHERINGHAM AND M. E. CHARLTON (1996). Geographically Weighted Regression: A method for exploring spatial nonstationarity. *Geographical Analysis* **28**(4): 282-297.
- BURROUGH, P. A. AND R. A. MCDONNELL (1998). Principles of Geographical Information Systems. New York, Oxford University Press: 190.
- CARRARA, A., G. CROSTA AND P. FRATTINI (2003). Geomorphological and historical data in assessing landslide hazard. *Earth Surface Processes and Landforms* **28**(10): 1125-1142.
- CARRARA, A. AND R. J. PIKE (2008). GIS technology and models for assessing landslide hazard and risk. *Geomorphology* **94**(3-4): 257-260.
- CASADEI, M., W. E. DIETRICH AND N. MILLER (2003). Controls on shallow landslide size. *Debris-flow Hazards Mitigation: Mechanics, Prediction, and Assessment* **1-2**: 91-101.
- CATANI, F., D. LAGOMARSINO, S. SEGONI AND V. TOFANI (2013). Landslide susceptibility estimation by random forests technique: sensitivity and scaling issues. *Natural Hazards and Earth System Science* **13**(11): 2815-2831.
- CHA, K.-S. AND T.-H. KIM (2011). Evaluation of slope stability with topography and slope stability analysis method. *KSCE Journal of Civil Engineering* **15**(2): 251-256.

- CHEN, Y. AND X. ZHU (2013). An integrated GIS tool for automatic forest inventory estimates of *Pinus radiata* from LiDAR data. *GIScience and Remote Sensing* **50**(6): 667-689.
- CONFORTI, M., S. PASCALE, G. ROBUSTELLI AND F. SDAO (2014). Evaluation of prediction capability of the artificial neural networks for mapping landslide susceptibility in the Turbolo River catchment (northern Calabria, Italy). *Catena* **113**: 236-250.
- D'AMATO AVANZI, G., R. GIANNECCHINI AND A. PUCCINELLI (2004). The influence of the geological and geomorphological settings on shallow landslides. An example in a temperate climate environment: the June 19, 1996 event in northwestern Tuscany (Italy). *Engineering Geology* **73**(3-4): 215-228.
- DAI, F. AND C. F. LEE (2002). Landslides on natural terrain. Physical characteristics and susceptibility mapping in Hong Kong. *Mountain Research and Development* **22**(1): 40-47.
- DALGAARD, P. (2008). *Introductory Statistics with R*. New York, Springer Science+Business Media.
- DANCEY, C. P. AND J. REIDY (2011). *Statistics without maths for psychology*, Pearson Education.
- DASSOT, M., T. CONSTANT AND M. FOURNIER (2011). The use of terrestrial LiDAR technology in forest science: application fields, benefits and challenges. *Annals of Forest Science* **68**(5): 959-974.
- DE'ATH, G. AND K. E. FABRICIUS (2000). Classification and regression trees: a powerful yet simple technique for ecological data analysis. *Ecology* **81**(11): 3178-3192.
- EDSON, C. AND M. G. WING (2011). Airborne Light Detection and Ranging (LiDAR) for individual tree stem location, height, and biomass measurements. *Remote Sensing* **3**(12): 2494-2528.
- ESRI (2013). Software ESRI ArcGIS 10.2.
- FAWCETT, T. (2003) ROC Graphs: notes and practical considerations for data mining researchers. 28.
- FELICÍSIMO, Á. M., A. CUARTERO, J. REMONDO AND E. QUIRÓS (2012). Mapping landslide susceptibility with logistic regression, multiple adaptive regression splines, classification and regression trees, and maximum entropy methods: a comparative study. *Landslides* **10**(2): 175-189.
- FERNANDES, N. F., R. F. GUIMARÃES, R. A. T. GOMES, B. C. VIEIRA, D. R. MONTGOMERY AND H. GREENBERG (2004). Topographic controls of landslides in Rio de Janeiro: field evidence and modeling. *Catena* **55**(2): 163-181.
- FORTIN, M.-J. AND M. R. T. DALE (2005). *Spatial analysis. A guide for ecologists*. Cambridge, Cambridge University Press.
- FREHNER, M., B. WASSER AND R. SCHWITTER (2005). Nachhaltigkeit und Erfolgskontrolle im Schutzwald. Wegleitung für Pflegemassnahmen in Wäldern mit Schutzfunktion. . *Vollzug Umwelt. Bundesamt für Umwelt, Wald und Landschaft, Bern.*: 564.
- GINZLER, C., H. BÄRTSCHI, A. BEDOLLA, P. BRASSEL, M. HÄGELI, M. HAUSER, M. KAMPHUES, L. LARANJEIRO, L. MATHYS, D. UEBERSAX, E. WEBER, P. WICKI AND D. ZULLIGER (2005). *Luftbildinterpretation LFI3. Interpretationsanleitung zum dritten Landesforstinventar*. Birmensdorf, Swiss Federal Institut for Forest, Snow and Landscape Research WSL.

- GOETZ, J. N., R. H. GUTHRIE AND A. BRENNING (2011). Integrating physical and empirical landslide susceptibility models using generalized additive models. *Geomorphology* **129**(3-4): 376-386.
- GORSEVSKI, P. V., P. E. GESSLER, J. BOLL, W. J. ELLIOT AND R. B. FOLTZ (2006). Spatially and temporally distributed modeling of landslide susceptibility. *Geomorphology* **80**(3-4): 178-198.
- GRAF, F., P. BEBI, C. RIXEN, C. RICKLI, S. SPRINGMAN AND M. FREI (2012). Soil stability and natural hazards: from knowledge to action. *Full proposal NRP 68: Sustainable use of soil as a resource*. Berne, Swiss National Science Foundation: 25.
- GRAY, D. H. (1973). Effects of Forest Clear-Cutting on the Stability of Natural Slopes: Results of Field Studies. Michigan, Department of Civil Engineering, University of Michigan: 134.
- GRAY, D. H. (1996). *Biotechnical and soil bioengineering slope stabilization: a practical guide for erosion control*, John Wiley & Sons, Inc.
- GUNS, M. AND V. VANACKER (2013). Forest cover change trajectories and their impact on landslide occurrence in the tropical Andes. *Environmental Earth Sciences* **70**(7): 2941-2952.
- GUZZETTI, F., A. CARRARA, M. CARDINALI AND P. REICHENBACH (1999). Landslide hazard evaluation: a review of current techniques and their application in a multi-scale study, Central Italy. *Geomorphology* **31**: 181-216.
- HASTIE, T., R. TIBSHIRANI AND J. FRIEDMAN (2008). *The Elements of Statistical Learning. Data Mining, Inference, and Prediction*, Springer.
- HEDIGER, M., GINZLER, CH., KÖCHLI, D. (2012). Erkennung von Waldstrukturen aus flugzeuggestützten Fernerkundungsdaten - Vergleich von Airborne Laserscanning und digitaler Photogrammetrie. *Angewandte Geoinformatik*. Berlin/Offenbach, Strobl, J., Blaschke, T., Griesebner, G.
- HOSMER, D. W. AND S. LEMESHOW (2000). *Applied logistic regression*. New York, John Wiley and Sons, Inc.
- HOTHORN, T., K. HORNIK, C. STROBLE AND A. ZEILEIS (2013). A Laboratory for Recursive Partitioning.
- HYPPÄ, J., H. HYPPÄ, D. LECKIE, F. GOUGEON, X. YU AND M. MALTAMO (2008). Review of methods of small-footprint airborne laser scanning for extracting forest inventory data in boreal forests. *International Journal of Remote Sensing* **29**(5): 1339-1366.
- IMAIZUMI, F., R. C. SIDLE AND R. KAMEI (2008). Effects of forest harvesting on the occurrence of landslides and debris flows in steep terrain of central Japan. *Earth Surface Processes and Landforms* **33**(6): 827-840.
- JING, L., B. HU, J. LI AND T. NOLAND (2012). Automated delineation of individual tree crowns from Lidar data by multi-scale analysis and segmentation. *Photogrammetric Engineering & Remote Sensing* **78**(12): 1275-1284.
- KEIM, R. F. AND A. E. SKAUGSET (2003). Modelling effects of forest canopies on slope stability. *Hydrological Processes* **17**(7): 1457-1467.
- KELLER, M. R. (2005). Schweizerisches Landesforstinventar. Anleitung für die Feldaufnahmen der Erhebung 2004-2007. E. F. WSL. Birmensdorf: 393.
- KIM, D., S. IM, C. LEE AND C. WOO (2013). Modeling the contribution of trees to shallow landslide development in a steep, forested watershed. *Ecological Engineering* **61**: 658-668.

- KOUKOULAS, S. AND G. A. BLACKBURN (2004). Quantifying the spatial properties of forest canopy gaps using LiDAR imagery and GIS. *International Journal of Remote Sensing* **25**(15): 3049-3072.
- LATELTIN, O. (1997). Berücksichtigung der Massenbewegungsgefahren bei raumwirksamen Tätigkeiten - Empfehlungen. B. f. R. BRP et al. Bern: 42.
- LEATHWICK, J. R., J. ELITH AND T. HASTIE (2006). Comparative performance of generalized additive models and multivariate adaptive regression splines for statistical modelling of species distributions. *Ecological Modelling* **199**(2): 188-196.
- LEFSKY, M. A., W. B. COHEN, G. P. PARKER AND D. J. HARDING (2002). Lidar remote sensing for ecosystem studies. *Bioscience* **52**(1): 20-31.
- LEGENBRE, P. (1993). Spatial autocorrelation: trouble or new paradigm? *Ecology* **74**(6): 1659-1673.
- LIU, X., J. PETERSON AND Z. ZHANG (2005). *High-resolution DEM generated from LiDAR data for water resource management*. MODSIM05: International Congress on Modelling and Simulation: Advances and Applications for Management and Decision Making, Melbourne, Australia.
- MA, J., G. LIN, J. CHEN AND L. YANG (2010). An improved Topographic Wetness Index considering topographic position. *Geoinformatics, 2010 18th International Conference on*. Beijing: 1-4.
- MATHYS, L. (2005). Erfassung von Waldlücken mittels Laserscanning. *Schweizerische Zeitschrift für Forstwesen* **156**(10): 372-377.
- MILLER, D. J. AND K. M. BURNETT (2007). Effects of forest cover, topography, and sampling extent on the measured density of shallow, translational landslides. *Water Resources Research* **43**(3).
- MONTGOMERY, D. R. AND W. E. DIETRICH (1994). A physically based model for the topographic control on shallow landslide *Water Resources Research* **30**(4): 1153-1171.
- MONTGOMERY, D. R., K. M. SCHMIDT, H. M. GREENBERG AND W. E. DIETRICH (2000). Forest clearing and regional landsliding. *Geology* **28**(4): 311-315.
- MOORE, D. S. AND G. P. MCCABE (2005). *Introduction to the practice of statistics*, W.H. Freeman & Co.
- MORS DORF, F. (2011). Erfassung struktureller Waldparameter mithilfe von flugzeuggetragenem Laserscanning | Deriving structural forest parameters using airborne laser scanning. *Schweizerische Zeitschrift für Forstwesen* **162**(6): 164-170.
- MORS DORF, F., E. MEIER, B. KÖTZ, K. I. ITTEN, M. DOBBERTIN AND B. ALLGÖWER (2004). LIDAR-based geometric reconstruction of boreal type forest stands at single tree level for forest and wildland fire management. *Remote Sensing of Environment* **92**(3): 353-362.
- NEFESLIOGLU, H. A., E. SEZER, C. GOKCEOGLU, A. S. BOZKIR AND T. Y. DUMAN (2010). Assessment of landslide susceptibility by decision trees in the metropolitan area of Istanbul, Turkey. *Mathematical Problems in Engineering* **2010**: 1-16.
- NILAWEEERA, N. S. AND P. NUTALAYA (1999). Role of tree roots in slope stabilisation. *Bulletin of Engineering Geology and the Environment* **57**: 337-342.
- PACHEPSKY, Y., D. E. RADCLIFF AND M. H. SELIM (2004). *Scaling methods in soil physics*. Y. Pachepsky et al., CRC Press: 456.
- PECKHAM, S. D. (2011). Profile, plan and streamline curvature: a simple derivation and applications. *Geomorphometry.org*: 27-30.

- PETSCHKO, H., A. BRENNING, R. BELL, J. GOETZ AND T. GLADE (2014). Assessing the quality of landslide susceptibility maps – case study Lower Austria. *Natural Hazards and Earth System Science* **14**(1): 95-118.
- PIACENTINI, D., F. TROIANI, M. SOLDATI, C. NOTARNICOLA, D. SAVELLI, S. SCHNEIDERBAUER AND C. STRADA (2012). Statistical analysis for assessing shallow-landslide susceptibility in South Tyrol (south-eastern Alps, Italy). *Geomorphology* **151-152**: 196-206.
- POPESCU, S. C. AND R. H. WYNNE (2004). Seeing the trees in the forest: using Lidar and multispectral data fusion with local filtering and variable window size foresting tree height. *Photogrammetric Engineering & Remote Sensing* **70**(5): 589-604.
- PRASAD, A. M., L. R. IVERSON AND A. LIAW (2006). Newer classification and regression tree techniques: bagging and random forests for ecological prediction. *Ecosystems* **9**(2): 181-199.
- PRETI, F. (2013). Forest protection and protection forest: Tree root degradation over hydrological shallow landslides triggering. *Ecological Engineering* **61**: 633-645.
- REUBENS, B., J. POESEN, F. DANJON, G. GEUDENS AND B. MUYS (2007). The role of fine and coarse roots in shallow slope stability and soil erosion control with a focus on root system architecture: a review. *Trees* **21**(4): 385-402.
- RICKLI, C. AND H. BUCHER (2003). Oberflächennahe Rutschungen, ausgelöst durch die Unwetter vom 15.-16.7.2002 im Napfgebiet und vom 31.8.-1.9.2002 im Gebiet Appenzell - Projektbericht zuhanden des Bundesamtes für Wasser und Geologie BWG., Swiss Federal Institute for Forest, Snow and Landscape Research, WSL: 100.
- RICKLI, C. AND F. GRAF (2009). Effects of forests on shallow landslides – case studies in Switzerland. *Forest, Snow and Landscape Research* **82**(1): 33-44.
- RICKLI, C., S. KAMM AND H. BUCHER (2008). Projektbericht Ereignisanalyse Hochwasser 2005 - Teilprojekt "Flachgründige Rutschungen": 114.
- RICKLI, C., K. ZÜRCHER, W. FREY AND P. LÜSCHER (2002). Wirkungen des Waldes auf oberflächennahe Rutschprozesse. *Schweizerische Zeitschrift für Forstwesen* **153**(11): 437-445.
- RICKLI, C. R. (2001). Vegetationswirkungen und Rutschungen - Untersuchung zum Einfluss der Vegetation auf oberflächennahe Rutschprozesse anhand der Unwetterereignisse in Sachslen OW am 15. Augsut 1997. . W. u. L. B. Bundesamt für Umwelt. Birmensdorf, Bern, Eidgenössische Forschungsanstalt WSL: 97.
- SCHICKER, R. AND V. MOON (2012). Comparison of bivariate and multivariate statistical approaches in landslide susceptibility mapping at a regional scale. *Geomorphology* **161-162**: 40-57.
- SCHMIDT, K. M., J. J. ROERING, J. D. STOCK, W. E. DIETRICH, D. R. MONTGOMERY AND T. SCHAUB (2001). The variability of root cohesion as an influence on shallow landslide susceptibility in the Oregon Coast Range. *Canadian Geotechnical Journal* **38**(5): 995-1024.
- SIDLE, R. C. (1992). A Theoretical Model of the Effects of Timber Harvesting on Slope Stability. *Water Resources Research* **28**(7): 1897.
- SIDLE, R. C. (2006). Landslides: processes, prediction, and land use. R. C. Sidle and H. Ochiai. Washington, DC, American Geophysical Union.
- SØRENSEN, R., U. ZINKO AND J. SEIBERT (2006). On the calculation of the topographic wetness index: evaluation of different methods based on field observations. *Hydrology and Earth System Sciences* **10**: 101-112.

- STAHEL, W. (2013). *Lineare Regression*. Seminar für Statistik, ETH Zürich.
- STARWEATHER, J. (2011). Cross Validation techniques in R: A brief overview of some methods, packages, and functions for assessing prediction models. *JDS*.
- STEYERBERG, E. W., F. E. HARRELL JR, G. J. J. M. BORSBOOM, E. R. M.J.C. AND H. J. D. F. VERGOUWE YVONNE (2001). Internal validation of predictive models: Efficiency of some procedures for logistic regression analysis. *Journal of Clinical Epidemiology* **54**: 774-781.
- STOJANOVA, D., M. CECI, A. APPICE, D. MALERBA AND S. DŽEROSKI (2013). Dealing with spatial autocorrelation when learning predictive clustering trees. *Ecological Informatics* **13**: 22-39.
- STROBL, C., A. L. BOULESTEIX, T. KNEIB, T. AUGUSTIN AND A. ZEILEIS (2008). Conditional variable importance for random forests. *BMC Bioinformatics* **9**: 307.
- STROBL, C., J. MALLEY AND G. TUTZ (2009). An introduction to recursive partitioning: rationale, application and characteristics of classification and regression trees, bagging and random forests. München, University of Munich: 50.
- SWISSTOPO (2001). SWISSIMAGE. B. f. Landestopographie. Wabern, Bern.
- SWISSTOPO (2013). Vector25: TLM Gebaeude Footprint 2013. s. (DV033594). Wabern, Bern.
- SWISSTOPO (2014). Kartendaten DTM-AV DOM-AV E. V. (CV033531).
- TEAM, R. D. C. (2012). R: A language and environment for statistical computing. . Vienna, Austria, R Foundation for Statistical Computation.
- TEMPERLI, R. (2006). *Analyse der Rutschaktivität in Waldflächen in Bezug auf deren Zustand und Nutzung. Fallstudie in St. Antönien GR*. Diplomarbeit, Hochschule Wädenswil.
- ULRICH, M. (2008). *Strukturerfassung und Dynamik von waldgrenznahen Wäldern mit verminderter Lawinenschutzwirksamkeit in der Landschaft Davos* Bachelorarbeit, Zürcher Hochschule für Angewandte Wissenschaften.
- VERGANI, C., E. A. CHIARADIA AND G. B. BISCHETTI (2012). Variability in the tensile resistance of roots in Alpine forest tree species. *Ecological Engineering* **46**: 43-56.
- VON RUETTE, J., A. PAPRITZ, P. LEHMANN, C. RICKLI AND D. OR (2011). Spatial statistical modeling of shallow landslides—Validating predictions for different landslide inventories and rainfall events. *Geomorphology* **133**(1-2): 11-22.
- VORPAHL, P., H. ELSENBEEER, M. MÄRKER AND B. SCHRÖDER (2012). How can statistical models help to determine driving factors of landslides? *Ecological Modelling* **239**: 27-39.
- WASEL, Y., A. ESHEL AND U. KAFKAFI (2002). Plant roots - The hidden half. Y. Waisel et al., CRC Press: 1136.
- WANG, L., GONG, P., BIGING, G.S. (2004). Individual tree-crown delineation and treetop detection in high-spatial-resolution aerial imagery. *Photogrammetric Engineering & Remote Sensing* **70**(3): 351-357.
- WARD, A. D. AND S. W. TRIMBLE (2004). Environmental hydrology. A. D. Ward and W. J. Elliott, CRC Press: 504.
- WU, W. AND R. C. SIDLE (1995). A distributed slope stability model for steep forested basins. *Water Resources Research* **31**(8): 2097-2110.

YEON, Y.-K., J.-G. HAN AND K. H. RYU (2010). Landslide susceptibility mapping in Injae, Korea, using a decision tree. *Engineering Geology* **116**(3-4): 274-283.

ZELLWEGER, F., V. BRAUNISCH, A. BALTENSWEILER AND K. BOLLMANN (2013). Remotely sensed forest structural complexity predicts multi species occurrence at the landscape scale. *Forest Ecology and Management* **307**: 303-312.

ZEVENBERGEN, L. W. AND C. R. THRONE (1987). Quantitative analysis of land surface topography. *Earth Surface Processes and Landforms* **12**: 47-56.

ZHAO, M. AND X. LI (2011). *An application of spatial decision tree for classification of air pollution index*. 19th International Conference on Geoinformatics, IEEE.

ZWEIG, M. H. AND G. CAMPBELL (1993). Receiver-Operating Characteristic (ROC) plots: A fundamental evaluation tool in clinical medicine. *Clinical Chemistry* **39**(4): 561-577.

Appendix A: Field protocol

Aufnahmeformular Rutschungen im Wald

Untersuchungsgebiet: St. Antönien

Protokollführer: _____

Datum: _____

1. Lokalisierung

1.1 Nr. _____ 1.2 Koordinaten: _____ / _____

1.3 Rutschung Kontroll

1.4 Exposition: _____ ° 1.5 Höhe: _____ m.ü.M.

1.5 Fotonummer: _____

2. Topographie

2.1 Geomorphologietyp (nach Rickli und Bucher, 2003): _____

2.2 Neigung Anrisspunkt: _____ °

2.3 Neigung 15 m oberhalb: _____ °

2.4 Neigung 15 m unterhalb: _____ °

2.5 Bemerkungen: _____

3. Waldstruktur (30x30 m² um (pot.) Anrisspunkt)

3.1 Oberhöhe (geschätzte maximale Höhe der Bäume): _____ m

3.2 Kronendeckungsgrad (auf 5%): _____ %

3.3 Schlussgrad: unbestockt aufgelöst (20%) lückig (40%) normal (80%) gedrängt (90%)

3.4 Vertikale Struktur

Deckungsgrad in der Bestandesschicht (auf 5%) Unter-: _____ % Mittel-: _____ %

Oberschicht: _____ %

3.5 Sukzessionsstadium

Anteil Bäume (auf 5%) 13-30 cm _____ % 30-50 cm _____ % > 50 cm _____ %

3.6 Waldzustand: W1 W2 W3

3.7 Totholz (Wurzelstock, stehend, liegend)

Abstand Anriss zum nächsten Totholz: _____ m > 10 m Art: _____

Zustand: _____

Anteil Totholz stehend: < 1% 1-5% 5-20% > 20%

Anteil Totholz liegend: < 1% 1-5% 5-20% > 20%

3.8 Distanz zu den 5 nächsten Bäumen (ab BHD = 12 cm)

Baum 1 _____ m 13-30cm 30-50 cm > 50 cm

Baum 2 _____ m 13-30cm 30-50 cm > 50 cm

Baum 3 _____ m 13-30cm 30-50 cm > 50 cm

Baum 4 _____ m 13-30cm 30-50 cm > 50 cm

Baum 5 _____ m 13-30cm 30-50 cm > 50 cm

3.9 Bemerkungen: (Baumarten falls etwas anderes als Fichte) _____

3.10 Bestandeslücke (grösste Lücke im Untersuchungsplot)

Max. Länge (m): _____

Max. Breite (m): _____

4. Verjüngung (BHD < 12 cm) im Untersuchungsplot

4.1 Arten (nach Menge geordnet): _____

4.2 Ansamung/Jungwuchs (<40 cm): <1% 1-9% 10-25% > 25%

4.3 Dückung (40 cm-12 cm BHD): <1% 1-9% 10-25% > 25%

4.4 Bemerkungen: _____

4.5 Deckungsgrad Bodenvegetation (auf 10%): _____

5. Boden (nur in Kontrollflächen)

5.1 Bezeichnung Horizont 1: _____ Mächtigkeit (cm): _____

5.2 Bezeichnung Horizont 2: _____ Mächtigkeit (cm): _____

5.3 Bezeichnung Horizont 3: _____ Mächtigkeit (cm): _____

5.4 Bezeichnung Horizont 4: _____ Mächtigkeit (cm): _____

5.5 Bezeichnung Horizont 5: _____ Mächtigkeit (cm): _____

5.6 Bezeichnung Horizont 6: _____ Mächtigkeit (cm): _____

5.7 Anzeichen alter Rutschbewegungen: keine undeutlich markant

5.8 Bemerkungen: _____

6. Hydrologie

6.1 Anzeichen von Vernässung: nein undeutlich markant

6.2 Bemerkungen: _____

6.3 Hangwasseraustritte und/oder Versickerungsstellen: ja nein

6.4 Anzeichen von Verdichtung (Fahrspuren, stehendes Wasser): nein undeutlich
 markant

6.5 Bemerkungen: _____

7. Beweidung / Bewirtschaftung

6.1 Anzeichen von Beweidung / landwirtschaftliche Bewirtschaftung: nein schwach
 intensive Beweidung / Bewirtschaftung

6.2 Bemerkungen: _____

Anleitung und Kommentar zum Aufnahmeformular

Untersuchungsplots:

- Rutschung: gemäss Koordinaten der Rutschungsinventur von Rickli et al., 2005, Anrisspunkt in der Mitte des Anrisses, Untersuchungsplot: 30 m x 30 m um Anrisspunkt
- Kontrollfläche: Der potentielle Anrisspunkt entspricht dem Kontrollpunkt (Koordinaten gemäss GIS-Analysen). Untersuchungsplot: 30 m x 30 m um pot. Anrisspunkt

1.1 Nummer: K_ für Kontrollfläche, R_ für Rutschung

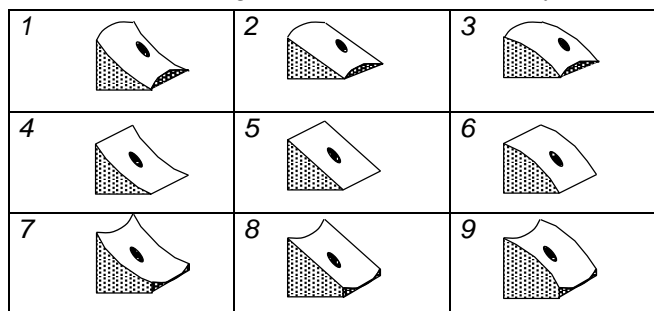
1.2 Koordinaten mit GPS, falls kein Empfang: mit Landkarte

1.4 Exposition: Hangrichtung, mit dem Kompass auf 10° genau.

1.5 Höhe über Meer: GPS

2.1 Geomorphologietyp nach Rickli und Bucher, 2003: Zahl 1 bis 9

Table A1: Codierung der verschiedenen Geländeformen.



2.2 – 2.4 Neigung: Messung mit Neigungsmesser

3.1 Oberhöhe: Geschätzte Höhe der höchsten Bäume im Plot. Zuerst Eichung mit Höhenmesser, dann schätzen

3.2 Kronendeckungsgrad: auf 5% genau schätzen

3.3 Schlussgrad: Basierend auf Kronendeckungsgrad.

3.4 Deckungsgrad in der Bestandesschicht (→ Anteil der einzelnen Schichten an DG): auf 5% Schätzen. Unterschicht: 0.40m Höhe bis 1/3 der Oberhöhe, Mittelschicht: 1/3 bis 2/3 der Oberhöhe, Oberschicht: 2/3 bis 3/3 der Oberhöhe.

3.5 Sukzessionsstadium: Anteil der Bäume in den versch. Durchmesserklassen auf 5% schätzen (Stammzahl).

3.6 Waldzustand: Gemäss Rickli, 2001

3.7 Totholz: Abstand zwischen (potentiellem) Anrisspunkt und dem nächsten Totholz mit Messband messen. Unter Totholz fallen liegende und stehende abgestorbene Stämme und Wurzelstöcke (> Art).

> Zustand:

- | | |
|---------------|---|
| 1 Frischholz: | saftführend |
| 2 Totholz: | saftlos, fest; das Messer dringt in Faserrichtung nur sehr schwer ein |
| 3 Morschholz: | weniger fest; das Messer dringt in Faserrichtung leicht ein, nicht aber quer. |
| 4 Moderholz: | weich; das Messer dringt in jeder Richtung leicht ein. |
| 5 Mulmholz: | sehr locker oder pulverig; kaum noch zusammenhängend. |

Anteil Totholz stehend / liegend in Kategorien schätzen.

Falls kein Totholz vorhanden: leer lassen.

3.8 Abstand zu den 5 nächsten Bäumen mit Messband messen. Baum einer Durchmesser-kategorie zuordnen. Falls keine Fichte, wird Baumart in den Bemerkungen festgehalten.

3.10 Bestandeslücke: Grösste Lücke im Untersuchungsplot (auch wenn sie über den Plot hinausgeht). Maximale Länge / Breite abschätzen.

4.1 Verjüngung im Untersuchungsplot: Arten nach Menge geordnet. Schätzung des Anteils (Stammzahl) versch. Verjüngungsstufen in Kategorien.

4.2 Ansamung/Jungwuchs: < 40 cm Höhe

4.3 Dickung: 40 cm Höhe – 12 cm BHD.

4.5 Deckungsgrad der Bodenvegetation auf 10% genau schätzen.

5. Boden: Untersuchung des Bodens nur in Kontrollflächen mit Bohrstock (bei pot. Anrisspunkt). Bestimmung der Horizontabfolge und der Mächtigkeit der Horizonte.

5.7 Anzeichen alter Rutschbewegungen: Anhand Geländeform, evt. Vegetation → in Bemerkungen festhalten.

6.1 Anzeichen von Vernässung: Feuchtezeiger, anhand Bodenprofil, stehendes Wasser → unter Bemerkungen festhalten.

6.4 Anzeichen von Verdichtung anhand Fahrspuren, Trittbermen, stehendes Wasser.

7. Anzeichen von Beweidung / landwirtschaftlicher Bewirtschaftung: Trittspuren, Zäune, Frassspuren, etc.

Appendix B: Correlation diagram

I plotted the variables measured in the field and derived from LiDAR data against each other and computed the *Spearman* correlation coefficient in order to assess whether they are correlated.

B1. St. Antoenien field data



Fig. 1: Pairs plot with Spearman correlation coefficient of 12 variables measured in St. Antoenien. Abbreviations for variable names are explained in Tab. 1.

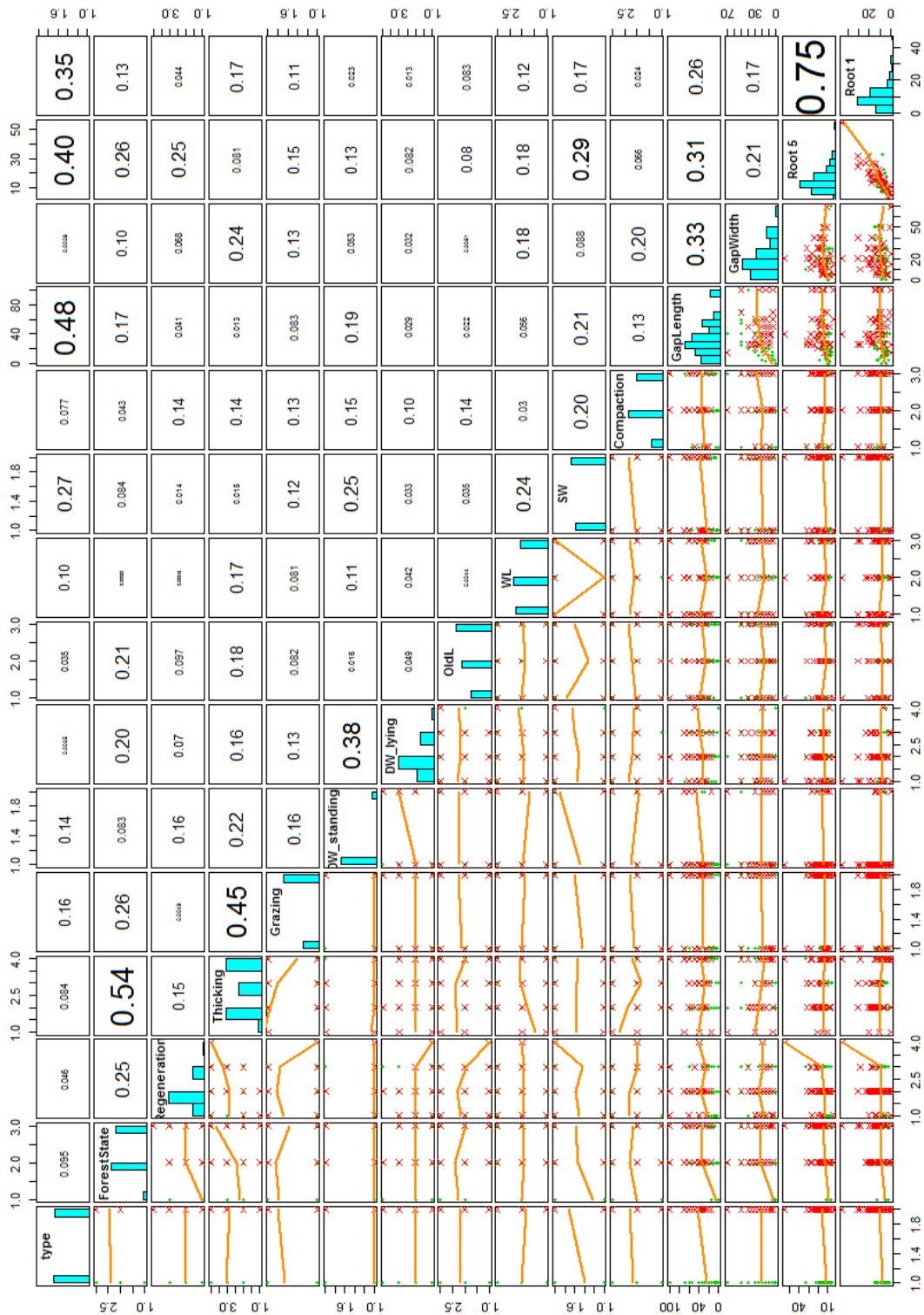


Fig. 2: Pairs plot with Spearman correlation coefficient of the remaining variables measured in St. Antoenien. Abbreviations for variable names are explained in Tab. 1.

Tab. 1: Abbreviations used in Fig. 1 and Fig. 2 for the variables assessed in the field.

Abbreviation	Explanation
Geo	Geomorphology typ
Slope	Slope angle release point
Slope above	Slope angle 15 m above
Slope below	Slope angle 15 m below
maxHeight	Maximum tree height
TreeCoverage	Tree coverage
SubLayer	Coverage of the sub layer
MiddleLayer	Coverage of the middle layer
UpperLayer	Coverage of the upper layer
dbh1	dbh 13-30 cm
dbh2	dbh 30-50 cm
dbh3	dbh > 50 cm
ForestState	Forest state
Regeneration	Regeneration (young growth) < 40 cm
Thinning	Thinning 40 cm height – 13 cm dbh
Grazing	Signs of grazing cattle
DW_standing	Deadwood standing
DW_lying	Deadwood lying
OldL	Signs of old landslides
WL	Signs of water logging
SW	Signs of slope water discharge
Compaction	Soil compaction
GapLength	Length of the largest gap
GapWidth	Width of the largest gap
Root 5	Proxy-variable for root penetration of the 5 nearest trees
Root 1	Proxy-variable for root penetration of the nearest tree

B2. St. Antoenien LiDAR data

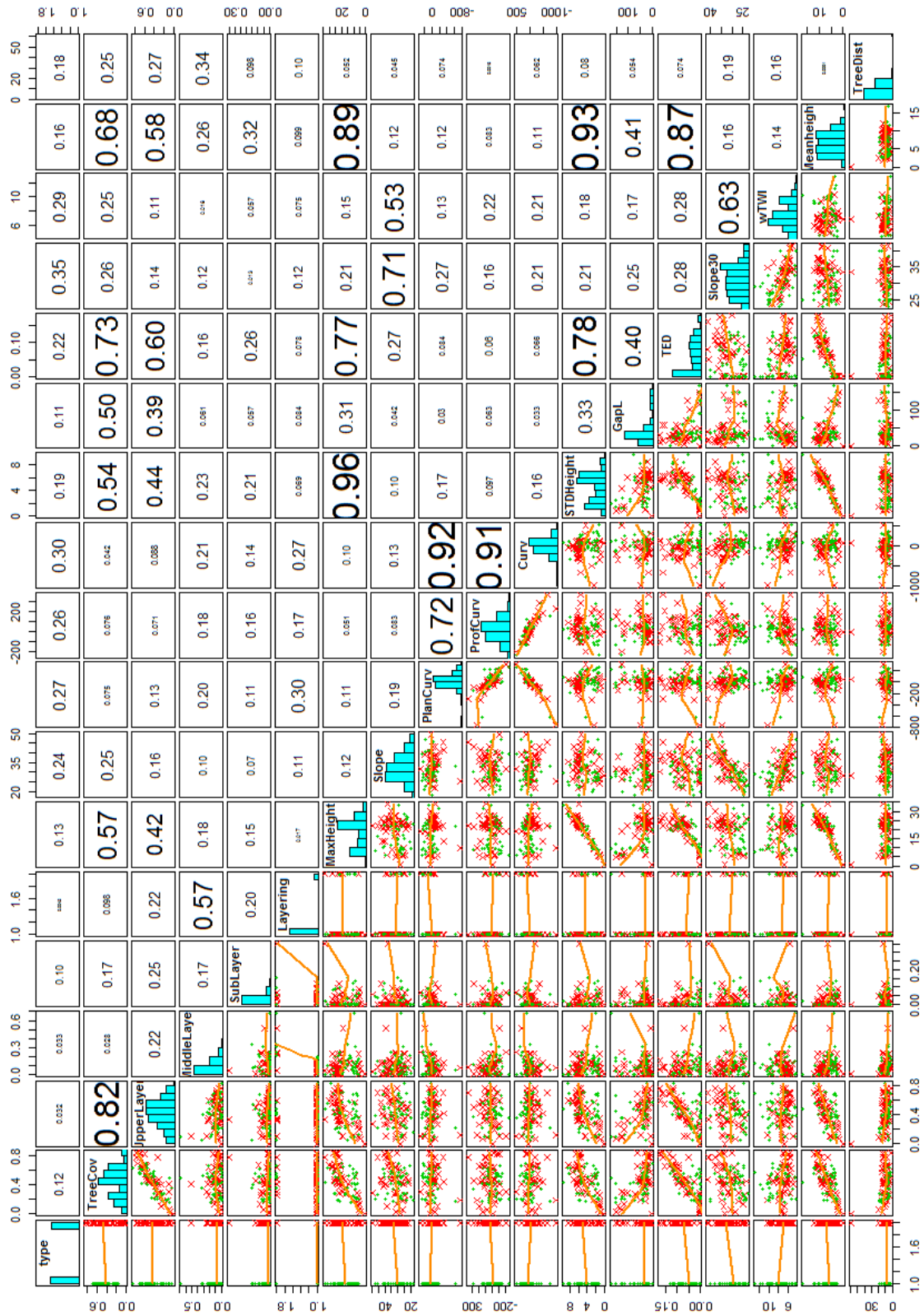


Fig. 3: Pairs plot with Spearman correlation coefficient of the variables derived from LiDAR data of St. Antoenien. Abbreviations for variable names are explained in Tab. 2.

Tab. 2: Abbreviations used in Fig. 3 for the variables derived from LiDAR data.

Abbreviation	Explanation
TreeCov	Tree coverage
UpperLayer	Coverage of the upper layer
MiddleLayer	Coverage of the middle layer
SubLayer	Coverage of the sub layer
Layering	Layering
MaxHeight	Maximum tree height
Slope	Slope angle at the release point
PlanCurv	Planform curvature (30 m x 30 m)
ProfCurv	Profile curvature (30 m x 30 m)
Curv	Curvature (30 m x 30 m)
STDHeight	Standard deviation tree height
GapL	Length of the largest gap
TED	Tree edge density
Slope30	Mean slope (30 m x 30 m)
OldL	Signs of old landslides
wTWI	Weighted Topographic Wetness Index (30 m x 30 m)
meanheight	Mean tree height
TreeDist	Distance to the nearest tree

B3. Sachseln

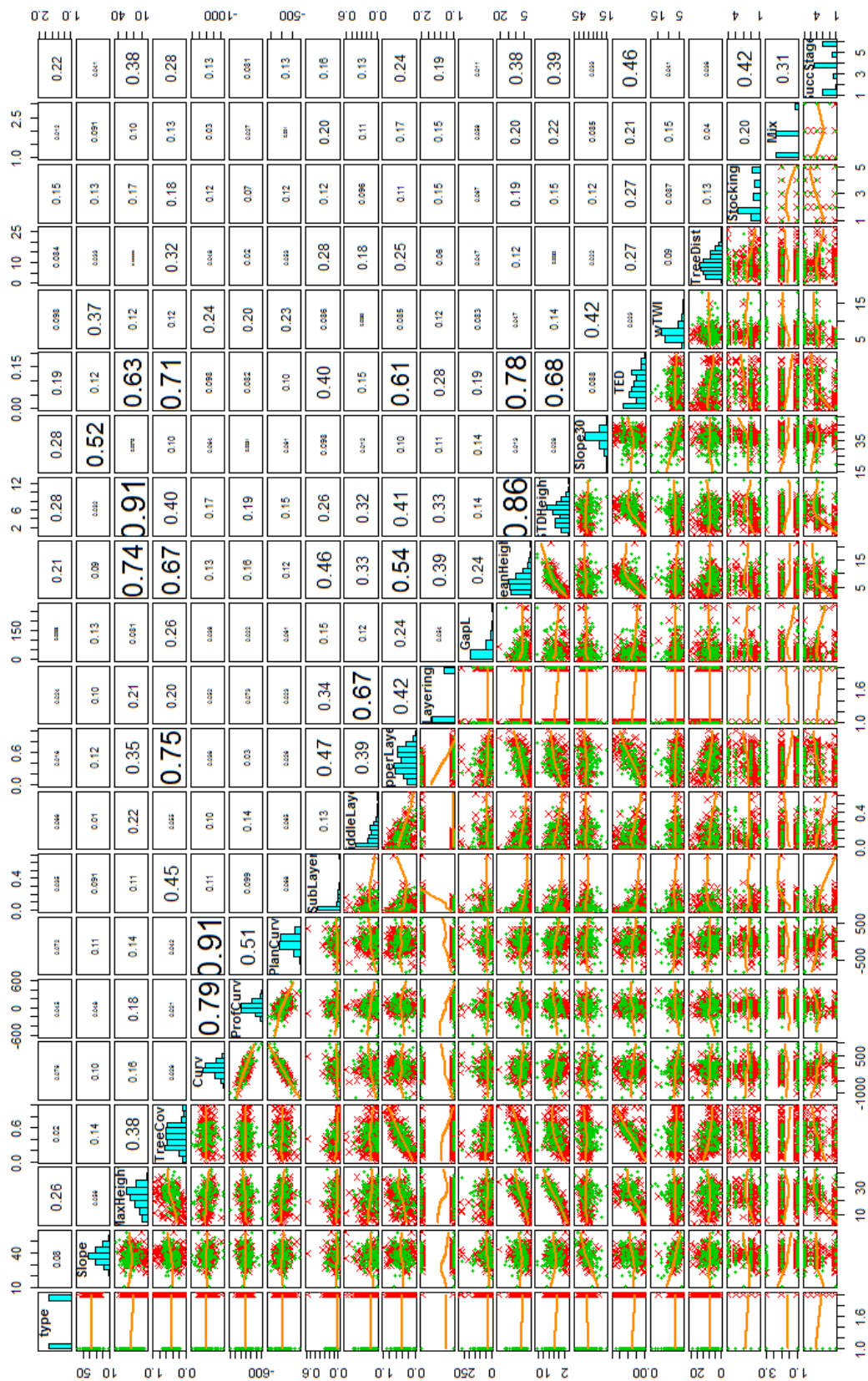


Fig. 4: Pairs plot with Spearman correlation coefficient of the variables derived from LiDAR data of St. Antoenien. Abbreviations for variable names are explained in Tab. 3.

Tab. 3: Abbreviations used in **Fehler! Verweisquelle konnte nicht gefunden werden.** for the variables derived from LiDAR data.

Abbreviation	Explanation
Slope	Slope angle at the release point
MaxHeight	Maximum tree height
TreeCov	Tree coverage
Curv	Curvature (30 m x 30 m)
ProfCurv	Profile curvature (30 m x 30 m)
PlanCurv	Planform curvature (30 m x 30 m)
SubLayer	Coverage of the sub layer
MiddleLayer	Coverage of the middle layer
UpperLayer	Coverage of the upper layer
Layering	Layering
GapL	Length of the largest gap
meanheight	Mean tree height
STDHeight	Standard deviation tree height
Slope30	Mean slope (30 m x 30 m)
TED	Tree edge density
OldL	Signs of old landslides
wTWI	Weighted Topographic Wetness Index (30 m x 30 m)
TreeDist	Distance to the nearest tree
Stocking	Stocking level
Mix	Species mixture
SuccStage	Successional stage

Appendix C: Model Builder diagrams ArcGIS

C1. Determination of control points

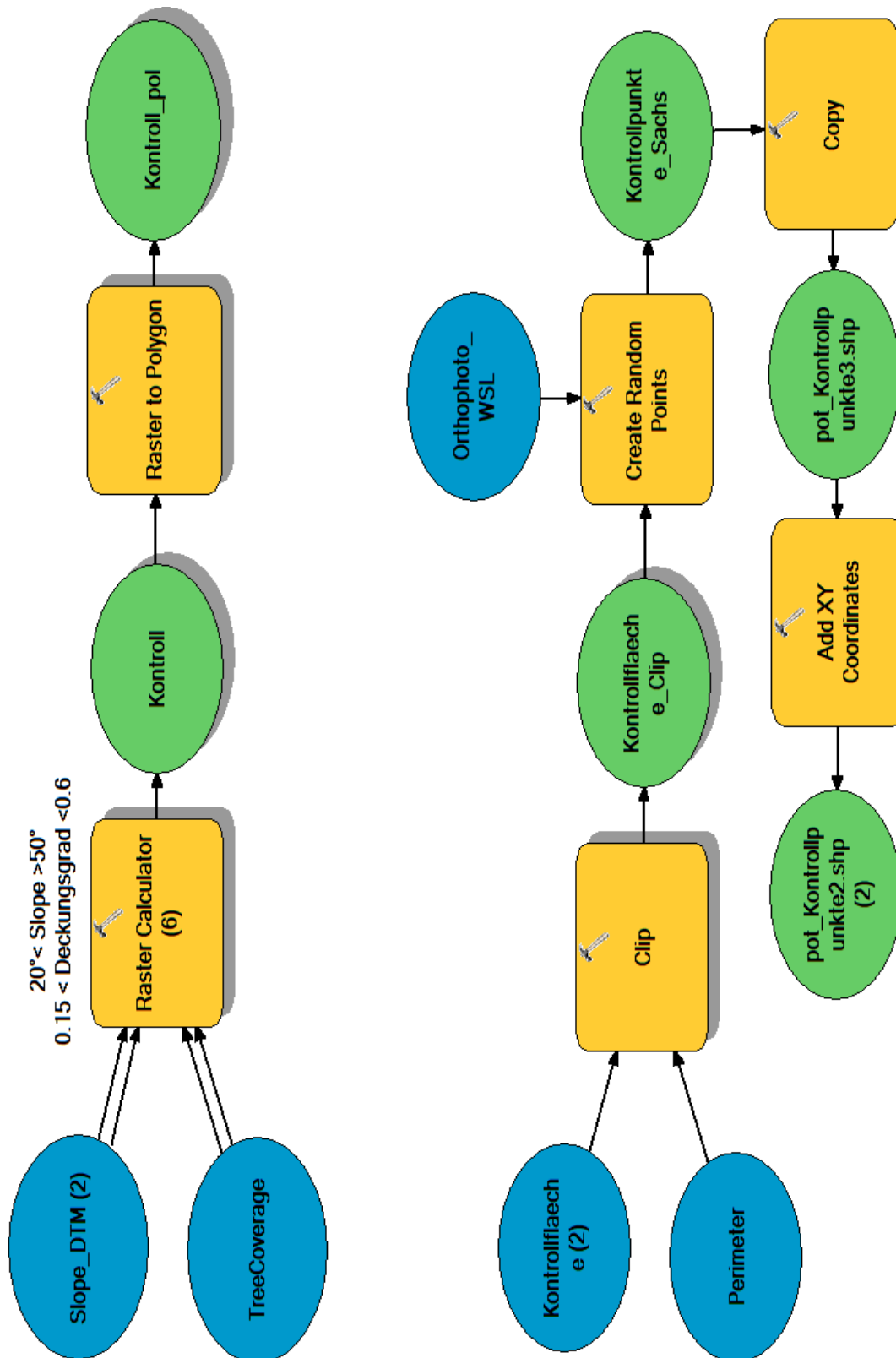


Fig. 5: Model Builder diagram of ArcGIS (ESRI 2013) for the determination of control points.

C3. Gap length

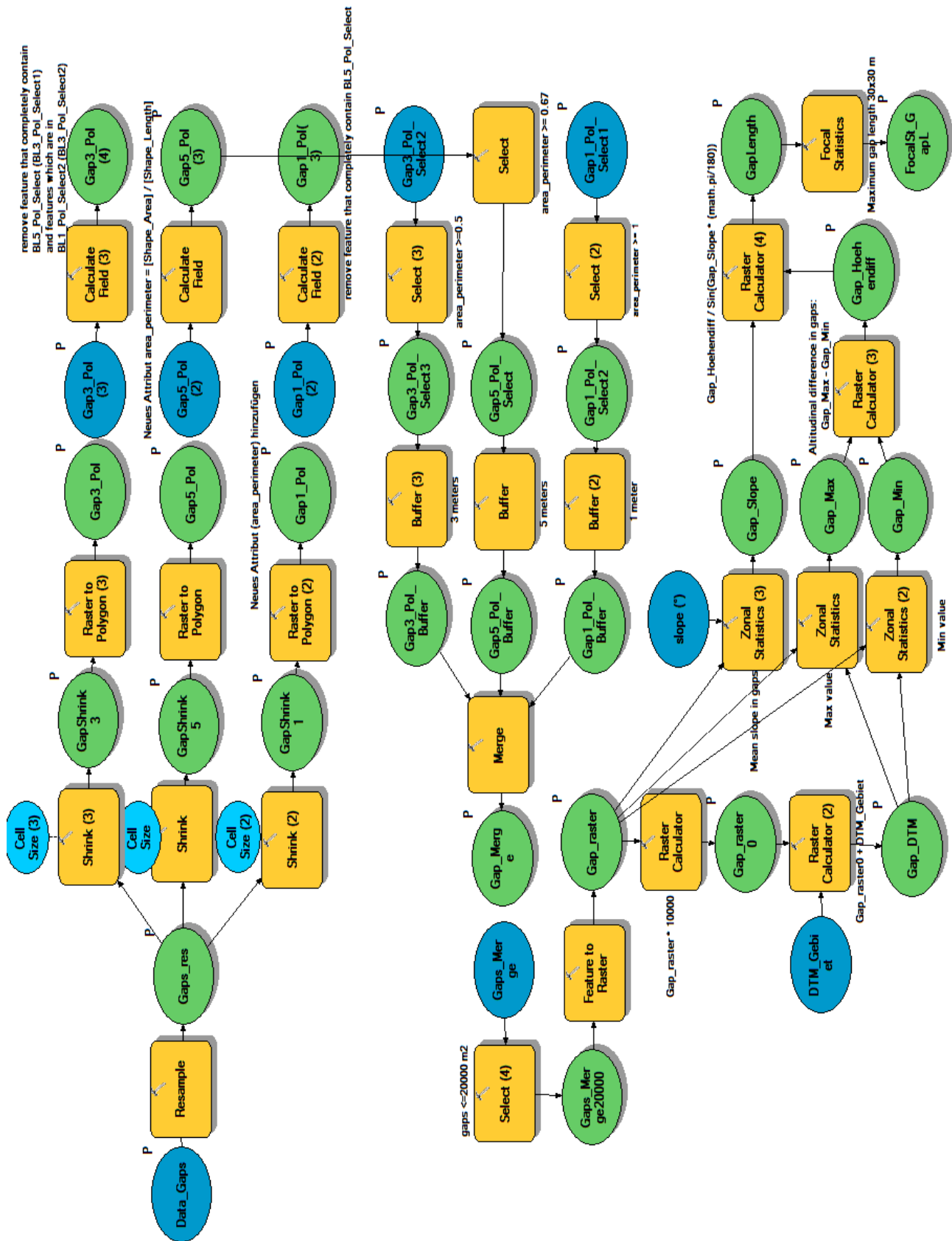


Fig. 7: Model Builder diagram of ArcGIS (ESRI 2013) for the calculation of gap length.

C4. Tree edge density

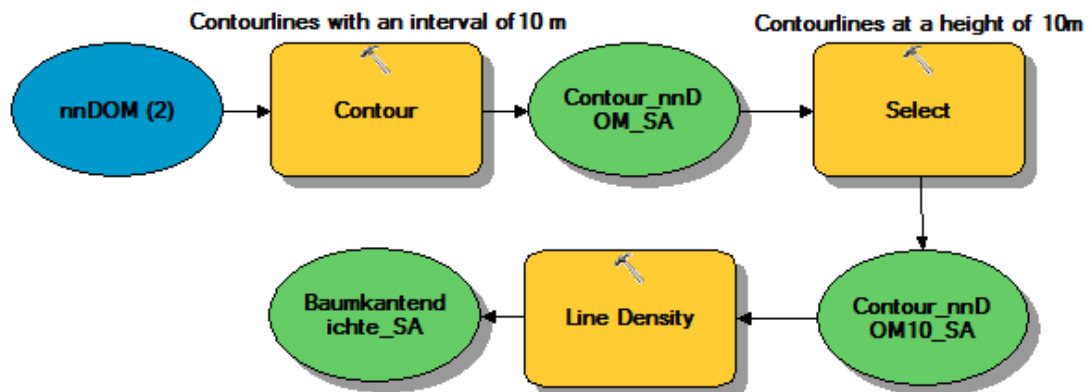


Fig. 8: Model Builder diagram of ArcGIS (ESRI 2013) for the calculation of tree edge density.

C5. Weighted Topographic Wetness Index

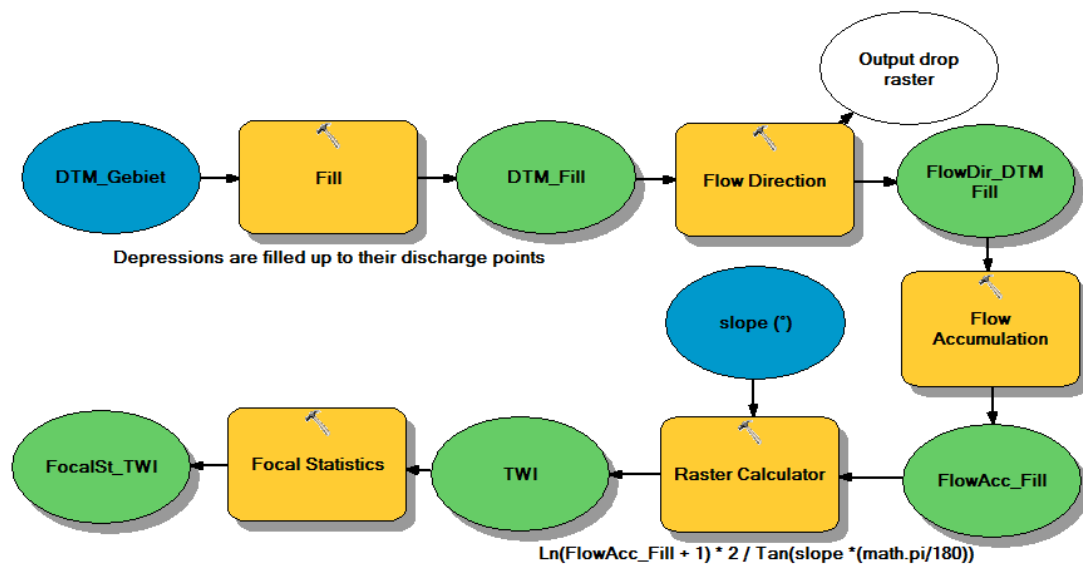


Fig. 9: Model Builder diagram of ArcGIS (ESRI 2013) for the calculation of the TWI (*Topographic Wetness Index*), which is the basis for the wTWI.

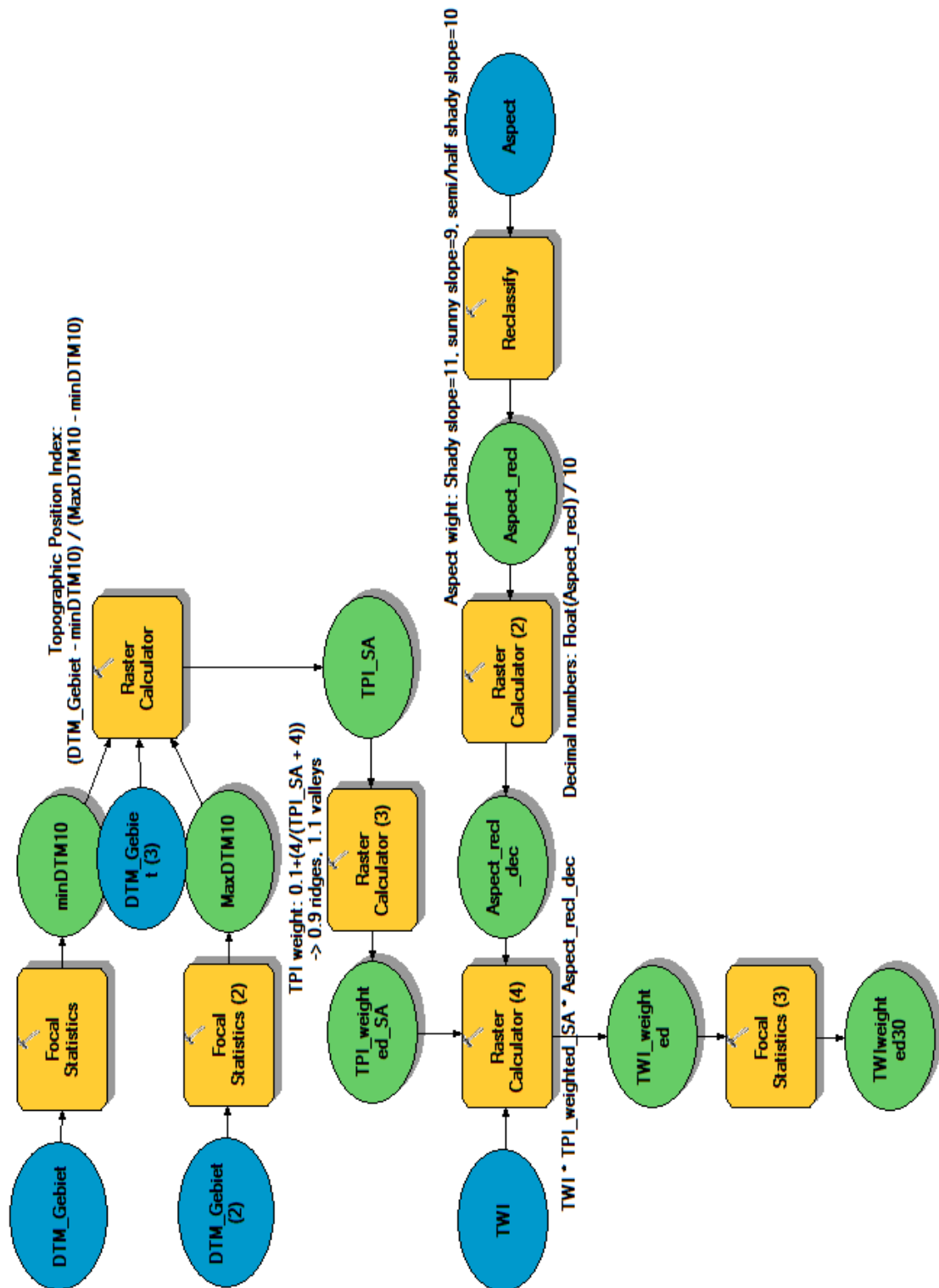


Fig. 10: Model Builder diagram of ArcGIS (ESRI 2013) for the calculation of the wTWI (weighted Topographic Wetness Index) based on the TWI (cf. Fig. 10).

Appendix D: Explanatory variables

Plots of explanatory variables which are not in the results (chapter 0) are shown here.

D1. St. Antoenien field data

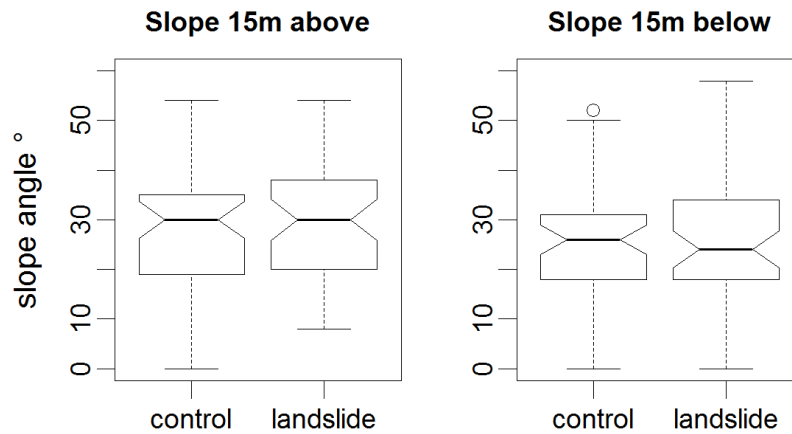


Fig. 11: Boxplots of slope angles measured 15 m above and below the (potential) release point in control and landslide plots. Differences between control and landslides are not significant.

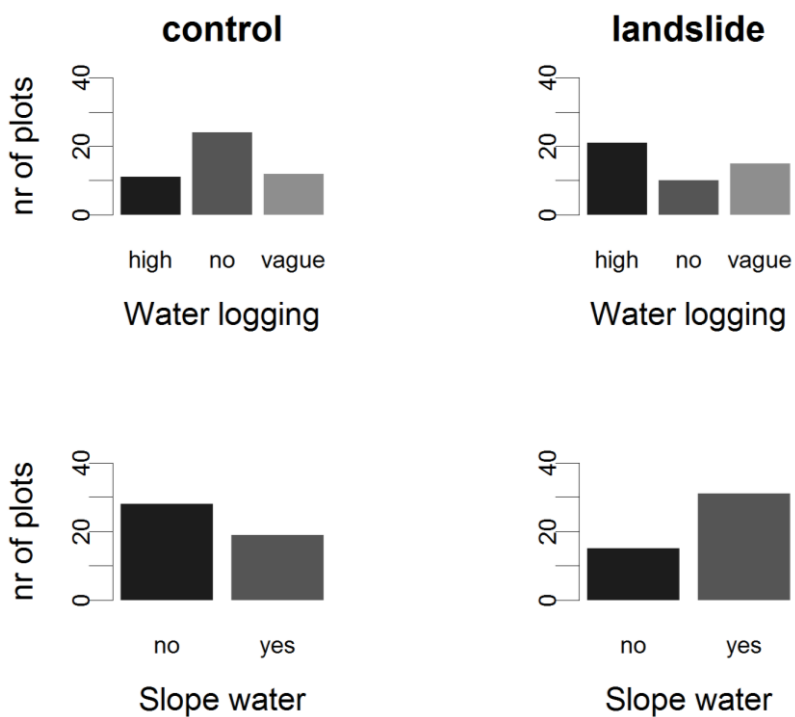


Fig. 12: Number of control (left) and landslide (right) plots with signs of water logging (above) and slope water discharge (below) in St. Antoenien. Differences between control and landslide plots are for both variables significant.

Signs of old landslides

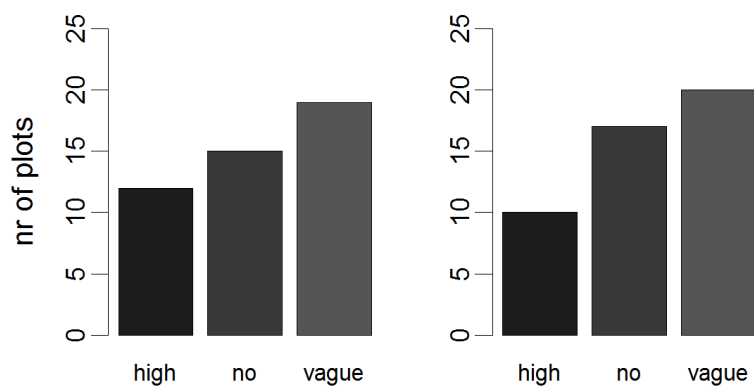


Fig. 13: Number of landslide (left) and control (right) plots in St. Antoenien with high, vague or no signs of past soil movements. Control and landslide plots do not differ significantly.

Soil compaction

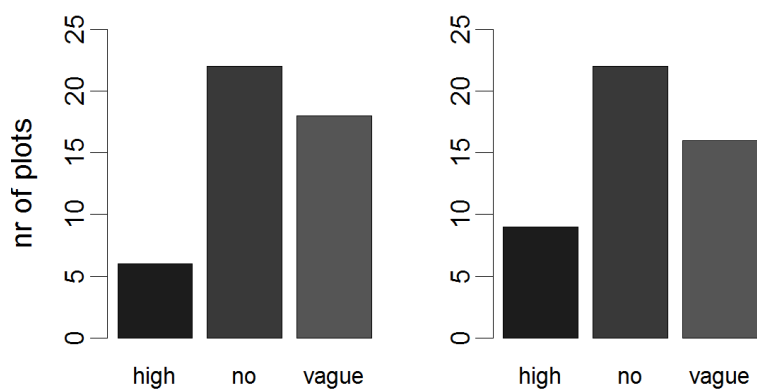
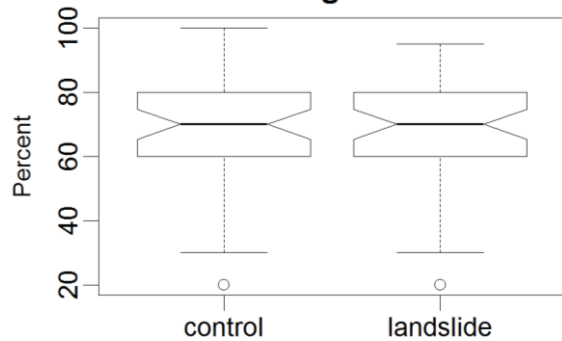


Fig. 14: Number of landslide (left) and control (right) plots in St. Antoenien with signs of compaction (high, no, vague). The difference between landslide and control plots is not significant.

Soil vegetation



Grazing

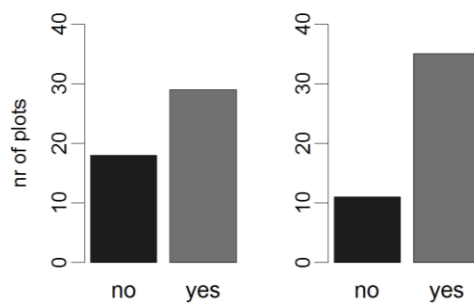


Fig. 15: Coverage of soil vegetation in control and landslide plots (left; no significant difference) and number of plots with signs of grazing (right; no significant difference).

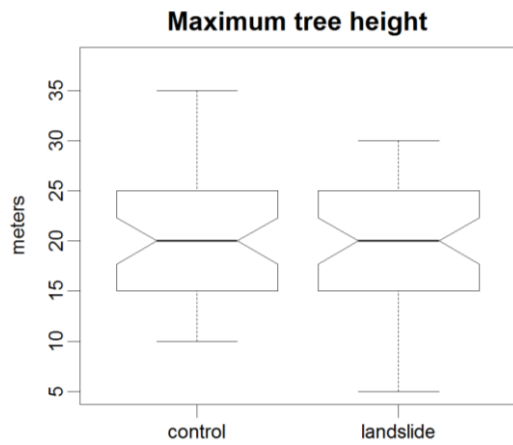


Fig. 16: Distribution of maximum tree heights in control (left) and landslide (right) plots. The difference is not significant.

Tree coverage of different tree layers

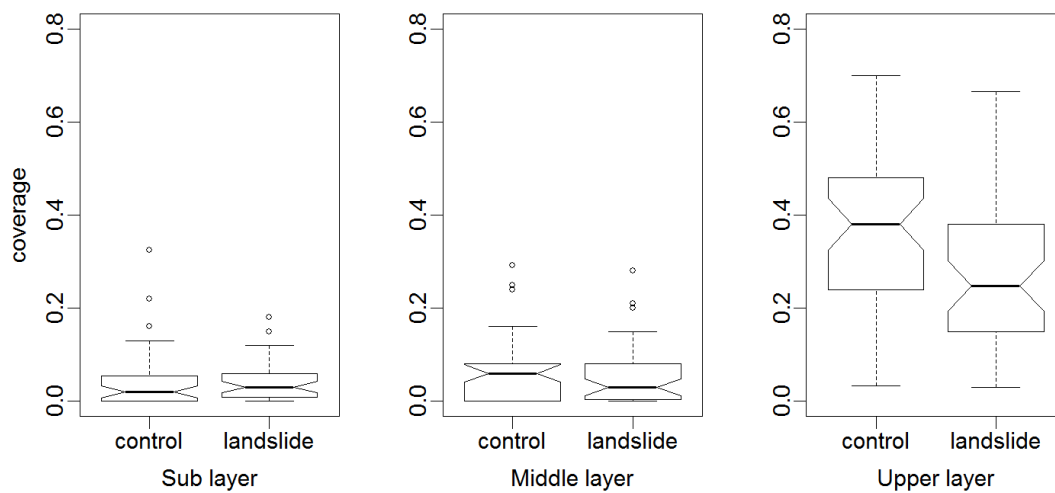


Fig. 17: Boxplot of the tree coverage of different tree layers estimated in the field. Sub layer = $1.3\text{m} - 1/3 \times$ maximum height, middle layer = $1/3 - 2/3 \times$ maximum height, upper layer = $2/3 \times$ maximum tree height – maximum tree height

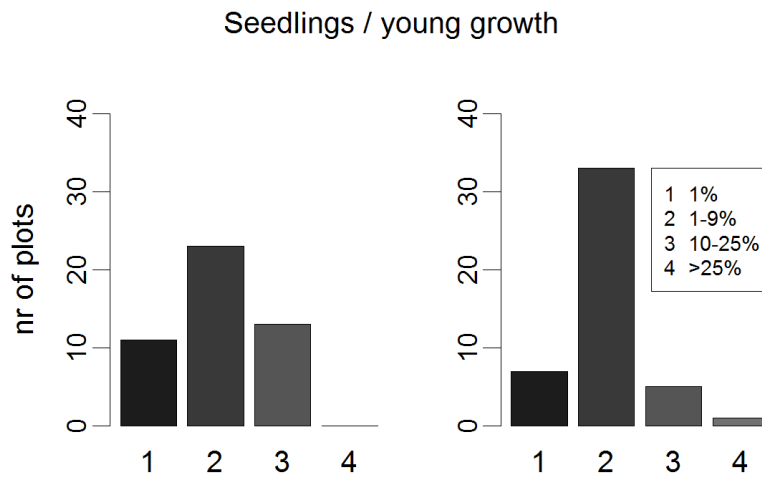


Fig. 18: Percentage of seedlings and young growth in control (left) and landslide plots (right) (difference not significant).

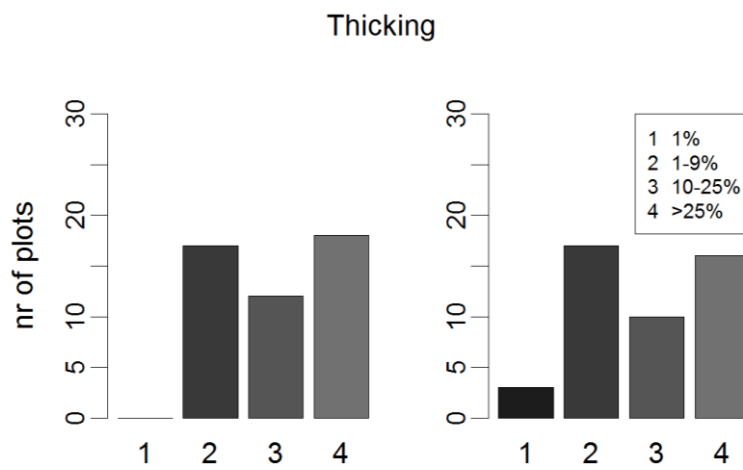


Fig. 19: Percentage of thickening in control (left) and landslide plots (right) (difference not significant).

D2. St. Antoenien LiDAR data

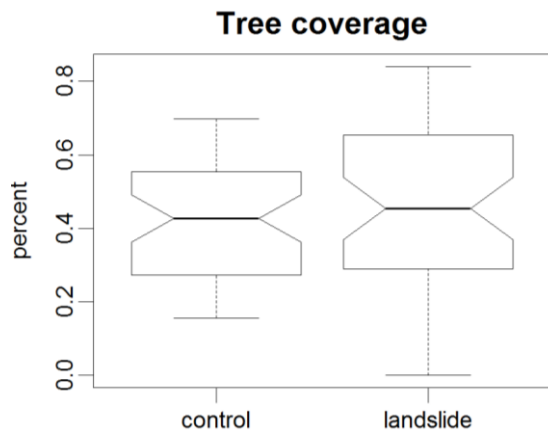


Fig. 20: Boxplots of tree coverage (left) and maximum tree height (right) calculated with the CHM for control and landslide plots in St. Antoenien. Differences are not significant.

Tree coverage of different layers

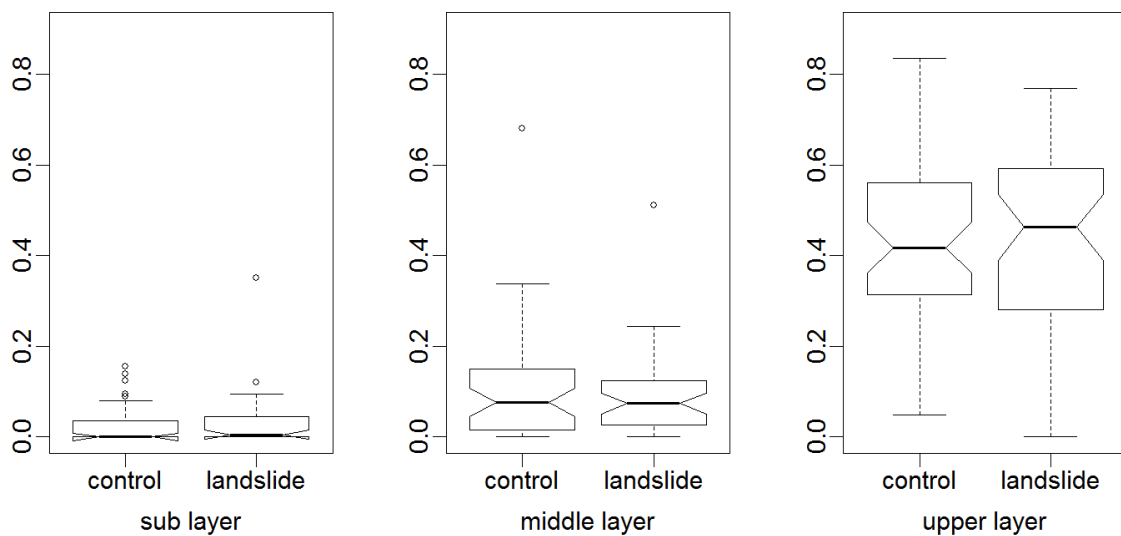


Fig. 21: Distribution of the tree coverage of different layers calculated with the CHM for control and landslide plots in St. Antoenien. Differences are not significant. Sub layer = $0.40 \text{ m} - 1/3 \times \text{maximum tree height}$, middle layer = $1/3 \times \text{maximum tree height} - 2/3 \times \text{maximum tree height}$, upper layer = $2/3 \times \text{maximum tree height} - \text{maximum tree height}$.

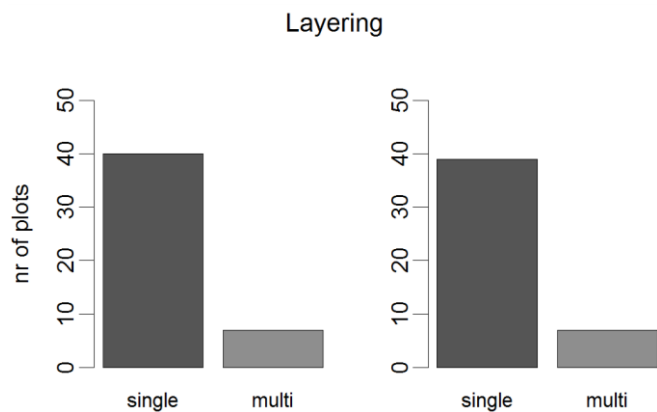


Fig. 22: Number of control (left) and landslide (right) plots with single- and multi-layered forest structure. Differences are not significant. Multi-layered = Tree coverage of sub or middle layer $\geq 20\%$.

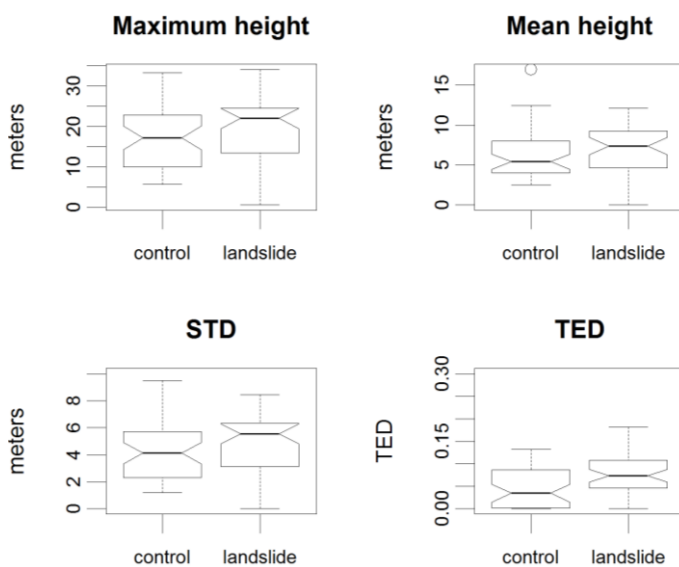


Fig. 23: Boxplots of the maximum (above left; not significant) and minimum (above right; not significant) tree height, the standard deviation of tree height (below left; not significant) and the tree edge density (below right; significant) calculated with the CHM for control and landslide plots.

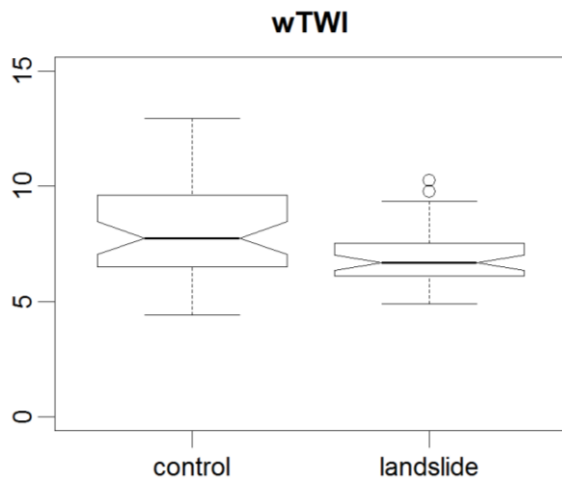


Fig. 24: Distribution of the weighted Topographic Wetness Index (wTWI) in control (left) and landslide (right) plots in St. Antoenien (significant difference).

D3. Sachseln

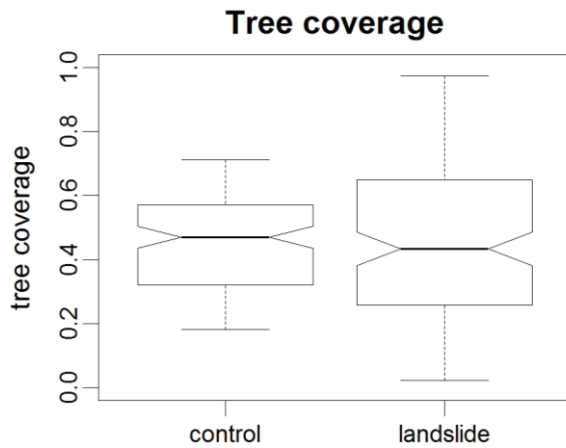


Fig. 25: Distribution of tree coverage calculated with the CHM in control (left) and landslide (right) plots in Sachseln. Differences are not significant.

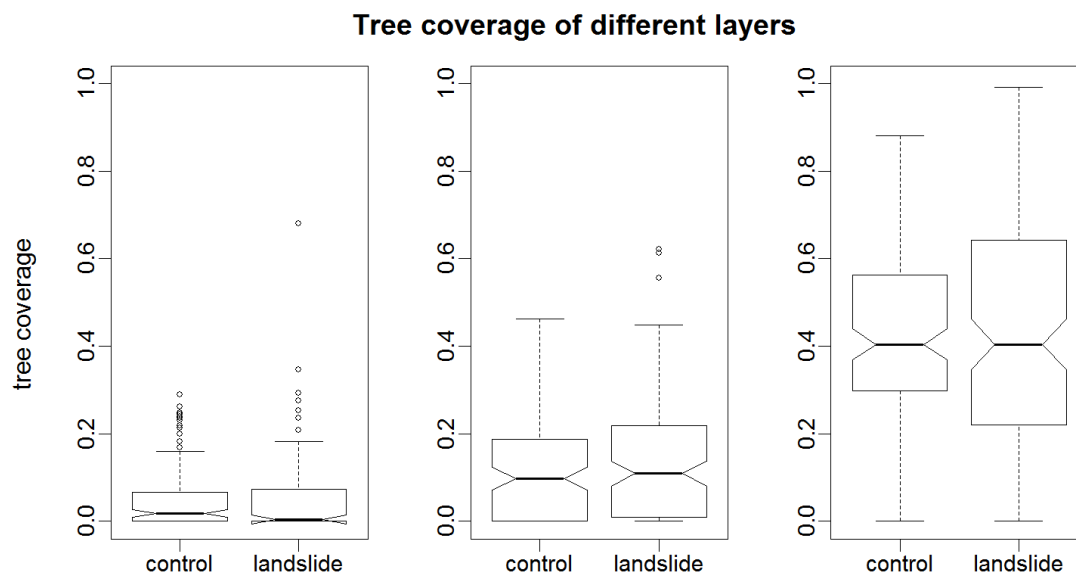


Fig. 26: Boxplots of the coverage of different tree layers in Sachseln. Differences between control and landslide plots are not significant. Sub layer = 0.40 m – 1/3 x maximum tree height, middle layer = 1/3 x maximum tree height – 2/3 x maximum tree height, upper layer = 2/3 x maximum tree height- maximum tree height.

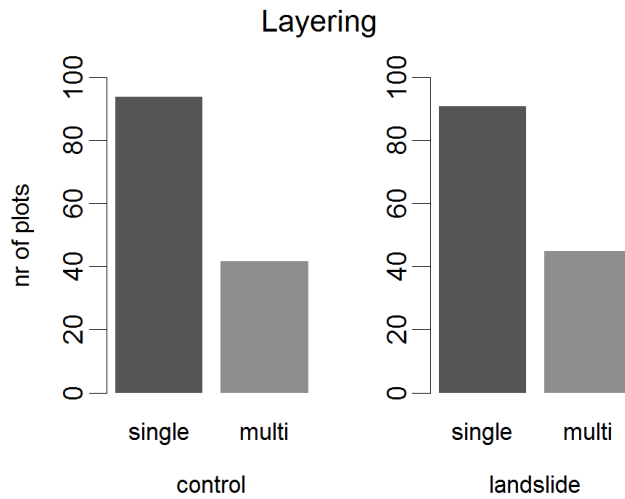


Fig. 27: Number of control (left) and landslide (right) plots in Sachseln with single- and multi-layered forest structure. Differences are not significant.

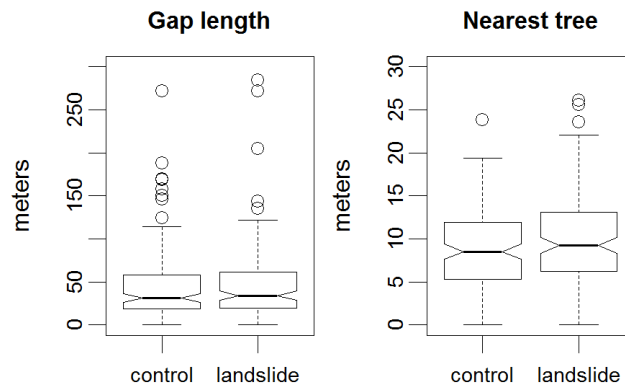


Fig. 28: Boxplots of the distance to the nearest tree (left) and the length of the largest gap (right) calculated with the CHM for control and landslide plots in Sachseln. Differences are not significant.

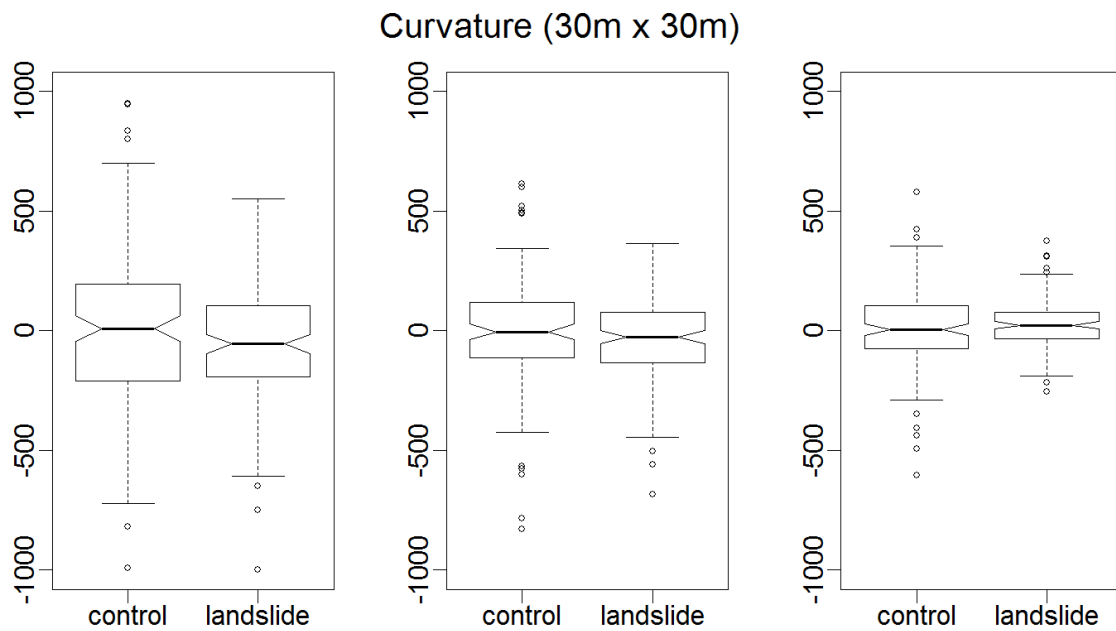


Fig. 29: Boxplots of the mean curvature (left), mean plan curvature (middle) and mean profile curvature (right) in control and landslide plots in Sachseln. Differences are not significant.

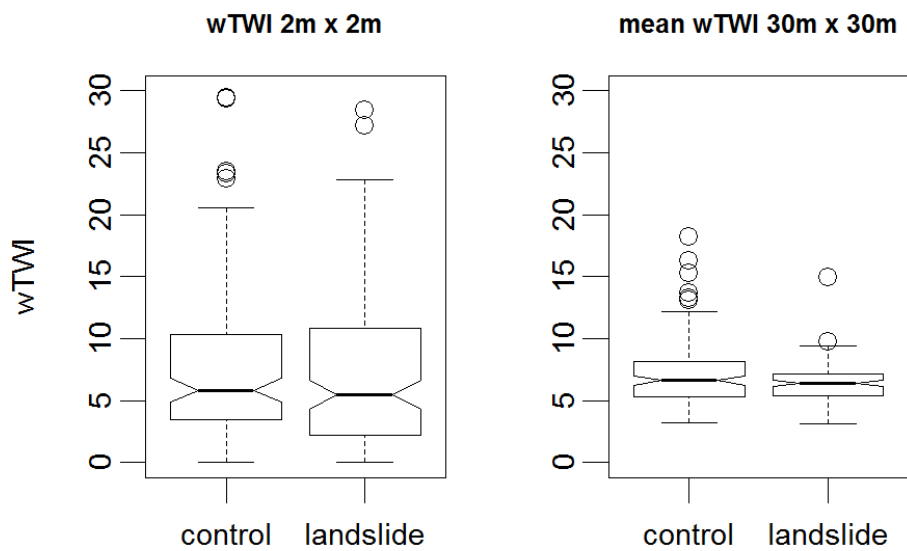


Fig. 30: Distribution of wTWI values for control and landslide points (left) and wTWI values averaged over an area of 30 m x 30 m (right). Differences between control and landslide plots are not significant.

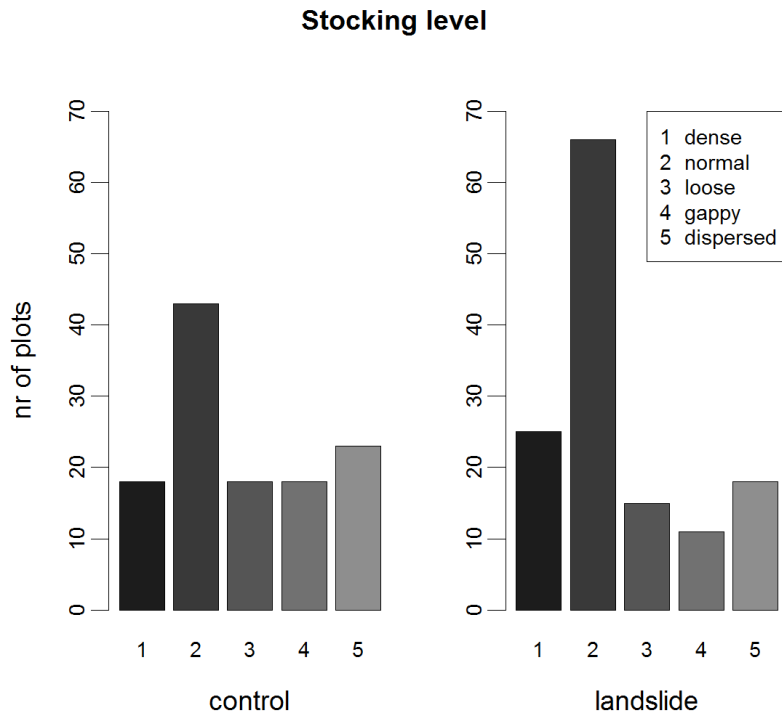


Fig. 31: Number of control (left) and landslide (right) plots per stocking level. Differences between control and landslide plots are not significant.

Appendix E: Residual analysis logistic regression

E1. LOG topo

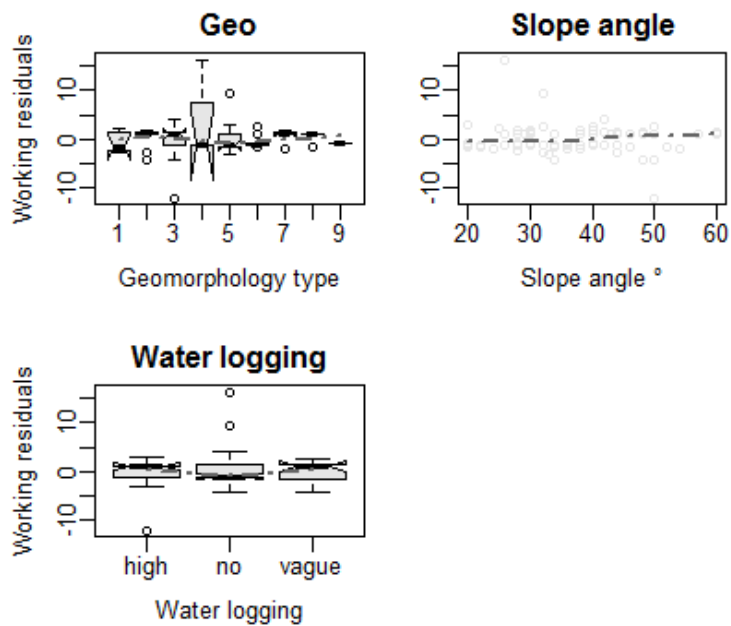


Fig. 32: Working residuals against explanatory variables of the logistic regression model based on terrain and hydrological field variables of St. Antoerien (*LOG topo*).

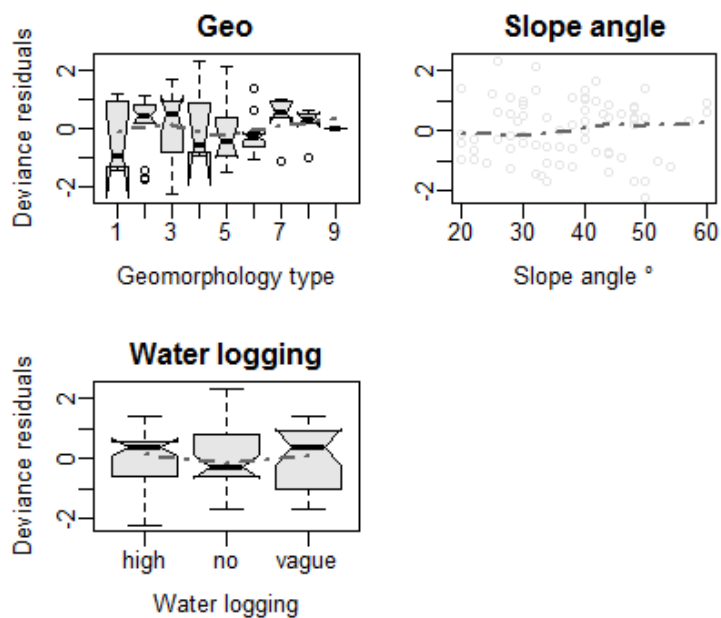


Fig. 33: Deviance residuals against explanatory variables of the logistic regression model based on terrain and hydrological field variables of St. Antoerien (*LOG topo*).

E2. LOG mix

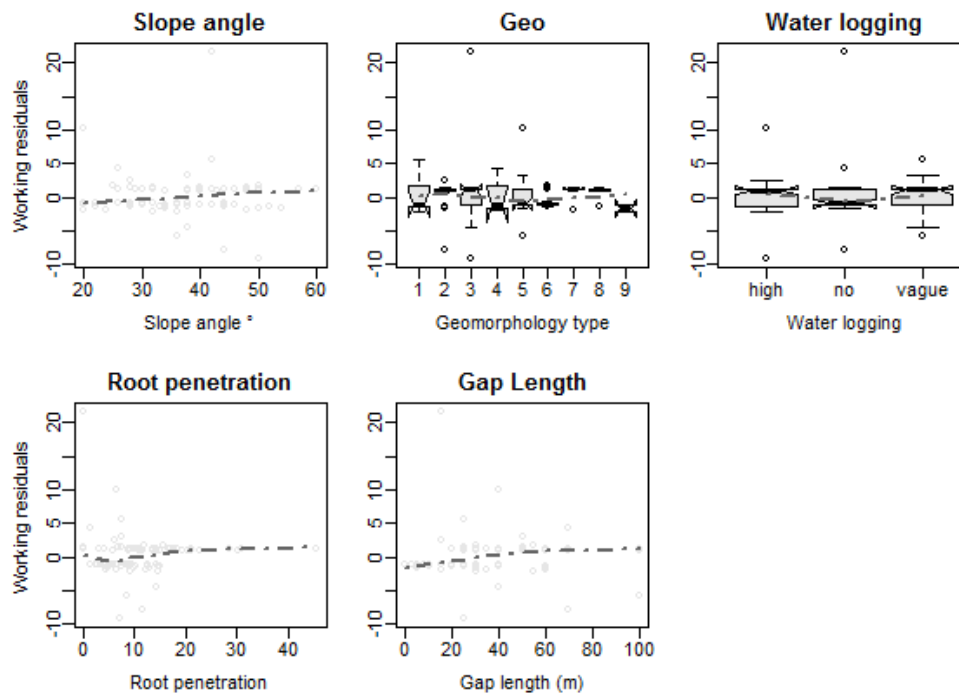


Fig. 34: Working residuals against explanatory variables of the logistic regression model based on terrain, hydrological and forest variables assessed in St. Antoenien (*LOG mix*).

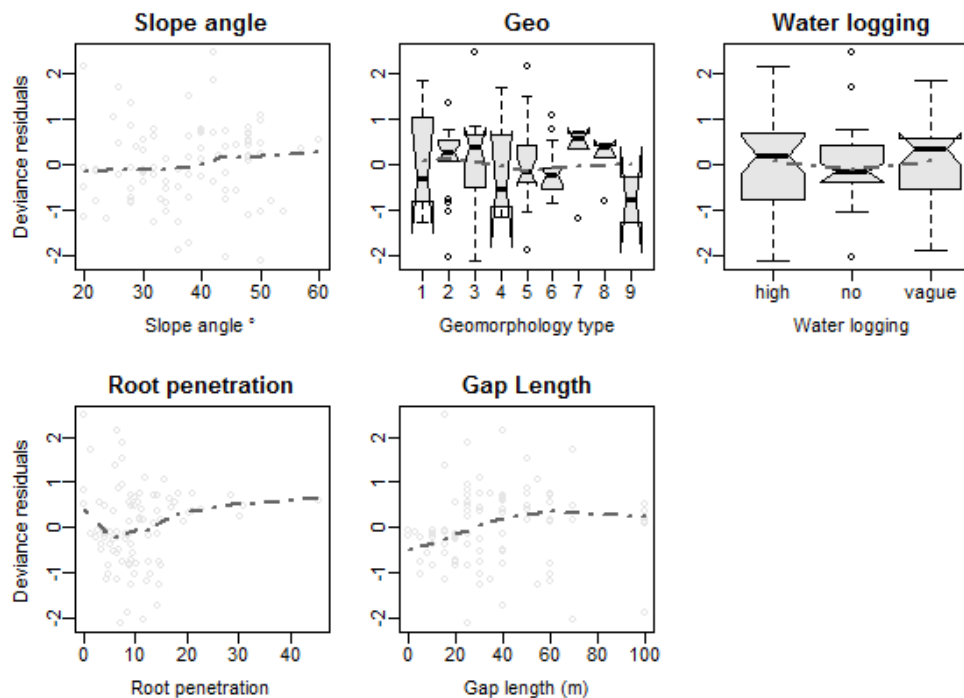


Fig. 35: Deviance residuals against explanatory variables of the logistic regression model based on terrain, hydrological and forest variables assessed in St. Antoenien (*LOG mix*).

E3. LOG LiDAR

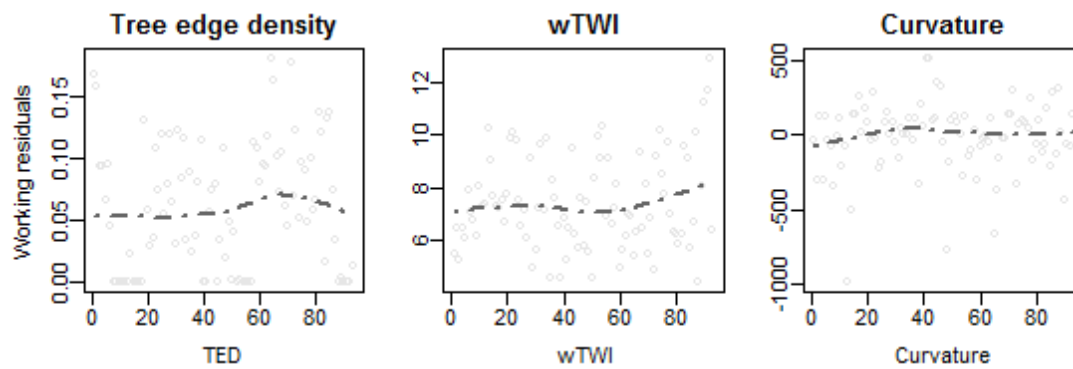


Fig. 36: Working residuals against explanatory variables of the logistic regression model based on LiDAR derived variables from St. Antoenien (*LOG LiDAR*).

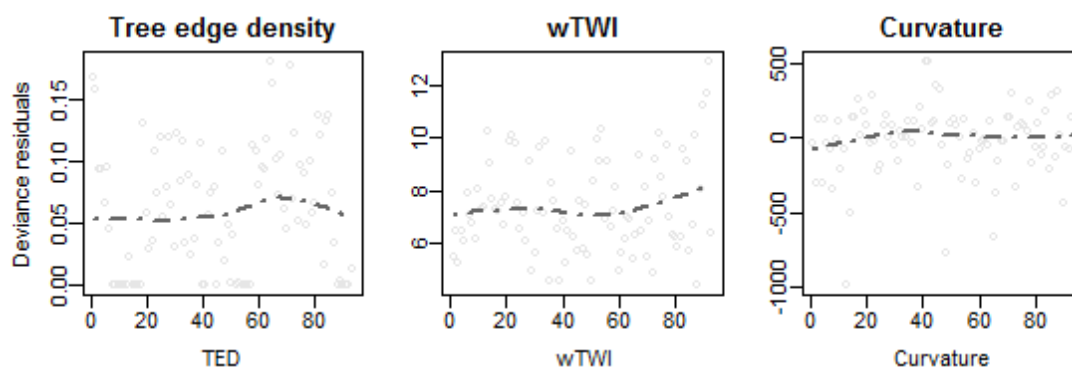


Fig. 37: Deviance residuals against explanatory variables of the logistic regression model based on LiDAR derived variables from St. Antoenien (*LOG LiDAR*).

E4. LOG Sachseln

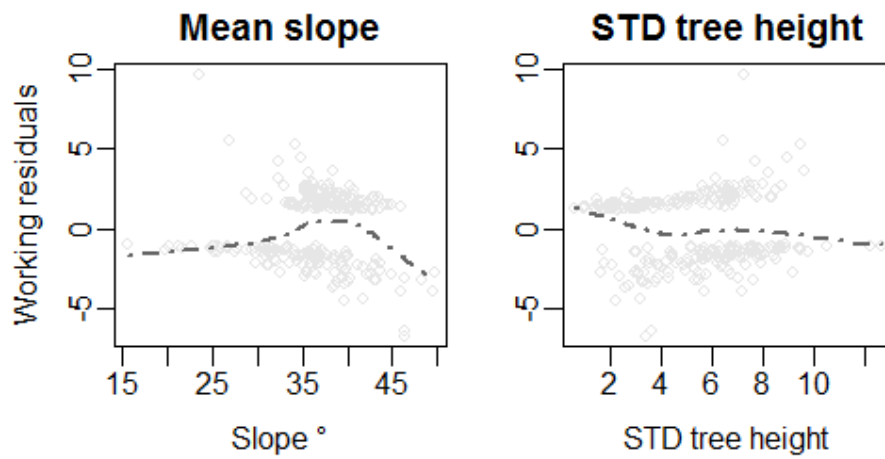


Fig. 38: Working residuals against explanatory variables of the logistic regression model based on LiDAR derived variables from Sachseln (*LOG Sachseln*).

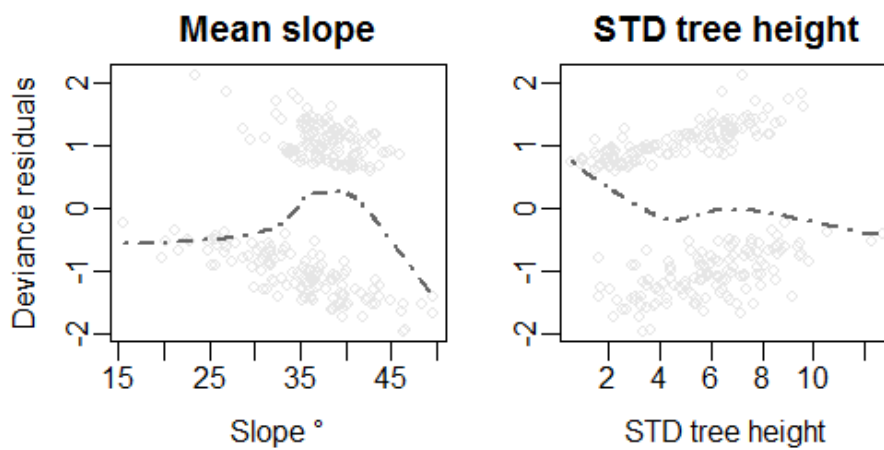


Fig. 39: Deviance residuals against explanatory variables of the logistic regression model based on LiDAR derived variables from Sachseln (*LOG Sachseln*).

E5. LOG Sachseln+

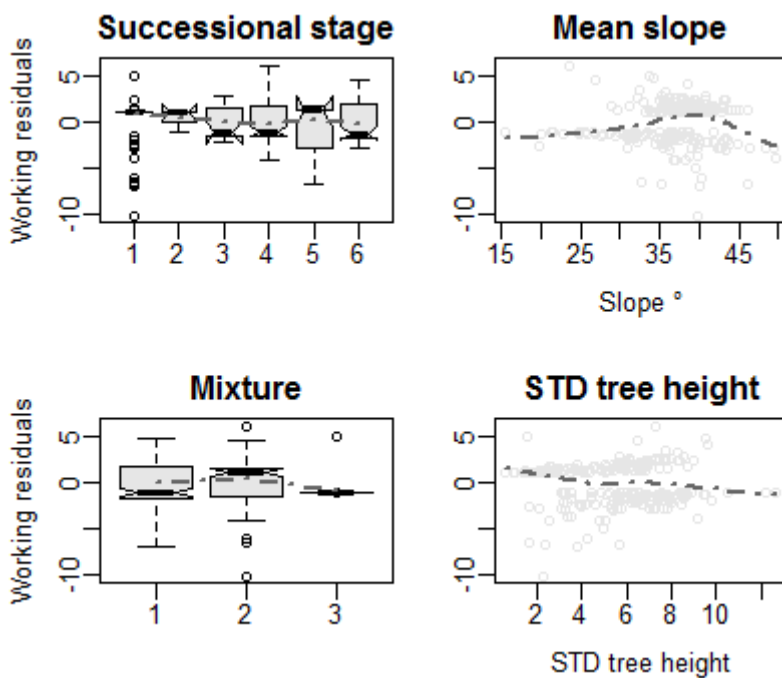


Fig. 40: Working residuals against explanatory variables of the logistic regression model based on variables derived from LiDAR and the stand classification from Sachseln (*LOG Sachseln+*).

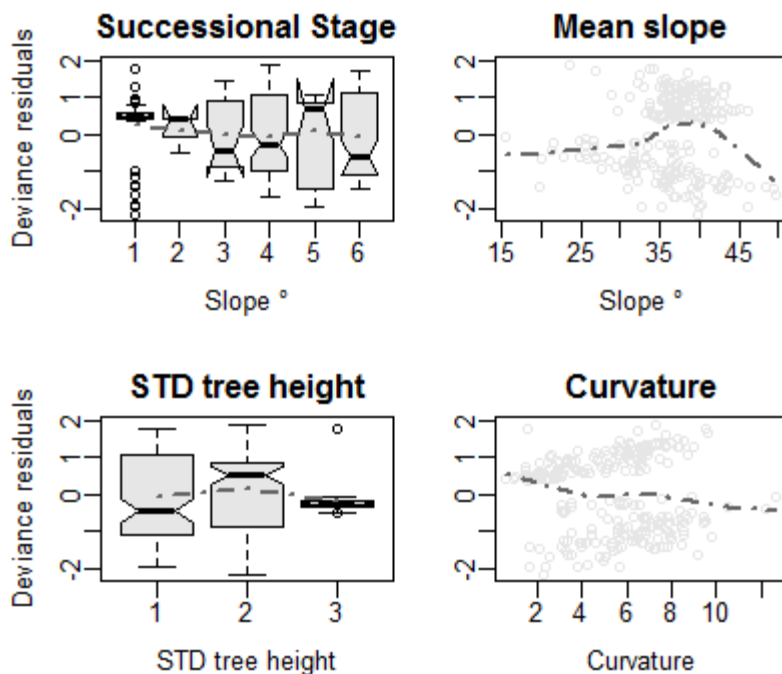


Fig. 41: Working residuals against explanatory variables of the logistic regression model based on variables derived from LiDAR and the stand classification from Sachseln (*LOG Sachseln+*).

Appendix F: Declaration of originality

This signed "Declaration of originality" is a required component of any written work (including any electronic version) submitted by a student during the course of studies in Environmental Sciences. For Bachelor and Master theses, a copy of this form is to be attached to the request for diploma.

I hereby declare that this written work is original work which I alone have authored and written in my own words, with the exclusion of proposed corrections.

Title of the work

Author(s)

Last name

First Name

With my signature, I hereby declare:

- I have adhered to all rules outlined in the form on „Citation etiquette“, www.ethz.ch/students/exams/plagiarism_s_en.pdf.
- I have truthfully documented all methods, data and operational procedures.
- I have not manipulated any data.
- I have identified all persons who have substantially supported me in my work in the acknowledgements.
- I understand the rules specified above.

I understand that the above written work may be tested electronically for plagiarism.

Place, Date

Signature*

* The signatures of all authors are required for work submitted as a group. The authors assert the authenticity of all contents of the written work submitted with their signatures.